The Adsorption of Arsenic Oxyacids to Iron Oxyhydroxide Columns

Including Studies of Weakly Hydrated Ions and Molecules in Aqueous Solution

Johan Mähler

Faculty of Natural Resources and Agricultural Sciences
Department of Chemistry
Uppsala

Doctoral Thesis
Swedish University of Agricultural Sciences
Uppsala 2013

Acta Universitatis Agriculturae Sueciae
2013:54

Cover: Arsenic enriched well in Lilgomdé village, Burkina Faso. The image was used as the cover of *Dalton Transactions*, 42, 2013, featuring the article *Hydration of Arsenic Oxyacid Species*.
(photo: Mr. J. Mähler, image editing Dr. D. Lundberg)

ISSN 1652-6880
ISBN (print version) 978-91-576-7846-1
ISBN (electronic version) 978-91-576-7847-8

Print: SLU Service/Repro, Uppsala 2013

The Adsorption of Arsenic Oxyacids to Iron Oxyhydroxide Columns. Including Studies of Weakly Hydrated Ions and Molecules in Aqueous Solution.

Abstract

The fundamental side of this project includes determination of ionic radii and plausible hydration numbers for the weakly hydrated alkali metal ions in solution, as well as an investigation of the intramolecular bond lengths of arsenic oxyacid species and orthotelluric acid. Experimental methods such as EXAFS, XANES and LAXS have been used for these purposes, as well as thorough screening for relevant structures in crystal structure databases. The improved ionic radius for the sodium ion in six-coordination is of particular interest as current literature data to a large extent is derived from structures not representative for aqueous solutions. The improved larger value is 1.07 Å in six-coordinated crystal structures and increases to 1.09 Å in aqueous solution due to hydration effects. Furthermore it has been discussed how alkali metal ions affect the three-dimensional network of hydrogen bound water molecules in aqueous solution, based on investigations with double difference infrared spectroscopy. Only the lithium ion was found to be a true structure making ion, even though the status of the border-line sodium ion can be discussed.

The applied studies have focused on the rapid removal of arsenic from aqueous solution using columns filled with iron oxyhydroxide based adsorbents, complemented with additional batch experiments. Atomic absorption spectrophotometry has been used to determine concentrations of arsenic in the effluent of columns and iron content of the adsorbent material. Experiments have shown that adsorption does occur rapidly and since there is no need for reaching equilibrium in practical water cleaning applications, short empty bed contact times are sufficient for removing practically all arsenic. However, somewhat longer empty bed reaction times are desirable for a more efficient material utilization, as both diffusion into porosities and desorption of competing species are kinetic hindrances. Adsorption capacity in a column is quite dependent on the presence of competitors such as phosphate, hydrogen carbonate and fluoride, as well as on pH, possibly due to desorption kinetics. Scanning electron microscopy as well as XANES and EXAFS have been used to study the structural and chemical status of the adsorbents. The arsenic part of the project can be seen as an initiation of a future project, aiming at developing a simple but efficient adsorption filter for arsenic removal from drinking water in Burkina Faso.

Keywords: column, adsorption, arsenic, arsenous, oxyacid, arsenic removal, arsenic enriched water, Burkina Faso, ionic radii, alkali ions, iron oxyhydroxide, GFH

Author's address: Johan Mähler, SLU, Department of Chemistry,
P.O. Box 7015, 750 07 Uppsala, Sweden
E-mail: johan.mahler@ slu.se

Dedication

To my wife Roya

Ofta illa veta,
de som inne sitta,
vad slags folk, som farande komma.

Ingen är så bra,
att ej brist han äger,
eller så dålig, att till intet han duger.

Hávamál (133).

Contents

List of Publications

This thesis is based on the work contained in the following papers, referred to by Roman numerals in the text:

I Mähler, J.; Persson, I. (2012). A Study of the Hydration of the Alkali Metal Ions in Aqueous Solution. *Inorganic Chemistry* 51, 425-438.
Reproduced by permission of ACS publications
http://pubs.acs.org/doi/full/10.1021/ic2018693

II Mähler, J.; Persson, I.; Herbert R.B. (2013). Hydration of Arsenic Oxyacid Species. *Dalton Transactions* 42, 1364-1377.
Reproduced by permission of The Royal Society of Chemistry
http://pubs.rsc.org/en/content/articlelanding/2013/dt/c2dt31906c

III Mähler J.; Persson I. Rapid Adsorption of Arsenic from Aqueous Solution by Ferrihydrite Coated Sand and Granular Ferric Hydroxide. *Applied Geochemistry*, in press.
Reproduced by permission of Elsevier.
http://authors.elsevier.com/sd/article/S0883292713002060
DOI 10.1016/j.apgeochem.2013.07.025

IV Mähler J.; Persson I. Competition for Adsorption Sites on Iron Oxyhydroxide based Column Adsorbents for the Removal of Arsenic Oxyacid Species. *Manuscript*

Supplementary material for publications may be downloaded from their respective web location as given above, or requested J. Mähler.

The contribution of Johan Mähler to the papers included in this thesis was as follows:

I DDIR experiments, some LAXS raw data collection, preliminary data analysis, literature study and writing of the article.

II Experimental work except preparation of organic arsenic solutions. Preliminary analysis of LAXS and XAS data. Responsible for literature study and for writing the article.

III Experimental work with columns and preparation of solutions and materials. Responsible for data analysis and writing of the article.

IV Experimental work, data analysis and writing of the article.

Abbreviations

AAS	Atomic Absorption Spectrophotometry (Spectroscopy)
AGP	Antimicrobial Growth Promoter
APL	Acute Promyelocytic Leukemia
ATP	Adenosine triphosphate
BET	"Brunauer, Emmet, Teller" (surface measurement method)
CAO	Chemolithotrophic Arsenite Oxidizer
CF	Charge Field
CN	Coordination Number
CSD	Cambridge Structural Database
D	Deuterium, $^{2}_{1}H$
DARP	Dissimilatory Arsenate Reducing Prokaryote
DDIR	Double Difference Infrared Spectroscopy
DMA^{III}	Dimethyl arsonous acid
DMA^{V}	Dimethyl arsonic acid
DMPU	*N*,*N*′-Dimethylpropylenurea
DMSO	Dimethyl sulfoxide
DNA	Deoxyribonucleic acid
EBCT	Empty Bed Contact Time
EDS	Energy Dispersive Spectroscopy
EPA	United States Environmental Protection Agency
eV	electron volt, $\approx 1.6022 \cdot 10^{-19}$ J
EXAFS	Extended X-ray Absorption Fine Structure
FDA	United States Food and Drug Adminstration
GEH®	Granuliertes Eisenhydroxid
GF	Graphite Furnace
GFH®	Granular Ferric Hydroxide
H-bond	Hydrogen bond
HAO	Heterotrophic Arsenite Oxidizer
ICSD	Inorganic Crystal Structure Database

IOCS	Iron Oxyhydroxide (Oxide) Coated Sand
LAXS	Large Angle X-ray Scattering
MD	Molecular Dynamics
MM	Molecular Mechanics
MMA^{III}	Monomethyl arsonous acid
MMA^{V}	Monomethyl arsonic acid
N	Affected number in DDIR
NTU	Nephelometric Turbidity Units
pH_{pzc}	pH point of zero charge
ppm	parts per million
QM	Quantum Mechanical
RDF	Radial Distribution Function
ROS	Reactive Oxygen Species
SEM	Scanning Electron Microscopy
SIDA	Swedish International Development cooperation Agency
SLU	Sorption Limiting Unit (proposed measure)
TCLP	Toxicity Characteristic Leaching Procedure
THF	Tetrahydrofuran
UV	Ultraviolet
VR	Swedish Research Council
WAXS	Wide Angle X-ray Scattering
XANES	X-ray Absorption Near Edge Structure
XAS	X-ray Absorption Spectroscopy

1 Introduction

Water is one of the very basic requirements for human life but the quality of employed sources range from excellent to rather poor. To avoid the biological risks of foul surface water, societies often turn to ground water found deep down in the bedrock. Several drilling programs in developing countries have been carried out in order to provide rural communities with tube wells for safe drinking water supply (Smith *et al.*, 2000). However, the crystal clear water emerging from the many tube wells may not always be as clean as it appears. The last few decades, arsenic content of ground water used for human consumption have become a growing source of concern (Smedley & Kinniburgh, 2002).

1.1 Arsenic

Arsenic was among the first of elements to be isolated by mankind, possibly by Albertus Magnus in the 13th century, Paracelsus in the 16th century or latest in the 17th century by Schroeder (Weeks, 1932). The use of arsenic compounds began much earlier and both Aristotle and Hippocrates mention a mineral likely to be realgar (As_4S_4) several centuries B.C. Arsenic is well known as a poison in literature and many alleged non-fictional victims also exist, although elevated arsenic concentrations may also result from overmedication or unintentional exposure. The highly poisonous and tasteless arsenous oxide (As_2O_3) was a particularly popular choice for poisoners. The compound produces ill-defined and various disease-like symptoms at repeated ingestion, before death occurs (Bentley & Chasteen, 2002). Today the qualitative analysis of arsenic in biological material is straightforward, and arsenic substances are best avoided by the careful poisoner.

During the 19th century, inhabitants in the Austrian province Styria have been claimed to eat large quantities of arsenic for cosmetic reasons as well as health purpose (Bentley & Chasteen, 2002). It was thought to improve figure

(plumpness), and skin smoothness, and also to improve physical condition. Inhabitants of Victorian England heard of this habit and adapted it as their own. Arsenic had many uses in the society at that time, such as pest control, in agricultural applications and in pigments such as Scheele green (Bentley & Chasteen, 2002; Scheele, 1778). The inhabitants started to eat arsenic compounds to cure illnesses as well as for cosmetic reasons. Even before that era, physicians had become increasingly enthusiastic about the use of arsenic compounds as cytostatics, which compared to alternative mercury compounds appeared to give less side effects (Rönnow, 1778). Naturally, they were also aware of the dangers of acute arsenic poisoning (Gahn, 1800; Swedelius, 1800). During the centuries of co-existence between humans and arsenic compounds, the two faces of the element - poison and therapeutic drug - has been apparent (Bentley & Chasteen, 2002). Since the mid-20th century, medical use is limited due to insufficient knowledge about biological reaction mechanisms and due to adverse side effects (Ni Dhubhghaill & Sadler, 1991). Medical applications do however exist and as late as 2001, an arsenic trioxide (As_2O_3) based drug was approved by FDA for treatment of acute promyelocytic leukemia, APL (Bentley & Chasteen, 2002).

Arsenic compounds are still used in lead alloys for car batteries, wood preservation agents, glass industry, herbicides and animal feed additives. High purity arsenic have found a growing market in the semiconductor industry as doping agents in silicon or germanium crystals, and arsenic compounds are also used in other fields of the electronics industry (Bentley & Chasteen, 2002). Humans may come into contact with arsenic compounds in the smelting of copper ore, and health effects have been noted for workers in this kind of plants, especially in the past (Hughes *et al.*, 2011).

Arsenic is a medium abundant element in the earth crust with about 2 ppm (Greenwood & Earnshaw, 1997). Small deposits of the metalloid in elemental form have been reported in nature although its surface oxidizes in moist air. The element is frequently associated with sulphur in nature (realgar As_4S_4, orpiment As_2S_3), but occurs also as oxide (arsenolite As_2O_3) and in mixed minerals with iron, cobalt or nickel (Greenwood & Earnshaw, 1997).

All naturally occurring arsenic consists of the only stable isotope, ^{75}As. The atomic number of the element is 33 and the electron configuration can be described as $[Ar]3d^{10}4s^24p^3$. The most common oxidation states in nature are arsenic(III), arsenite, where the valence 4p electrons are lost and arsenic(V), arsenate, where valence 4p and 4s electrons are lost. Under laboratory conditions arsenic(-III) can also be produced with relative ease by the addition of three electrons into molecular orbitals of p character. The formal oxidation state of arsenic in realgar, As_4S_4, is +2 as the mineral contain covalent As-As

bonds. Located between phosphorus and antimony in the nitrogen group of the periodic table, Figure 1, arsenic shares many chemical properties of both elements in addition to the most common oxidation states. It differs from phosphorus for example by an increased preference for the +3 oxidation state and a less varied flora of oxides and oxyacids. Arsenic form stronger covalent bonds than the less common and substantially larger neighboring antimony. Antimony is less reactive in general and also less electronegative (Greenwood & Earnshaw, 1997).

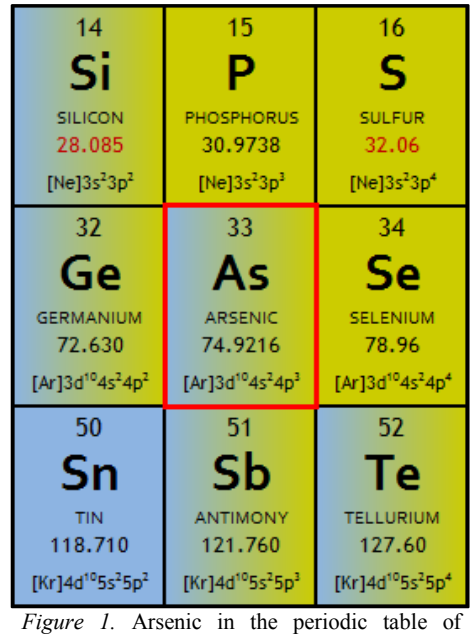

Figure 1. Arsenic in the periodic table of elements.

1.2 As in drinking water

Anthropogenic arsenic contamination of water exists particularly in connection with mining or historical industry sites but although severe, these are rather local phenomena. The widespread problem of arsenic in ground water with associated human health problems is mainly caused by geology (Smedley & Kinniburgh, 2002). A higher utilization of ground water releases substantial quantities of arsenic which might never have entered the biosphere if it was not for the drilling of new wells. The arsenic concentration is generally higher in ground water from drilled tube wells than from dug wells and the former collect ground water at larger depths than the latter. However, the quality of surface waters often has other shortcomings such as unhealthy microbiology, which is a reason why dug wells are being replaced with tube wells in the first place (Smith *et al.*, 2000).

Reductive dissolution of arsenic bearing iron minerals is one way ground water can be enriched in arsenic. Reducing conditions also increases arsenic mobility by reduction of the pentavalent arsenic form to the supposedly more mobile trivalent form (Smedley & Kinniburgh, 2002). This effect, as well as increased arsenic release at alkaline pH is further discussed in subsequent sections. Use of phosphorus fertilizers may worsen the problem as phosphate competes with arsenic species for adsorption sites on mineral surfaces,

although this is primarily a concern of soil above the bedrock. Phosphorus may also increase biological growth, and thereby facilitate mineral reduction (Acharyya *et al.*, 1999).

1.2.1 Global situation

Arsenic enriched ground water can be found in many parts of the world, although the situation is most thoroughly studied in Bangladesh and the Indian province West Bengal, both located in the Ganges delta. This is probably also where most people are affected and the concentrations are occasionally very high (Smith *et al.*, 2000). High ground water arsenic concentrations occur in large parts of the world, and other problematic regions include south western USA and Mexico, parts of Argentina and Chile, Romania and Hungary, northern China, Taiwan and Vietnam (Smedley & Kinniburgh, 2002). Even within a problematic region, there are huge differences and it is often not possible to estimate the arsenic concentration of one well based on known conditions of neighboring wells (Jakariya *et al.*, 2007).

1.2.2 Burkina Faso

Burkina Faso is a land locked country in western Africa, its territory having a long but sparsely studied prehistory. Burkina Faso faces substantial challenges, being an agriculturally based economy in a region haunted by recurring droughts - life expectancy as well as median age is low. There are however reasons for good hope about the Burkina future, as the country also have assets, most notably a growing middle class, peace and relative order. Another asset of Burkina Faso is gold ore. Unfortunately, arsenic prevalence is often correlated to the presence of gold, found in the bedrock of large parts of western Africa. The rural farming population north of the town Ouahigouya, Yatenga province, is particularly struck by arsenic enriched water, Figure 2 (Smedley *et al.*, 2007; Some *et al.*, 2012). Even while the geological causes differ from those in the Ganges delta, there are also similarities in the undertaken expansion of tube well drinking water to avoid the microbial hazards of dug wells. In this particular area, most of the arsenic enriched water contains arsenate rather than arsenite, although arsenic concentrations are often higher in wells with more reducing conditions (Smedley *et al.*, 2007). In the investigation by Smedley, the median arsenic concentration of 36 drilled wells in the Yatenga province was 17 µg/L, although a maximum concentration as high as 1630 µg/L was found. No precise measurements have been made, but it has been estimated that around 2 m^3 water per day is extracted from an average well. However, during the dry season this number become substantially higher as continuous pumping is performed for longer periods in order to provide water for farm ani-

Figure 2. Left panel: A girl pumping water from a well in the Lilgomdé village, north of Ouahigouya. Right panel: During dry season, water is also pumped into a special tray to water farm animals. The picture is taken towards the end of the rainy season.

mals such as goats and donkeys, Figure 2 right panel. It is not common but in a few rare installations in larger villages, water is pumped to an intermediate storage water tower located some meters above the ground, for subsequent use as tap water.

1.3 Biological aspects

Reasons why a compound is poisonous to humans are connected to reactivity and water solubility, but also to its abundance in the environment around us. Life has had a long time of evolution to adapt to compounds prevalent in the biosphere and these pose only moderate threats to the health of organisms even if they are reactive. The most convincing example is the oxygen molecule

which despite its reactivity (technically the reactivity of its radical derivatives) has shaped the world and the biosphere to what they are today (Lane, 2003). While arsenic is fairly prevalent in the bedrock, it has been too uncommon in the biosphere for most organisms to evolutionary prioritize a large scale-protection against it; some exceptions are mentioned in a subsequent section. The first documented statement that toxicity is a matter of dose was that of 16th century medical writer Paracelsus (Waddell, 2010), and today it is generally accepted that compounds may be toxic to harmless, or even beneficial, depending on the amount intaken.

Organoarsenic compounds have been and are still to some extent used to prevent diseases and promote growth in farm animals. A general understanding is that the observed growth enhancing effect of antibiotics is due to changes in the intestine microbial flora which promote a more efficient use of compounds in the feed (van den Bogaard & Stobberingh, 1999). A common feed additive is the antimicrobial growth promoter (AGP) 4-hydroxy-3-nitrobenzenearsonic acid (or Roxarsone), which possibly also act by chelating to metal ions present in detrimental concentrations (Czarnecki & Baker, 1984). After the withdrawal of Roxarsone from the American market, Nitarsone (or Histostat) is the most widely used arsenic containing AGP, and the primary purpose is prevention of the blackhead disease in chicken and turkey. No specific metabolic pathway requiring arsenic have been proven, which is a formal requirement for defining an element as essential (Ni Dhubhghaill & Sadler, 1991). Positive effects of arsenic based drugs for humans and animals are more likely due to their destructive behavior against certain undesired cells, may they be of cancer or microbial origin. Arsenite compounds may react with thiol containing proteins for the regulation of reactive oxygen species (ROS) and inhibiting them (Ralph, 2008). This is certainly not desirable for healthy cells, but in cancer treatment the effect in rapidly growing cells might weigh up the disadvantages.

Different schemes have been proposed for the arsenic detoxification process in humans, but there is some agreement that a first step is the reduction of arsenate to arsenite in the bloodstream (Tseng, 2009). During the detoxification process, oxidation state may be changed again (Tseng, 2009). If humans consume monomethylarsonic acid (MMA^V) and dimethylarsonic acid (DMA^V), they are excreted in more or less unchanged form, indicating that these are the preferred end products of arsenic metabolism (Tseng, 2009). This cannot be directly proven since arsenic metabolism is slow in humans, who excrete several arsenic species (Tseng, 2009). Differences in methylation capacity are large between individuals, positively correlated to young age, pregnancy and general health, while negatively correlated to smoking, alcohol and high arsenic intake (Tseng, 2009). Genetic differences are also thought to be rather

large (Tseng, 2009). Inorganic arsenite is thought to be transported into cells through aquaglycoporins intended for water and glycerol, while arsenate is likely to be transported by the phosphate transporter (Rossman, 2003).

Vegetables may take up arsenic from irrigation water, particularly accumulating it in the roots (Huq, 2006; Marin *et al.*, 1992; Smith *et al.*, 2008). Arsenate appears to be less accessible for plants than arsenite (Marin *et al.*, 1992). There seems to be a rather large difference in arsenic accumulation by different species of vegetables (Huq, 2006), possibly due to metabolic differences. An investigation of dairy animals have shown that arsenic can be found in the milk from an area with arsenic enriched water, and then mainly in the yet not metabolized inorganic form (Datta *et al.*, 2010). Arsenic concentrations in milk from an area with 47 µg As/L in the water were about 62% higher than in a control area with 15µg As/L in the water, although uncertainties were rather large. Arsenic concentrations in the straw fed to animals were approximately proportional to the differences in water concentration (Datta *et al.*, 2010). No signs of arsenic poisoning were noted in the cows (Datta *et al.*, 2010), possibly due to their shorter life span. Arsenic is accumulated in the hair of the animals or excreted through feces (Bera *et al.*, 2010; Datta *et al.*, 2010), but little is known about arsenic accumulation in meat through contamination of feed and water.

Goats are common farm animals in the affected villages of northern Burkina Faso, Figure 3. During the dry period they may drink water from the affected tube wells but it is yet not known to what extent arsenic is transferred to the milk or meat.

Figure 3. Goats are common farm animals in northern Burkina Faso.

1.3.1 Health problems

Skin lesions such as melanosis and keratosis are frequently observed in areas with high content of arsenic in the drinking water (Kapaj *et al.*, 2006), and due to their visibility they are the most easily detectable sign of chronic arsenic poisoning. The skin lesions have been linked to a high urinary arsenic content (Ahsan *et al.*, 2000), and there is also a correlation to cancer (Rahman *et al.*, 2003). Arsenic is known to cause cancer, especially in the skin, the lungs and the bladder (Kapaj *et al.*, 2006). It has been shown that time spans of several decades can pass between first exposure and cancer diagnosis (Bates *et al.*, 2004; Chiou *et al.*, 2001; Steinmaus *et al.*, 2003). Interestingly, consequences of high arsenic exposure is less severe in the USA than in developing countries, which could possibly be explained by nutritional status of the population (Rahman *et al.*, 2003; Rossman *et al.*, 2004), amount of UV radiation from the sun or genetic differences (Rossman *et al.*, 2004). The statistics about cancer related to arsenic intake is often better in industrialized countries than in developing countries, as an economically challenged population hesitate to, or does not have the opportunity to, undergo full medical examinations. (Rahman *et al.*, 2003). It has however been noted that people who die from cancer in the problematic regions often suffer from arsenic induced skin lesions in addition to the lethal disorder (Rahman *et al.*, 2003).

Many non-cancer effects have been noted (Kapaj *et al.*, 2006), including neurobehavioral and neuropsychological ones such as effects on memory and intellect (Calderón *et al.*, 2001; Tsai *et al.*, 2003; Wasserman *et al.*, 2004), reproductive effects (Milton *et al.*, 2005) and heart diseases (Lee *et al.*, 2002; Tseng *et al.*, 2003). Non-cancer effects have also been seen on the respiratory system (Guha Mazumder *et al.*, 2000; Milton & Rahman, 2002).

In the Yatenga province of northern Burkina Faso, urinary arsenic content was correlated to concentrations in tube wells. While 48% of the studied population was under 18 years old, only 10% of reported skin lesions were found in this group, consistent with symptoms evolving under a fairly long time. Arsenic was not detected in investigated vegetables, although these were primarily irrigated with surface water low in arsenic (Some *et al.*, 2012).

1.3.2 Paths of action

Mechanisms behind arsenic toxicity are not completely unraveled but one major route is the inhibition of enzymes. This occurs often, but not always, through the binding of thiol groups. The effect is thought to be worse for organic arsenic(III) compounds than for inorganic arsenite (Ni Dhubhghaill & Sadler, 1991). Organic arsenic compounds are still considered less poisonous as they do not enter cells with the same ease as inorganic ones (Tseng, 2009).

Arsenous acid shows toxicity either by binding to proteins, disruption of H-bonding in proteins or by reduction of other compounds (Ni Dhubhghaill & Sadler, 1991). Arsenic toxicity may also arise from the replacement of phosphate in molecules, for example causing diminished formation of adenosine triphosphate, ATP (Hughes *et al.*, 2011). Yet another path is increased production of reactive oxygen species, ROS (Hughes *et al.*, 2011), perhaps by inhibiting regulatory proteins (Ralph, 2008). Observed genotoxic effects of arsenic may be explained by ROS or by other oxidants (Rossman, 2003).

It has been observed that arsenite induced skin cancer arises mainly in the presence of UV-light, indicating that arsenite damages the DNA repair mechanism rather than being the origin of the cancer (Rossman *et al.*, 2004). This hypothesis also derives support from the fact that a synergistic effect has been observed between smoking and arsenic intake in the development of bladder and lung cancer (Ferreccio *et al.*, 2000; Steinmaus *et al.*, 2003).

1.3.3 Microorganisms and arsenic

It has recently been proposed that certain bacteria have the ability to incorporate arsenic into DNA instead of phosphate (Wolfe-Simon *et al.*, 2011), although even more recent papers cast very serious doubts onto this hypothesis (Elias *et al.*, 2012; Erb *et al.*, 2012; Reaves *et al.*, 2012). Undisputable, some microorganisms have an impressive ability to withstand high arsenic concentrations and occasionally species of microorganisms are involved in rather complex arsenic cycling (Oremland & Stolz, 2003).

A number of species is known to utilize arsenate in respiration, although all of them may exchange it for other electron acceptors such as sulphate or ferric compounds. These dissimilatory arsenate-reducing prokaryotes, or DARPs, can use a variety of simple organic *electron* donors such as lactate to gain energy (Oremland & Stolz, 2003). The chemolithotrophic arsenite oxidizers, CAOs, on the other hand use arsenite as a substrate in oxygen or nitrate respiration to produce energy for CO_2 fixation. Type reactions for both are shown below:

$$CH_3CH(OH)COO^- + 6\,H_2AsO_4^- + 7\,H_3O^+ \xrightarrow{\text{DARP}} 3\,CO_2 + 6\,As(OH)_3 + 10\,H_2O$$

$$2\,As(OH)_3 + O_2 + 2\,H_2O \xrightarrow{\text{CAO}} 2H_2AsO_4^- + 2\,H_3O^+ \qquad \text{(Eqs 1 and 2)}$$

Increased oxygen supply to the bedrock through tube well boreholes may increase microbial oxidation of reduced arsenic minerals such as realgar or orpiment (Oremland & Stolz, 2003). Reduction of arsenic bearing ferric minerals by iron(III) respirating microorganisms is another path of which microbiology contributes to the problem of arsenic in ground water (Herbel & Fendorf, 2005). Biogeochemical laboratory experiments have shown that somewhat

reducing conditions where arsenate and iron(III) reduction occurs without extensive release of iron(II), promote arsenic mobility (Herbel & Fendorf, 2006). It has been shown that arsenic(III) release is actually suppressed in the beginning of ferrihydrite reduction by iron respiring bacteria, and then increases and exceed abiotic controls (Tufano & Fendorf, 2008). This behavior was attributed to two consecutive phases: mineral transformation to magnetite, and dissolution, with arsenic(III) first being assimilated into the newly formed mineral in the first phase (Tufano & Fendorf, 2008). In the transformation of arsenic-bearing ferrihydrite to magnetite, arsenic(V) appears to be incorporated into the structure while arsenic(III) remain as surface complexes (Coker *et al.*, 2006). This difference has been suggested to be responsible for higher arsenic(III) mobility due to decrease in surface area and competition for surface sites (Coker *et al.*, 2006).

1.4 Remediation techniques

In large scale water plants, arsenite is frequently oxidized to arsenate prior to removal. Oxidation by oxygen from air is slow, and therefore oxidants such as ozone, chlorine, hypochlorite, chlorine dioxide, or hydrogen peroxide are added (Bissen & Frimmel, 2003). Following oxidation, arsenate is frequently co-precipitated with iron hydroxides or other coagulants and removed in fixed bed sand filters. Other methods such as anion exchange or reverse osmosis have also been applied (Bissen & Frimmel, 2003).

None of these methods are particularly suitable for the small scale of a well under the sometimes rough conditions found in rural communities of developing countries. In Bangladesh different small scale filters have been applied and one of the more known ones is the SONO filter (Hussam & Munir, 2007). In this device, arsenic enriched water is poured into a multilayer container where it is trickles through sand, a rusted iron matrix, brick chips and wood charcoal (for removal of organics)(Hussam & Munir, 2007). The filters have been applied on a scale of hundreds of thousands to a low cost and with good results. One draw-back is that it is working on household level and not applied at the source of the problem - the well. A high social acceptance is required for the inconvenience of a separate cleaning procedure. The household units are also fairly space-demanding and the material weighs about 57 kg per piece. Apart from inorganic approaches, organic material have also been used for arsenic cleaning (Fox *et al.*, 2012; Teixeira & Ciminelli, 2005), although these materials are more suitable for the cleaning of mine waste than for production of drinking water, as it is hard to control the microbial ecology thriving in this kind of matrix.

2 Background and concepts

In the beginning of this project a plan was developed, aiming at studying interactions between arsenic oxyacid species and water molecules in their vicinity. Water has the intriguing property of having a fair degree of order also in the liquid phase, deriving from its ability to create networks of hydrogen bonds between molecules. These networks can be disturbed or enhanced upon hydration of other species, depending on the strength with which such species interact with the solvent (Marcus, 2009). The goal was to study the effect from environmentally important arsenic oxyacid species but the weakly hydrated alkali metal ions appeared to require a visit to facilitate interpretations. The scope of the project changed somewhat during its implementation, moving from primarily fundamental research to emphasizing an analysis of how arsenic enriched water can be cleaned through adsorption.

A background is supplied in the subsequent sections, dealing with the chemical systems of interest as well as concepts such as hydration, adsorption and more. Previous work in this or closely related fields are briefly reviewed within this section.

2.1 Arsenic oxyacid systems

Compared to the multitude of phosphorus oxyacids described, the fauna of inorganic oxyacids of arsenic are rather straightforward (Greenwood & Earnshaw, 1997). Oxidation state +V is represented in aqueous solution by arsenic acid, H_3AsO_4, which can successively deprotonate until the arsenate ion, AsO_4^{3-}, remains. Oxidation state +III is represented by arsenous acid, $As(OH)_3$, which can deprotonate completely to the arsenite ion, AsO_3^{3-}. Arsenic is less keen than phosphorus to form bonds to atoms of the same element but such compounds certainly exist, such as realgar or As_4S_4. It has been proposed that solvated multinuclear units such as As_4O_6 or $As_3O_3(OH)_3$

can form in concentrated solutions of arsenous acid (Tossell, 1997), but if so the concentration is low compared to the one of the normal oxyacid species. Simple organic oxyacids in both oxidation states may result from biological activity.

2.1.1 Arsenic(V)

Arsenic acid, H_3AsO_4, is quite similar to phosphoric acid, H_3PO_4, both being triprotonic acids with a group 15 element in oxidation state +V, surrounded by four oxygen atoms in near tetrahedral arrangement. Infrared spectroscopy, IR, have shown that the tetrahedron can be substantially distorted upon partial deprotonation (Myneni *et al.*, 1998). Formally arsenic acid can be written $O=As(OH)_3$ in analogy with $O=P(OH)_3$ for phosphoric acid. The pK_a values are also rather similar between arsenic and phosphoric acid with pK_{a1} = 2.25, pK_{a2} = 7.05 and pK_{a3}= 11.58 for the former (Raposo *et al.*, 2002). This means that all protons can be dissociated in aqueous solution, which is illustrated in Figure 4, calculated with the equilibrium program Hydra-Medusa (Puigdomenech, 2004, 2009). It can be seen that in the pH range 6.5-8.5 relevant for drinking water (WHO, 2003), inorganic arsenic(V) occurs as either

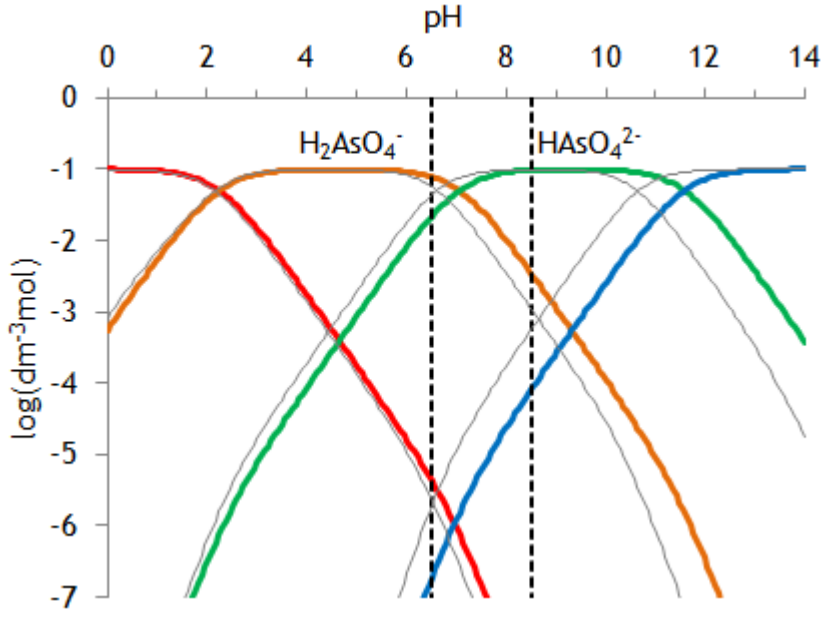

Figure 4. Logarithmic equilibrium diagram for the arsenic acid system at ionic strength I=0; H_3AsO_4 (red), $H_2AsO_4^-$ (orange), $HAsO_4^{2-}$ (green) and AsO_4^{3-} (blue). Corresponding lines when ionic strength is adjusted for the ionic concentration is given by thin grey lines, and the pH range relevant for drinking water is shown between dashed lines.

of the anionic species $H_2AsO_4^-$ or $HAsO_4^{2-}$ in aqueous solution. The difference between a hypothetical zero ionic strength and an ionic strength determined by the ionic content is also shown in Figure 4. Zero ionic strength is a fair approximation of ground water, while the lines for calculated ionic strength are more suitable for sample solutions around 0.1 mol dm^{-3}.

The intramolecular As-O distance has been reported as 1.69 Å by EXAFS spectroscopy for arsenate in solution (Manning *et al.*, 2002a) and a Quantum Mechanical Charge Field Molecular Dynamics, QMCF-MD, simulation have reported similar results (Bhattacharya *et al.*, 2007). EXAFS spectroscopy has also been used by several authors to study arsenate species adsorbed to mineral surfaces (Chakraborty *et al.*, 2011; Farquhar *et al.*, 2002; Fendorf *et al.*, 1997; Loring *et al.*, 2009; Manning *et al.*, 1998, 2002a; O'Reilly *et al.*, 2001; Waychunas *et al.*, 1993), as will be disucussed in subsequent sections.

2.1.2 Arsenic(III)

Unlike the anionic arsenate, arsenic in oxidation state +III remain as the fully protonated neutral arsenous acid, $As(OH)_3$, in the pH range relevant for drinking water (WHO, 2003), Figure 5. This very weak triprotonic acid has

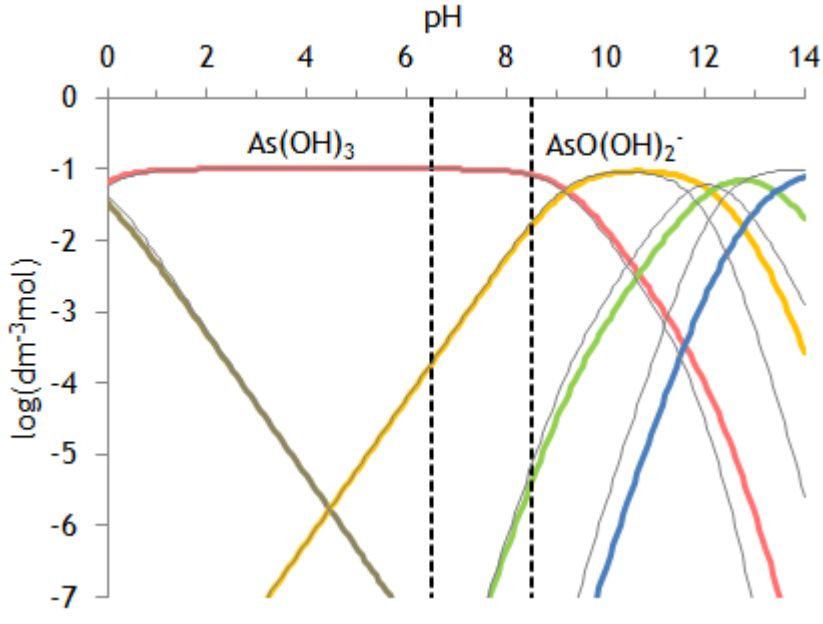

Figure 5. Logarithmic equilibrium diagram for the arsenous acid system at ionic strength I=0; $As(OH)_3$ (light red), $AsO(OH)_2^-$ (light orange), AsO_2OH^{2-} (light green) and AsO_3^{3-} (light blue blue). Corresponding lines when ionic strength is adjusted for the ionic concentration is given by thin grey lines, and the pH range relevant for drinking water is shown between dashed lines. The solid phase As_2O_3 precipitates at concentrations somewhat higher than shown here, below pK_{a1}.

pK_a values of pK_{a1}=9.25, pK_{a2}=12.13 and pK_{a3}=13.4 (Konopik & Leberl, 1949; Zakaznova-Herzog *et al.*, 2006). Arsenous acid and its derivative species are formed by the dissolution of arsenic(III) oxide, As_2O_3, or salts containing the linear meta-arsenite anion, $[AsO_2^-]_n$. Arsenous acid have only been detected in aqueous solution and it has not been isolated in pure form (Greenwood & Earnshaw, 1997).

Arsenous acid is a trigonal pyramidal molecule, distorted from planar configuration by a lone pair of electrons (Loehr & Plane, 1968). The old view of trivalent arsenic existing as AsO_2^- in aqueous solution have by now been abandoned by practically everyone, although exceptions exist (Chen *et al.*, 2004). It has been proposed that the $As(OH)_3$ molecule is hydrated mainly at the hydroxyl groups and that the lone pair of electrons is surrounded by a clathrate like structure (Hernández-Cobos *et al.*, 2010), similar to the recently described situation for the sulfite ion, SO_3^{2-} (Eklund *et al.*, 2012). This kind of hydration might be a reason why arsenous acid can pass through membrane proteins originally meant for the transportation of water, glycerol and urea (Hernández-Cobos *et al.*, 2010). A computer simulation of arsenous acid and its deprotonation species have predicted the following As-O distances: $As(OH)_3$ - 3 x 1.751; $AsO(OH)_2^-$ 2 x 1.814 Å + 1 x 1.645 Å; AsO_2OH^{2-} 1 x 1.964 Å + 2 x 1.684 $Å_{average}$; AsO_3^{3-} 3 x 1.746 Å (Tossell, 1997). This means that the average As-O distance follows as 1.751 Å for $As(OH)_3$; 1.758 Å for $AsO(OH)_2^-$; 1.777 Å for AsO_2OH^{2-}; and 1.746 Å for AsO_3^{3-}. The O-As-O angles are predicted at 97-99° (Tossell, 1997).

2.1.3 Organic arsenic oxyacids

Some of the most common organic arsenic compounds in nature are monomethylarsonic acid, MMA^V, dimethylarsonic acid, DMA^V, monomethylarsonous acid, MMA^{III} and dimethylarsonous acid, DMA^{III}. In these species one or two hydroxo groups have been replaced with methyl groups on the near tetrahedral arsenic acid or the trigonal pyramidal arsonous acid (Smith *et al.*, 2005b). All four species are involved in human arsenic detoxification metabolism, although there is not general agreement on the exact order they appear (Tseng, 2009). The only pK_a value of DMA^V is 6.2 while MMA^V have pK_{a1}= 3.6 and pK_{a2}=8.2 (Bowell, 1994). Sometimes DMA^V is referred to as cacodylic acid (Ni Dhubhghaill & Sadler, 1991). Almost all arsenic in ground water is in inorganic form, although if it is used to irrigate crops methabolic processes may transform it to the organic species mentioned (Huq, 2006).

2.1.4 Comparison of mobility, bioavailability and toxicity

The concepts of mobility, bioavailability and toxicity is interlinked and a comparison might not be straightforward as toxicity works with different mechanisms, bioavailability may differ from species to species and mobility is very dependent on environment. The following trends have been suggested with some degree of interpretation from this author.

Mobility ("Reluctance to adsorption")
DMA^V > MMA^V = As(V) (Zhang *et al.*, 2007)
As(III) >MMA^V = DMA^V >As(V) below pH 7 (Bowell, 1994)
MMA^V=DMA^V > As(III) > As(V) above pH 7 (Bowell, 1994)
As(III) > As(V) (Korte & Fernando, 1991)$_{ref}$(Sun & Doner, 1998)$_{ref}$

Bioavailability
As(III) > MMA^V >As(V) > DMA^V (rice) (Marin *et al.*, 1992)

Toxicity
As(III) > As(V) > organic species, (humans) (Hall, 2002)$_{ref}$
MMA^V > As(III) > As(V) > DMA^V (rice), (Marin *et al.*, 1992)

2.2 Orthotelluric acid

Orthotelluric acid, $Te(OH)_6$, share some important features with arsenous acid, in that it is a neutral oxyacid molecule over a wide pH range. As orthotelluric acid have a higher solubility than arsenous acid (Weast, 1975), the possibility to use it as a model compound for studying the hydration of such acidic hydroxyl groups can be considered. The hydration could be similar for these very weak acids, although arsenous acid has a lone pair of electrons which orthotelluric acid lacks.

Othotelluric acid is a much weaker oxyacid than those of the preceding group 16 elements in oxidation state +VI, H_2SO_4 and H_2SeO_4. Instead of forming tetrahedral units such as SO_4^{2-} and SeO_4^{2-} in aqueous solution, orthotelluric acid is an octahedral molecule. A first pK_a value is found at 7.70 and a second one at 11.0 (Ellison *et al.*, 1962).

The mean Te-O distance from nine reported crystal structures is 1.916 ± 0.004Å (Averbuch-Pouchot, 1988; Averbuch-Pouchot & Durif, 1989, 1990; Averbuch-Pouchot & Schulke, 1996; Cisarova *et al.*, 1995; Driess *et al.*, 2001; Ilczyszyn *et al.*, 1992; Qui *et al.*, 1984, 1987), this distance also confirmed by EXAFS on the solid phase (Levason *et al.*, 1994). The crystal structures have mean Te-O-H angles of 112°± 6° and mean O-H distances of

0.84±0.09 Å, although these are uncertain values due to the difficulties in identifying positions of hydrogen atoms. Orthotelluric acid in aqueous solution have previously been investigated by Large angle X-ray scattering, LAXS, which gave a mean Te-O bond distance of 1.935 Å and first hydration sphere consisting of 12 hydrogen bonded water molecules (Andersson *et al.*, 1981).

Other oxyacids of tellurium include poorly soluble tellurous acid, $(HO)_2TeO$, polymeric metatelluric acid, $(H_2TeO_4)_n$ for low numbers of n, and peroxymonotelluric acid H_2TeO_5, all reviewed by reference (Dutton & Cooper, 1966).

2.3 Alkali metal ions

Due to low charge density, the alkali metal ions from group 1 of the periodic table are rather weakly hydrated in aqueous solution. The ubiquitous sodium and potassium ions are involved in biological, geological and industrial processes on a huge scale. As both cations form rather soluble salts, they are frequently used as counter ions for desired anions. The solubility also explains their abundance in marine water. Lithium ions are increasingly used in the field of rechargeable batteries (Tarascon & Armand, 2001), but also in lithium stearates for grease production, lithium carbonate for glass and porcelain industry and as psychiatric pharmaceutics (Greenwood & Earnshaw, 1997). The amount of rubidium and cesium for industrial applications is very limited compared to the lighter alkali metal ions. Emitted radioactive cesium isotopes from nuclear industry and testing of nuclear weapons are partly responsible for an environmental problem (Avery, 1995).

The heaviest alkali metal francium does not exist in sufficient amounts to perform laboratory work out of the trace element scale - the half-life of the relevant isotope ^{223}Fr is only about 22 minutes (Audi *et al.*, 2003), and it has been estimated that 15 g of the element exists in total in the earth crust at any given moment due to a branch in the ^{235}U decay series (Greenwood & Earnshaw, 1997). Consequently, naturally occurring francium is found in uranium and thorium ores. Elements produced by fission may decay via the neptunium series in which ^{221}Fr is an intermediate with a half-life of 4.9 minutes (Audi *et al.*, 2003; Greenwood & Earnshaw, 1997).

2.4 Hydrogen bonding in liquid water

Water is an amazing solvent due to its ability to form hydrogen bonds, responsible for the high boiling point and surface tension compared to H_2S, H_2Se and H_2Te. In ice, a fully developed network of hydrogen bonds causes a

rather porous and open structure, as the negative dipole of the water molecules, the oxygen atoms, strive to point away from each other in a H-bond, O-H···O, Figure 6. While it is difficult to exactly determine the physical appearance of water hydrogen atoms, a consideration with oxygen atom radii of 1.34 Å (Beattie *et al.*, 1981) and intermolecular O-O distances averaging 2.75 Å (Fortes *et al.*, 2004) indicate that water hydrogen atoms are not very space demanding. This is shown in detail in appendix I. Crystal coordinates in Figure 6 is retrieved from (Fortes *et al.*, 2004).

Hydrogen bonds remain to a fair degree even in solution, causing the open structure of water to be preserved to some extent. Without hydrogen bonding, the density of water would be larger. A classic view of liquid water is to consider it a structure consisting of a finite number of hydrogen bonded water molecules mixed with non-hydrogen bonded molecules. Clusters of tetrahedrally bonded molecules exist within a matrix where most molecules are closer packed, and the amount of cluster molecules would increase upon cooling of the liquid (Nilsson & Pettersson, 2011). In another view, all bulk water molecules are considered to be involved in hydrogen bonding but to a continuously varying extent (Smith *et al.*, 2005a). This is in line with the fact that any definition of a hydrogen bond in terms of distances or O-(H)···O angles is arbitrary (Smith *et al.*, 2005a). An angle closer to 180° and a shorter distance constitute a stronger hydrogen bond. Positions of hydrogen atoms are hard to determine by experimental methods and hydrogen bonds are often referred to as the entire distance O-H···O.

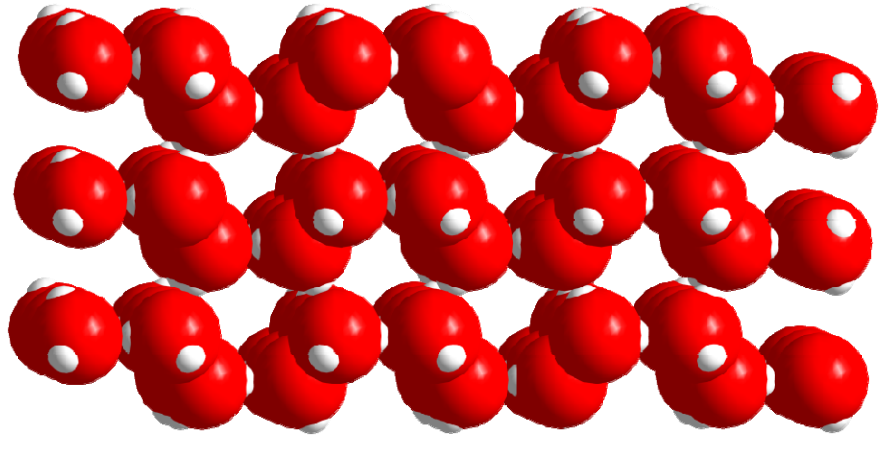

Figure 6. Three dimensional hydrogen bonded network of water molecules in hexagonal low-pressure ice (I_h). Proton ordering does not occur in this phase but possible disordered protons in the crystal structure of (Fortes *et al.*, 2004) have been manually removed for visual clarity.

2.5 Hydration of ions

The hydration of ions in aqueous solution is a process often overlooked by chemists, writing Fe^{2+} instead of the principally more correct $Fe(H_2O)_6^{2+}$ for a ferrous ion in water (Lundberg *et al.*, 2007b). The first coordination sphere in a complex represents the solvent molecules interacting directly with a central ion, in the case of water through ion-dipole interactions. Second and further coordination spheres can be seen as those water molecules interacting with previous coordination spheres, but here opinions differ about the exact definition. Scientists working with computer simulations may define many consecutive coordination spheres but the view adapted in this thesis is that second or third coordination spheres only exist if included water molecules are distinguishable from the bulk by spectroscopic or other experimental means.

Ion-pairs may be formed in electrolyte solutions although the extent of ion pairing is debated (Buchner & Hefter, 2009). While there are indications of ion-pairing even in solutions of weakly hydrated ions (Wachter *et al.*, 2005), the extent and strength of such interactions would be small and the effect on hydration studies presumably negligible.

Apart from the scientific importance from a fundamental point of view, applied scientists may also gain information from the hydration of ions. Working on a molecular level, the existence of hydration shells may be important in cell biology, regarding the passage of ions over cell membranes (Hernández-Cobos *et al.*, 2010), or it might affect capillary forces in plants or other biological systems.

2.5.1 Weak *vs.* strong hydration

Hydration of ions is not equally strong for all ionic species. Small highly charged ions - ions with a high charge density - are strongly hydrated and may have several coordination spheres (hydration shells), while those with low charge density do not. As a general observation, anions tend to be larger than cations due to a surplus of electrons, thus having lower charge density.

The exchange times of water molecules in the hydration shell of ions can sometimes be measured experimentally when they are sufficiently long, while it in other cases is necessary to rely on calculations (Helm & Merbach, 1999). Exchange time is related to charge density although not proportionally, as factors such as the presence of strong multiple hydration shells and valence d-orbital occupancy also matters (Helm & Merbach, 1999). Exchange times are very varying between different ions, spanning from 300 years in the first hydration shell of Ir^{3+} (Helm & Merbach, 1999), to just a few picoseconds for weakly hydrated ions such as Cs^+ or I^- (Rodnikova, 2003).

Heat of hydration is formally defined for the transfer of an ion from gas phase to aqueous solution, and this is always a strongly exothermic process (Persson, 2010). Upon dissolution of a salt this exothermic process occurs simultaneous with the breaking of ionic bonds which require energy. Also contributing is the breaking of hydrogen bonds and the formation of new ones. The resulting energy balance sometimes, as in the case of NaCl dissolution in water, turns out to be an endothermic process. With other salts, such as NaOH, considerable heat is released upon dissolution. It can be seen that the process of hydration differs in mode or strength between the chloride ion and the hydroxide ion. The fact that the dissolution of NaCl is spontaneous despite a positive enthalpy, can be explained by the entropy term ΔS in the relationship for Gibbs free energy, $\Delta G = \Delta H - T\Delta S$.

An alternative way to look at hydration strength is to consider how the process affects the structure of the solvent. The concept of structure makers and structure breakers have been introduced (Gurney, 1953), originally referring to ions or molecules causing increased and decreased viscosity in their vicinity. Definitions used today differ slightly and sometimes only effects on the environment outside the hydration shells are regarded (Marcus, 2009). Such a definition is clearly not compatible with the view in this thesis, that hydration shells are extra-ionic or extra-molecular layers of water molecules that can be distinguished from the bulk. A common denominator in the view of these concepts is that structure making ions increase hydrogen bonding within the solvent while the structure breakers decrease it, Figure 7.

Small highly charged ions such as multivalent metal ions are structure makers while large ions with a low charge density are structure breakers (Marcus, 2009). In addition to many metal ions, common anions such as OH^- and PO_4^{3-} can also be considered structure makers (Marcus, 2009). Examples of structure breakers include many anions but also the larger alkali metal ions (Marcus, 2009). It has been pointed out that the naming of the structure making/breaking concept is unfortunate in the sense that structure makers are in fact breaking the hydrogen bonds of the aqueous bulk in order to form new ones around themselves (Soper & Weckström, 2006).

A *Science* paper with the for solution chemists provocative title "Negligible effect of ions on the hydrogen bond structure in liquid water" (Omta *et al.*, 2003) contracted some criticism a few years ago (Marcus, 2009), but the substance of the paper is not completely consistent with the title. Instead it concludes that the effect on water structure is caused through molecules in the hydration shells of dissolved species. That said, experimental settings were not optimal for studying bulk water. Concentrations were so high that hydration

shells around ions were left incompletely filled, leaving no bulk water molecules to study.

Due to the strong dependence on charge density, the concept of structure makers and breakers show a high correlation to exchange times in the first hydration shell. Rodnikova uses this relationship and suggests by a modelling approach that a hypothetical univalent ion with a radius of 1.1 Å corresponds to the limit between positive and negative hydration (Rodnikova, 2003), that is structure making and breaking. Corresponding limit between negative hydration and hydrophobic hydration is set at 3.3 Å for a hypothetical univalent ion (Rodnikova, 2003). It was calculated that Li^+ and Na^+ had water exchange times of 1.60 and 1.12 times that of a bulk water molecule (8 ps), while water molecules in the hydration shells of the heavier alkali metal ions showed shorter exchange times than bulk water (Rodnikova, 2003). The sodium ion is considered a borderline ion in the structure maker/breaker context (Marcus, 2009).

The Hofmeister series, used by biochemists to predict effects from ions, show resemblance to the discussed structure making and breaking concept, with "kosmotropic" ions having a high charge density and "chaotropic" ions having a low one (Kunz, 2010). In this series however, ions are sorted after their effects, with kosmotrophs increasing surface tension and protein stability but decreasing the solubility of hydrocarbons. For chaotrophs the effects are opposite (Kunz, 2010).

Ionic diffusion rates in water (Li & Gregory, 1974) appear to coincide with the concept of weak and strong hydration to a large extent, where weakly hydrated ions move fast through the bulk.

2.5.2 Ionic radii and hydration numbers

There is no such thing as an atomic or ionic surface, and ionic or molecular particles are delimited only by the probability cloud of their filled orbitals. To assume that ions are hard spheres has however proved to be a fruitful approach at least when it comes to the ions classified as hard according to the Hard-Soft Acid-Base theory (Pearson, 1963). Anions with oxygen or fluorine would pass for such hard ions, as would most metal ions. Exceptions are univalent ions of transition or main group metals, noble metal ions, or ions of cadmium or mercury (Huheey *et al.*, 1993).

In this work, the structure regarding coordination number (hydration number for water) and ionic radii in solution are of principal interest. The direct measurement of coordination numbers is substantially more uncertain in solution than in a crystal but it is fortunately possible to predict them by comparing to the situation in solid phase. Linus Pauling was among the first to

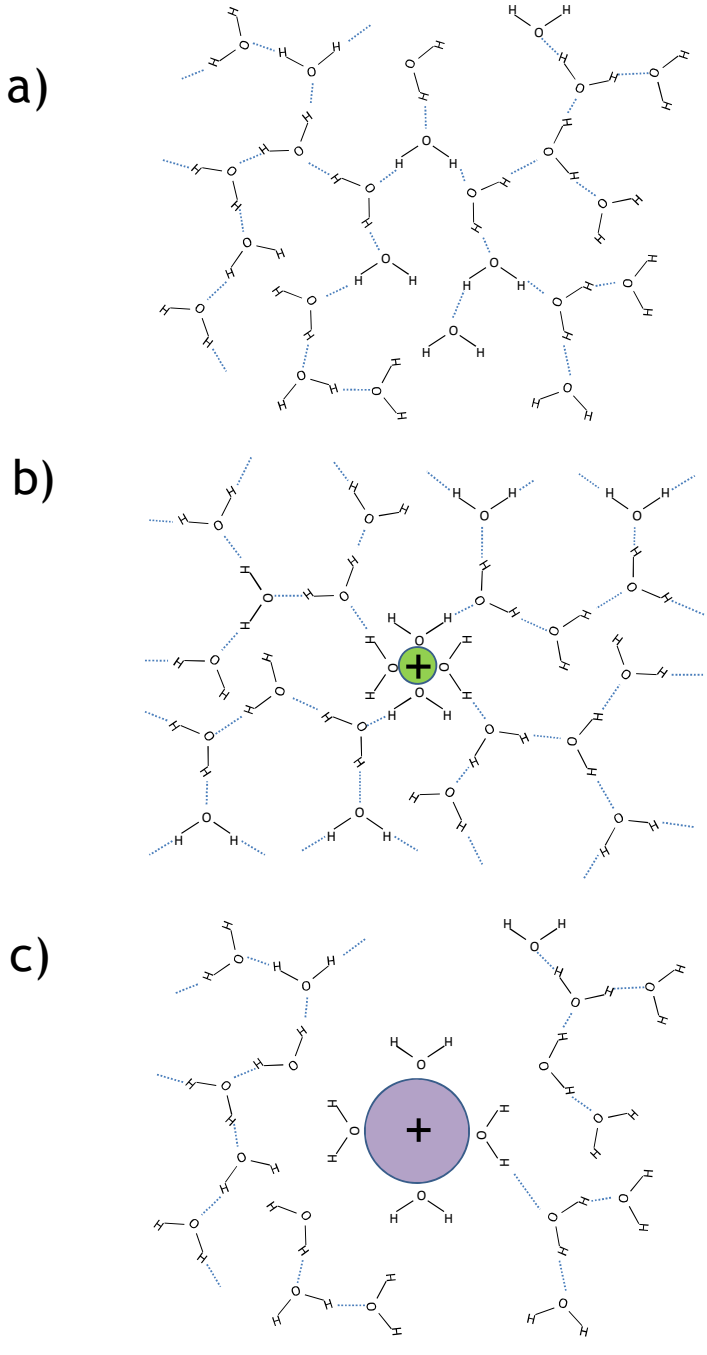

Figure 7. a) Schematic picture of bulk water structure. b) Schematic picture of the water structure around a structure maker. c) Schematic picture of the structure around a structure breaker. The ordering effects are exaggerated and the structure is shown only in two dimensions instead of 3D.

determine ionic radii on a larger scale but the modern holy article of ionic radii is Shannon's compilation "Revised Effective Ionic-Radii and Systematic studies of Interatomic distances in Halides and Chalcogenides" (Shannon, 1976), to a large extent based on earlier work (Shannon & Prewitt, 1969). Shannon pointed out that adding cationic and anionic radii reproduced interatomic distances well, as long as the correct coordination number is applied and covalence as well as geometrical distortion is negligible (Shannon, 1976). The 26271 citations of Shannon's article at the time of this writing - an impressive head start to the 19 citations for Paper I - is understandable considering that Shannon's work is used as the encyclopedia of ionic radii. It is however necessary to keep in mind that Shannon, being a crystallographer, was interested in the crystalline phase rather than solutions. The considered structures upon which he based the ionic radii were mostly oxide and fluoride based, showing high symmetry as such structures give the best crystallographic data. High symmetry is however correlated to high lattice energies, making obtained radii possibly unsuitable for representing the ion in a less ordered solution. Furthermore, Shannon used the Pauling ionic radius for the oxide ion, O^{2-}, which is 1.40 Å (Shannon, 1976). The radius of a neutral oxygen atom, such as the one in a water molecule, is 1.34 Å as shown in a work with different cesium alumns with crystal water (Beattie *et al.*, 1981). It is interesting to notice that Shannon suggests the same radius for 3-coordinated oxygen of hydroxide ions (Shannon, 1976), which could be considered equivalent to a water molecule interacting with one ion. That is, the water oxygen binds covalently in two directions to hydrogen atoms and electrostatically in one direction to the ion. Shannon also suggests 1.36 Å for the 3-coordinated oxide ion (Shannon, 1976). This is also close to the Beattie *et al.* value for water oxygen of 1.34 Å.

Considering crystals, a close-packing of spheres (e.g. anions) give tetrahedral as well as octahedral holes in its matrix. In these holes, smaller spheres (e.g. cations) may fit to give coordination numbers 4 and 6 respectively with a limiting radius ratio of r_{small}/r_{large} = 0.414 and r_{small}/r_{large} = 0.732 respectively (Huheey *et al.*, 1993). That is, if the cationic/anionic ratio is smaller than 0.414, a close-packed lattice of anions with cations in the tetrahedral holes would not be stable. Similarly, if the cationic/anionic ratio is smaller than 0.732, a close-packed lattice of anions with cations in the octahedral holes would not be stable. This radius ratio limiting rule can be geometrically deduced, knowing that anionic contact is avoided due to ligand-ligand repulsion (Huheey *et al.*, 1993).

It is difficult to determine hydration numbers or other coordination numbers in solution, as there is a very strong interdependence on the temperature or

Debye-Waller factor. It is simply not possible to refine coordination numbers at the same time as the temperature or Debye-Waller factor, and results regarding coordination numbers will often be nonsense. Yet this methodology has been used frequently, and therefore a wide range of coordination numbers has been suggested for ions in solution. Fortunately, recurring distances in the solution can often be determined with a fairly high certainty. Due to the very strong relationship between coordination number and interatomic distances (Shannon, 1976), it is possible to use the latter to deduce the most likely coordination number in solution. A solution being a dynamic system, it will contain a distribution of coordination number, although one should be considered the thermodynamically most stable one. The methodology have been used in several works of the Persson group, such as for alkali metal ions in Paper I, V^{3+}(Krakowiak *et al.*, 2012), Pb^{2+}(Persson *et al.*, 2011), lantanoids (Lundberg *et al.*, 2010), In^{3+} and Ga^{3+}(Topel *et al.*, 2010), Th^{4+}(Torapava *et al.*, 2009), Hg_2^{2+}(Rosdahl *et al.*, 2004), Zn^{2+} and Cd^{2+} (Lundberg *et al.*, 2007a), Fe^{2+} and Fe^{3+} (Lundberg *et al.*, 2007b), Sc^{3+} (Lindqvist-Reis *et al.*, 2006), Ni^{2+}(Kristiansson *et al.*, 2003), Cu^{+}, Ag^{+} and Au^{+} (Stålhandske *et al.*, 2001) and Bi^{3+} (Näslund *et al.*, 2000).

Some care must be taken when considering which crystal structures to be used in the comparison with results from aqueous solution. In order to avoid strong lattice effects, it is better to withdraw the radius of a neutral oxygen atom, 1.34 Å (Beattie *et al.*, 1981), from interatomic bond distances, than to use the radius for the oxide ion as in previous determinations (Shannon, 1976). One would expect the crystal structures of homoleptic hydrates to be the most reliable ones, and they can be used where such data exist. It has however been shown that the radius of the oxygen atom in a neutral compound is the same for most such compounds, including common oxygen donoring aprotic solvents such as dimethylsulfoxide, DMSO, and *N,N'*-Dimethylpropylenurea, DMPU (Lundberg *et al.*, 2010), where oxygen atoms are doubly bound. Cyclic ethers is an exception (Lundberg *et al.*, 2010), probably due to an unusual electronic configuration (Penczek *et al.*, 1980). It makes no sense to use heavily constraining ligands such as crown ethers, as it would be the ligand rather than inherent properties of the ion that would determine the size. Such a distorted complex would be an unsuitable representation of a species in solution. Homoleptic monodentate neutral oxygen donor ligands are however suitable, and this requirement often means hydrates or other solvates of small molecules.

Interatomic distances and hydration numbers for alkali metal ions

Authors attempting to determine Li-O distances for the lithium ion in aqueous solution by X-ray diffraction methods propose distances of 1.98 Å (Bouazizi & Nasr, 2007) to 2.17 Å (Palinkas *et al.*, 1980). As X-rays are diffracted by electrons, and Li^+ has only two, this method is far from optimal to study this very light atom. Attempts being made in the Persson group only gave very disputable results, heavily dependent on assumptions in the refinement. A Li-O distance of 1.90 Å was obtained from a neutron scattering study (Ohtomo & Arakawa, 1979). Simulation methods in which quantum-mechanics are calculated *ab inito* without prior preconceptions are the most scientifically sound of computer based methods. One such investigation suggests a Li-O distance of 1.95 Å (Loeffler & Rode, 2002). Other computer simulations have proposed distances such as 1.97 Å (Bouazizi & Nasr, 2007; Rudolph *et al.*, 1995) or 2.03 Å (Du *et al.*, 2007). The most probable hydration number is four (Loeffler & Rode, 2002; Novikov *et al.*, 1999; Ohtomo & Arakawa, 1979; Palinkas *et al.*, 1980). Smirnov and Trostin have reviewed a number of articles on lithium ion hydration and some authors suggest coordination number six (Smirnov & Trostin, 2006). Investigations of crystal structures show that lithium hydrates tend to crystallize with either four water molecules in tetrahedral fashion in the hydration shell or with six water molecules in repeating chains of shared water molecules. Available crystal structures of lithium hydrates will be further discussed in connection with obtained results.

Intermolecular Na-O distance of the sodium ion in aqueous solution have been experimentally suggested in a wide range, such as 2.34 Å (Mancinelli *et al.*, 2007), 2.40 Å (Maeda & Ohtaki, 1975), 2.42 Å (Palinkas *et al.*, 1980) and 2.50 (Ohtomo & Arakawa, 1980). An *ab initio* quantum mechanical simulation has suggested this distance to 2.34/2.36 Å (Azam *et al.*, 2009) and other computer simulations have reported similar values (Tongraar *et al.*, 1998), (Heinje *et al.*, 1987). Hydration numbers have been suggested in the range of 4 to 8 (Azam *et al.*, 2009; Bosi *et al.*, 1984; Chizhik *et al.*, 1987; Heinje *et al.*, 1987; Maeda & Ohtaki, 1975; Mancinelli *et al.*, 2007; Ohtaki & Fukushima, 1992; Ohtomo & Arakawa, 1980; Tongraar *et al.*, 1998). Investigations of sodium ion hydration have been reviewed by (Smirnov & Trostin, 2007a). The anhydrous sodium ion frequently crystallizes with small and symmetric counter ions, while full hydration shells seem to form solely with larger and less symmetric counter ions, (Paper I; Allen, 2002; *Inorganic Crystal Structure Database*, 2009). The crystallization often occurs as six-coordinated sodium ions in $[Na_2(H_2O)_{10}]^{2+}$ units, never observed in solution.

Experimental values of the interatomic K-O distance for the potassium ion in aqueous solution can be found in the range 2.65-2.97 Å (Mancinelli *et al.*,

2007; Nikologorskaya *et al.*, 2000; Ohtaki & Fukushima, 1992; Ohtomo & Arakawa, 1980; Palinkas *et al.*, 1980; Soper & Weckström, 2006) and *ab initio* quantum mechanical simulations suggest 2.80 Å (Azam *et al.*, 2009; Tongraar *et al.*, 1998). Hydration numbers in aqueous solution are suggested from 3.4 to 8.3 (Azam *et al.*, 2009; Mancinelli *et al.*, 2007; Ohtaki & Fukushima, 1992; Soper & Weckstrom, 2006; Tongraar *et al.*, 1998). Due to its low charge density, potassium does not crystallize with well-defined hydration shells, nor does it form other relevant (as defined before) solvates in the crystal phase. A number of tetrahydrofuran, THF, solvate structures may constitute a possible exception, although this kind of small cyclic ethers may not be fully representative for other neutral oxygen containing compounds (Lundberg *et al.*, 2010).

The rubidium ion has previously been investigated in the Persson group, in a combined LAXS and EXAFS study (D'Angelo & Persson, 2004). It was found that the Rb-O bond interatomic distance was 2.98 Å, which can be compared with other experimental results in the range 2.83-3.05 (Kubozono *et al.*, 1994; Ohkubo *et al.*, 2002; Ramos *et al.*, 2000). A computer simulation with a quantum mechanical approach suggested 2.95 Å (Hofer *et al.*, 2005) while another one suggested 2.9 Å (San-Román *et al.*, 2009). Reported hydration numbers in aqueous solution stretches from six to eight, where the two mentioned computer simulations are close to 7. The rubidium ion does not crystallize with any well-defined hydration shell, or with well-defined solvation shells of other neutral O-donor ligands (Paper I; Allen, 2002; *Inorganic Crystal Structure Database*, 2009).

Experimentally determined interatomic Cs-O distances in aqueous solutions of Cs^+ ranges from 2.95 Å to 3.21 Å (Ohtaki & Fukushima, 1992; Ohtomo & Arakawa, 1979; Palinkas *et al.*, 1980; Tamura *et al.*, 1987). The value 2.95 Å from reference (Ohtomo & Arakawa, 1979) has been misquoted in reviews (Smirnov & Trostin, 2007b; Vinogradov *et al.*, 2003). A computer simulation with a quantum mechanical approach suggests Cs-O distances of 3.20-3.30 Å (Schwenk *et al.*, 2004) while another computer simulation obtained 3.1 Å (Mile *et al.*, 2009). Suggested coordination numbers range from 6.5 to 9 (Chizhik *et al.*, 1987; Mile *et al.*, 2009; Novikov *et al.*, 1999; Ohtomo & Arakawa, 1979; Schwenk *et al.*, 2004) with deviating values at 2.3-5.3 (Ohtaki & Fukushima, 1992). Smirnov and Trostin have reviewed hydration studies of cesium ions in solution (Smirnov & Trostin, 2007b). As in the case with rubidium, cesium does not crystallize surrounded solely by water molecules. Neither does it form other crystalline solvates where it is surrounded solely by neutral oxygen donating ligands. In the structures by (Beattie *et al.*, 1981)

previously mentioned, the cesium atom is surrounded by six water molecules and two sulfate ions, the latter coordinating with three oxygen atoms each.

Structural work has not been performed with francium ions, as the element is not available in sufficient amounts. The ionic radii of the francium ion is listed as 1.80 Å by Shannon (Shannon, 1976), who refer to an earlier listing by Ahrens (Ahrens, 1952). The conclusion was reached after assuming that ionic radii for the period Fr^{+}, Ra^{2+} etc as a function of charge had the same shape as the period Rb^{+}, Sr^{2+} , Y^{3+}, Zr^{4+} etc. but with an offset. Ahrens had access to ionic radii for the latter period, as well as for Ra^{2+} (Ahrens, 1952).

Shannon's value for six-coordinated sodium

As it will turn out, the ionic radius obtained in this work for six-coordinated sodium deviates from that of Shannon (Shannon, 1976), and this require a deeper analysis of his paper. The listing of the six-coordinated sodium radius as 1.02 Å on page 753 is based on ten structures: $Na_4Sn_2Ge_4O_{12}(OH)_4$, $NaC_6O_7H_7$, $NaB(OH)_4.2H_2O$, NaUacetate, Na_2WO_4, $Na_2Al_2Si_3O_{10}.2H_2O$, $NaClO_3$, $(NaAsO_3)_x$, $NaSbF_4$ and $Na_2CO_3.H_2O$. These structures would not be approved in this work, as they contain strongly polarizing cations, anionic ligands and is very diverse in general. Shannon does notice the non-linearity in the relationship between different sodium coordination numbers but rather point out that the radii does not decrease as much as one would expect below CN=6. This reasoning is equivalent for the potassium ion below CN=7.

On page 761, Shannon lists 11 crystal structures containing sodium atoms with six ligands in octahedral configuration. They are the first five out of ten structures listed above, and in addtion also $Na_4P_2O_7.10H_2O$, $Na_4P_4O_{12}.4H_2O$ $NaAl(SO_4)_2.12H_2O$, $Na_2B_4O_6(OH)_2.3H_2O$, $C_{10}H_{13}N_5NaO_6P.6H_2O$ and $NaHCO_3$. By subtracting a value of 1.35-1.38 for the ligand atom radius, from the Na-ligand distance, a sodium radius of 1.05 Å was obtained, which is closer to the value deduced in Paper I. It is unclear why the value of 1.02 Å from the first ten structures was chosen for the listing at page 753, and not the value obtained from the last 11 structures.

Neither would the last structures pass the requirements of this work, although the structure $Na_4P_2O_7.10H_2O$ is closer than the others. In this structure one sodium ion is surrounded by 4 neutral water oxygens and two oxygen atoms from two different $P_2O_7^{4-}$ ions (Cruickshank, 1964). By subtracting the water oxygen radius of 1.34 Å (Beattie *et al.*, 1981) from the average distances of the neutral oxygens 2.41 Å, a sodium radius of 1.07 Å is obtained, identical to that of ours (Paper I). The other sodium ion in this structure has a distorted hydration shell with very different bond lengths (Cruickshank, 1964).

2.6 Ferrihydrite and other iron oxyhydroxides

Iron as an element is very prevalent on earth and a number of solid oxides and hydroxides can be formed. These iron oxyhydroxides are important in geology, soil science, corrosion science and industry, but also play a role in many microbial systems (Schwertmann & Cornell, 2000). The various iron oxyhydroxides and their interconversions are thoroughly described in a book by Schwertmann and Cornell (Schwertmann & Cornell, 2000), and only a partial summary is given here. The iron(III) ion is stable in aqueous solution only under very acidic conditions. The first iron oxyhydroxide to form upon pH increase is ferrihydrite, with the approximate formula $Fe_5HO_8.4H_2O$, while high pH and gentle heat treatment promote the formation of the more stable goethite, α-FeOOH. Akaganetie, β-FeOOH, can be formed in the presence of chloride ions (Schwertmann & Cornell, 2000). Perhaps β-FeO(OH,Cl) would be a more appropriate formula as the presence of chloride ions in this structure is required, and it breaks down upon their complete removal (Schwertmann & Cornell, 2000). Lepidocrocite, γ-FeOOH, can be formed via an oxidation/hydrolysis process from Fe^{2+}. Upon dehydration and thermal transformation, all these species may form hematite, α-Fe_2O_3. Other major iron oxides to mention are maghemite, γ-Fe_2O_3, and the iron(II,III) mineral magnetite, Fe_3O_4 (Schwertmann & Cornell, 2000).

The iron oxyhydroxide used in this work has mainly been ferrihydrite as it has a less well defined crystal structure (Schwertmann & Cornell, 2000), which often promote adsorption properties (Pierce & Moore, 1982). Ferrihydrite particles in freshly formed suspensions are very small and thus have large surface area per weight. While this is advantageous in batch experiments, it poses some difficulties when using the mineral as a column adsorbent. Two forms of ferrihydrite, 2-line, and 6-line, can be distinguished by powder diffraction, and the former is somewhat less structurally ordered. The microcrystalline structure of ferrihydrite has been studied by (Jansen *et al.*, 2002). Ferrihydrite is formed in natural environments where iron(II) is oxidized rapidly or in the presence of crystallization inhibitors (Schwertmann & Cornell, 2000). Crystallinity increases with time and ferrihydrite turns into goethite and other stable minerals by a dissolution/reprecipitation process. This process may take years but can be accellerated for example in the presence of organic reducing agents. The transformation can be retarded by organic matter, phosphate or silicate species (Schwertmann & Cornell, 2000). It has also been noted that the presence of arsenic suppress mineral transformation (Tufano & Fendorf, 2008). The pH value at which postive and negative charges on a surface counterbalance each other, pH_{pzc}, is high for iron oxyhydroxides. For ferrihydrite the value is somewhere around 8.1 (Dzombak & Morel, 1990;

Gustafsson, 2003). This aids ferrihydrite in the adsorption of anionic species around neutral pH, and the material is a promising adsorbent material. It should be noted that the surface charge of ferrihydrite decreases upon adsorption of arsenic oxyacid species, as has been thoroughly investigated before (Jain *et al.*, 1999).

2.7 Iron oxyhydroxide coated particles

As iron oxyhydroxide suspensions consists of very fine particles, it is not possible to use the material in columns, which would immediately clog. It is however possible to coat sand particles by treating them with such a suspension (Schwertmann & Cornell, 2000). More iron oxyhydroxide is attached to the grains with increasing pH until pH_{pzc} is reached but then drops sharply. A more homogenous coating distribution is obtained at somewhat lower pH (Schwertmann & Cornell, 2000). A moderate ionic strength of about ≈ 0.01 mol·dm^{-3} gives a good result for the process. A higher suspension concentration as well as temperature may affect the outcome of the coating process (Schwertmann & Cornell, 2000). Alternative pathways of iron oxyhydroxide coating are a dry contact method, as well as a method where iron hydroxide mineral is precipitated in the presence of sand (Khare *et al.*, 2008). The wet contact method described above seems to be most efficient for ferrihydrite (Khare *et al.*, 2008). It is possible to dope filter sand with impurities such as silicon, phosphorus and calcium to suppress recrystallization to goethite, and presence of manganese dioxide may aid oxidation of arsenite (Jessen *et al.*, 2005). The iron content of coatings has been reported in the range of 3-15 mg·g^{-1} (Herbel & Fendorf, 2006; Khare *et al.*, 2008; Schwertmann & Cornell, 2000; Thirunavukkarasu *et al.*, 2003b; Tufano & Fendorf, 2008; Vaishya & Gupta, 2003).

2.8 Granular ferric hydroxide

An iron oxyhydroxide based adsorbent is produced by the company GEH Wasserchemie GmbH & Co under the name granular ferric hydroxide, GFH®, or Granuliertes Eisen Hydroxid, GEH®. This material is used in municipal drinking water plants for arsenic removal and its properties have been studied in several studies (Badruzzaman *et al.*, 2004; Banerjee *et al.*, 2008; Driehaus *et al.*, 1998; Guan *et al.*, 2008; Saha *et al.*, 2005; Sperlich *et al.*, 2005; Thirunavukkarasu *et al.*, 2003a; Westerhoff *et al.*, 2005). The material is said to consist of low crystalline akaganeite - that is β-FeOOH with chloride ions incorporated in the structure. It has been shown to adsorb almost as much

arsenate as freshly prepared ferrihydrite (Driehaus *et al.*, 1998). The removal of other oxyanions is also feasible (Asgari *et al.*, 2008).
GFH® contains a significant amount of mesa-porosity with pore sizes around 20-95 Å and the internal surfaces may be more negatively charged than the external ones (Saha *et al.*, 2005). The BET specific surface was determined to 551 m^2g^{-1} in the same study. The material cost is high per mass unit but this is compensated by the high adsorption capacity. The material cost per gram of adsorbed arsenic is similar to other arsenic adsorbents (Kumar *et al.*, 2008).

2.9 Adsorption

The process in which an ion or molecule is adhered to a surface is known as adsorption, not to be confused with absorption. The potential species to be adsorbed is known as the adsorptive, while the surface material is the adsorbent. An already adsorbed species is called the adsorbate. The reverse adsorption process is known as desorption. Monolayers are formed upon adsorption, and the process is not to be confused with surface precipitation, in which a new material precipitates in a three-dimensional layer-by-layer structure. The broader term sorption can be used to include both adsorption and surface precipitation (Davis & Kent, 1990). Adsorption may occur as inner-sphere surface complexes by the formation of covalent bonds between the adsorptive and the surface, Figure 8. The adsorbate will then be embedded into

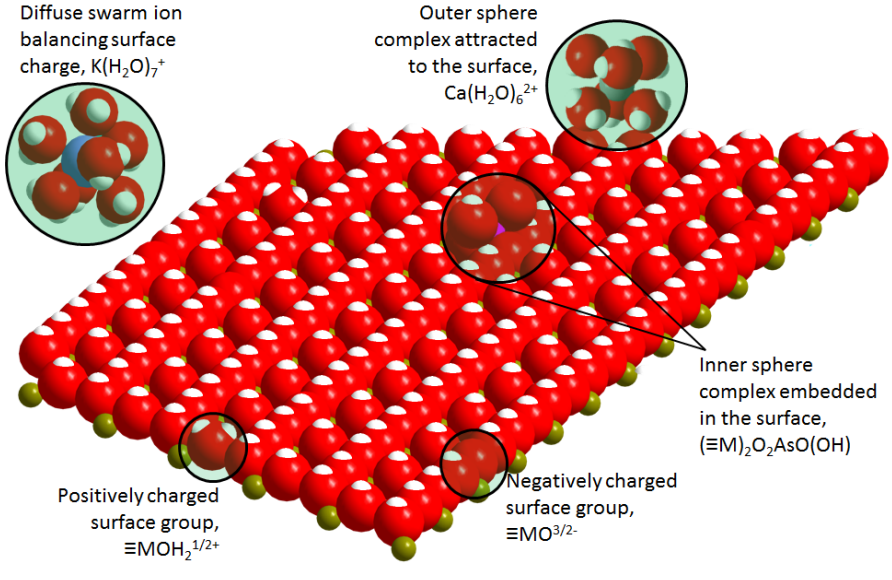

Figure 8. Schematic illustration of a mineral surface.

the mineral surface. Outer sphere complexes may be formed by electrostatic interactions between the adsorbed species and a charged surface (Stumm, 1992). Formation of outer sphere complexes often shows a high correlation to the ionic strength (Stumm, 1992). Ions not directly interacting with the surface but required for the charge balance, is said to be in the diffuse swarm, also Figure 8. Several layers of solvent molecules may separate them from the surface. The entire zone outside the formed inner-sphere complexes is known as the Helmholz layer.

2.9.1 The classical 2 p*K* model

In the classical 2 p*K* model, the charges of a surface are treated as point charges. The surface groups of a mineral in aqueous solution that show affinity for adsorption are considered to be neutral ≡MOH, negatively charged $\equiv MO^-$ or positively charged $\equiv MOH_2^+$ (Stumm, 1992). The pH at the point of zero charge, pH_{pzc}, is defined as the pH where the amount of positive and negative charges on the surface is the same, resulting in a neutral surface on average. Below pH_{pzc}, the surface will be positively charged and above it will be negatively charged. For a particular mineral, pH_{pzc} will be located exactly in between the minerals' pK_{a1} and pK_{a2}. These two refers to the equilibria where $\equiv MOH_2^+$ and ≡MOH are deprotonated (Stumm, 1992), that is the pH values when $\{\equiv MOH_2^+\}=\{\equiv MOH\}$ and $\{\equiv MOH\}=\{\equiv MO^-\}$ respectively. The classical 2 p*K* model is simple and illustrates adsorption in a convincing way. It does however have limitations and new models have been developed to confront discrepancies between measured and calculated surface charge (Hiemstra & van Riemsdijk, 1996).

2.9.2 The charge distribution model

That the classical 2 p*K* model is a simplification can be grasped by imaging a metal oxide Me_2O_3 (for example hematite Fe_2O_3) in which all metal ions are surrounded by six oxygen atoms and each oxygen atom is surrounded by four iron atoms. In the bulk of this material the +3 charge of the iron atom must be neutralized from six directions with -½ from each direction. At a surface where one of the oxygen atoms is missing, the iron atom would have a remaining positive charge of +½. This implies that the above mentioned surface groups for such a mineral would rather be written $\equiv MOH^{1/2-}$, $\equiv MO^{3/2-}$ and $\equiv MOH_2^{1/2+}$ respectively. Iron atoms of ferrihydrite and goethite are also surrounded by six oxygen atoms, which imply the same charges of these surface groups.

A full description of the charge distribution model can be found in reference (Hiemstra & van Riemsdijk, 1996), in which the charge localization of surface complexes is also discussed. It is convincingly argued that there are two

sometimes opposing incentives for the adsorbate to distribute its charge. The incentive for (1) an even charge distribution around the central atom of the adsorbate can be counteracted by an incentive for (2) charge neutralization of the previous surface interface (Hiemstra & van Riemsdijk, 1996). The authors propose that the true situation is often an intermediate where part of the excess charge is left at the mineral oriented ligands in the oxygen link between a surface metal atom and the adsorbate central atom, while part is transferred to the new surface (the solution oriented ligands of the adsorbate). Calculations regarding surface structures of As(III) and As(V) on goethite have been performed and results will be further mentioned in the subsequent section (Stachowicz *et al.*, 2006).

2.10 Surface structures

Inner sphere complexes between a surface and an anionic multiatomic adsorbate may be either monodentate or bidentate, depending on whether the adsorbate binds with one or two atoms. It may be either mononuclear or binuclear, depending on whether it interacts with one or two metal ions, Figure 9.

Arsenic(V) species form inner-sphere complexes, covalently embedded into the surface (Farquhar *et al.*, 2002; Goldberg & Johnston, 2001; Mamindy-Pajany *et al.*, 2009; Manning *et al.*, 2002b; Partey *et al.*, 2009) and this is lik-

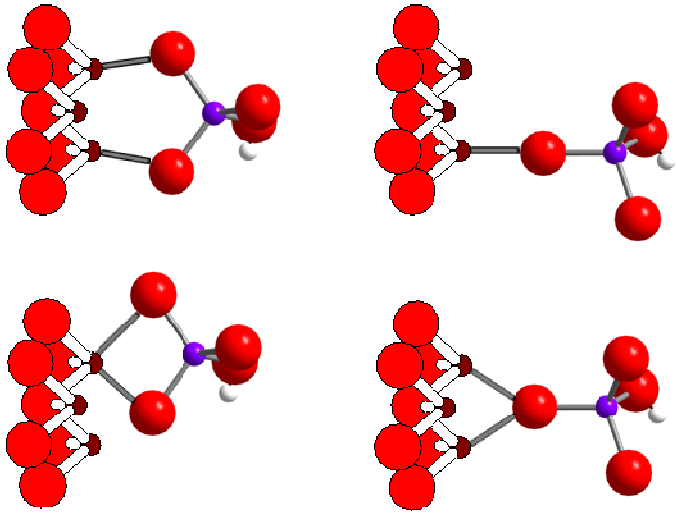

Figure 9. Different adsorption possibilities, inspired by reference (Zhang *et al.*, 2007). Upper left: bidentate, binuclear. Upper right: monodentate, mononuclear. Lower left: bidentate, mononuclear. Lower right: monodentate binuclear. Iron atoms do not face the solution as depicted, but instead the outermost layer consists of oxygen surface grooups and surface complexes as shown in Figure 8. These are not shown in this Figure for clarity reasons.

ely also true for arsenite (Bhandari *et al.*, 2011; Farquhar *et al.*, 2002; Manning & Goldberg, 1997; Partey *et al.*, 2009). The alternative adsorption mechanism for the neutral $As(OH)_3$ molecule would be weak electrostatic interactions, but the molecule is rather weakly hydrated. It would be possible that the fraction of arsenic(III) that occurs as the $AsO(OH)_2^-$ anion in the pH range of drinking water, Figure 5, could form outer sphere complexes. It is believed that arsenate forms mainly bidentate complexes which are either mononuclear or binuclear (Arai *et al.*, 2004; Farrell *et al.*, 2001; Manceau, 1995; Manning *et al.*, 2002a, 2002b; O'Reilly *et al.*, 2001; Sherman & Randall, 2003; Sun & Doner, 1996; Waychunas *et al.*, 1996). The hypothesis of bidentate arsenate surface complexes have been challenged by showing that a short metal-arsenic distance is insufficient proof for bidentate binding (Loring *et al.*, 2009). Arsenic(III) species have been suggested to form either bidentate mononuclear (Chakraborty *et al.*, 2011; Manning *et al.*, 1998, 2002b; Sun & Doner, 1996) or bidentate binuclear surface complexes. The previously mentioned study on surface charge and H_3O^+/OH^- stoichiometry indicate that several different arsenic surface complexes may exist (Jain *et al.*, 1999), and over-generalization is best avoided.

The charge distribution model have been applied for arsenic(III) and arsenic(V) complexes with a goethite surface (Stachowicz *et al.*, 2006). It was indicated that arsenic(III) mainly form bidentate surface complexes in which excess positive charge were directed towards the surface. For arsenic(V), a non-protonated bidentate complex and a protonated monodentate were found.

2.11 Column technology

Studying adsorption by batch experiments with suspensions is fairly quick and as the suspensions are homogenous, a high experimental repeatability can be obtained. There is however a disadvantage, as it cannot easily be determined whether an ion or molecule is strongly adsorbed or just show a slight preference of adsorption compared to solvation. From an applied point of view, batch experiments are poorly representative for the events taking place in a real decontamination plant, as suspensions of fine particles cannot be used in the latter situation. To study adsorption under more practical conditions, it is necessary to use columns packed with adsorbent. By comparing the adsorptive load before column break-through occurs, it is also possible to gain insight in the relative surface affinity of different species. To avoid clogging of the column, a length of five times the diameter has been recommended (Nikolaidis *et al.*, 2003).

For a particular material, a permeability coefficient B can be calculated (Coulson *et al.*, 1991).

$$u_c = B \cdot \frac{-\Delta P}{\mu \cdot h} \qquad \text{(Eq. 3)}$$

Parameters are the superficial velocity u_c ($m \cdot s^{-1}$), pressure loss $-\Delta P$ (Pa), viscosity μ ($kg \cdot m^{-1}s^{-1}$) and column height h (m). The superficial velocity is the velocity a liquid *seems to have* through a column cross area (m^3s^{-1} / m^2), as opposed to the pore velocity which require detailed knowledge (or assumptions) about the intra-material channels. The equation is valid under laminar flow (Coulson *et al.*, 1991) with a Reynolds number < 10 for flow through a bed of particles (Rhodes, 2008). Calculation of Reynolds number through beds of particles is further discussed in the supplementary material for Paper III.

Information about the permeability coefficient could be useful in estimating pressure loss in a larger column, even though up-scaling of adsorption columns is not completely straightforward. Westerhoff *et al*. studied upscaling of columns from a particle size point of view (Westerhoff *et al.*, 2005).

2.12 Adsorption of arsenic species to iron oxyhydroxides

There have been several studies of arsenite and arsenate adsorption onto iron minerals, as shown in Table 1. Most studies involved batch experiments but some used columns or sand filters (Benjamin *et al.*, 1996; Guo *et al.*, 2007; Herbel & Fendorf, 2006; Jessen *et al.*, 2005; Kocar *et al.*, 2010; Nikolaidis *et al.*, 2003; Thirunavukkarasu *et al.*, 2003a, 2003b; Tufano & Fendorf, 2008). Studies on the adsorption of organic arsenic species show that MMA^V and DMA^V are not adsorbed as efficiently as inorganic arsenate (Bowell, 1994).

2.12.1 Arsenic adsorption and pH

A mineral is net positively charged in water below its pH_{pzc}, thereby facilitating the attraction of negatively charged species. Therefore adsorption of the anionic arsenic(V) species increases with decreasing pH (Carabante *et al.*, 2009; Goldberg & Johnston, 2001; Grafe *et al.*, 2001; Partey *et al.*, 2008; Pierce & Moore, 1982; Su & Puls, 2008). As pH increases above the pH_{pzc}, the net charge of the surface become negative and adsorption is obstructed but not prevented. Arsenic(V) species are desorbed upon pH increase, and the desorption is faster and more efficient with increasing pH (Carabante *et al.*, 2009). Arsenic(III), mainly existing as the neutral $As(OH)_3$ molecule in the pH

range of interest, have a broad adsorption maximum around neutral pH or slightly above (Bowell, 1994; Grafe *et al.*, 2001; Partey *et al.*, 2008, 2009; Pierce & Moore, 1982; Su & Puls, 2008).

It is sometimes said that arsenic(III) should be oxidized to arsenic(V) prior to adsorption to increase efficiency and this is partly supported by studies (Hsu *et al.*, 2008; Stachowicz *et al.*, 2007). However, many investigations show that adsorption efficiencies at near-neutral pH is comparable for arsenic(III) and arsenic(V) (Chakraborty *et al.*, 2011; Farquhar *et al.*, 2002; Goldberg & Johnston, 2001; Grafe *et al.*, 2001; Guo *et al.*, 2007; Partey *et al.*, 2008, 2009; Pierce & Moore, 1982; Su & Puls, 2001, 2008; Thirunavukkarasu *et al.*, 2003a, 2003b). Column experiments at pH 7.6 support the hypothesis that arsenic(V) and arsenic(III) adsorbs to a similar extent (Thirunavukkarasu *et al.*, 2003a; Thirunavukkarasu *et al.*, 2003b). It is possible and likely that the discrepancies between different investigations can be explained with different experimental conditions, most notable different levels of pH as well as different reaction times.

The adsorption reaction can by itself change the pH of a solution, either by anionic exchange with $\equiv FeOH^{-\frac{1}{2}}$ groups or by expelling an oxonium ion from $\equiv FeOH_2^{+\frac{1}{2}}$ groups. The true situation is complex (Hiemstra & van Riemsdijk, 1996; Jain *et al.*, 1999) but pH increases upon adsorption of the anionic hydrogen and dihydrogen arsenate species while it decreases upon adsorption of the neutral arsenous acid (Jain *et al.*, 1999).

2.12.2 Competition

Differences in adsorption at different pH values show that hydroxide ions can - directly or indirectly - compete with anionic arsenic species for available adsorption sites. There are however also other species that can cause a decrease in arsenic adsorption. Only negligible competing ability have been found for sulfate (Liao *et al.*, 2011; Partey *et al.*, 2009; Zeng, 2004) but organic material such as humic and fulvic acids may decrease arsenic adsorption to goethite slightly (Grafe *et al.*, 2001). Hydrogen carbonate, HCO_3^-, may be relevant as an arsenic adsorption competitor in natural waters due to its relative high abundance. (Appelo *et al.*, 2002; Stachowicz *et al.*, 2007). Considering the similarities between phosphate and arsenate, it is not surprising that the former also adsorbs well to iron oxyhydroxide surfaces. In some studies it has been found that the adsorption of phosphate occurs to a similar extent as the one of arsenate (Hongshao & Stanforth, 2001; Manning & Goldberg, 1996). It has also been shown that phosphate and arsenate behave in a similar way when added to a goethite suspension sequentially (Hongshao & Stanforth, 2001). Experiments with a molar P:As ratio of about five at pH 7.7 (Driehaus *et al.*,

Table 1. Investigations of arsenite and arsenate adsorption on iron oxyhydroxide surfaces. References according to number *1(Sun & Doner, 1998), 2(Manning et al., 1998), 3(Farquhar et al., 2002), 4(Sun & Doner, 1996), 5(Bowell, 1994), 6(Stachowicz et al., 2007), 7(Grafe et al., 2001), 8(Loring et al., 2009), 9(O'Reilly et al., 2001), 10(Fendorf et al., 1997), 11(Waychunas et al., 1993), 12(Pedersen et al., 2006), 13(Zhang et al., 2007), 14(Mamindy-Pajany et al., 2009), 15(Fukushi & Sverjensky, 2007), 16(Hongshao & Stanforth, 2001), 17(Manning & Goldberg, 1996), 18(Thirunavukkarasu et al., 2003a), 19(Banerjee et al., 2008), 20(Saha et al., 2005), 21(Guan et al., 2008), 22(Driehaus et al., 1998), 23(Westerhoff et al., 2005), 24(Manning et al., 2002b), 25(Jessen et al., 2005), 26(Tufano & Fendorf, 2008), 27(Herbel & Fendorf, 2006), 28(Bhandari et al., 2011), 29(Ona-Nguema et al., 2010), 30(Voegelin & Hug, 2003), 31(Thirunavkukkarasu et al., 2001), 32(Raven et al., 1998), 33(Appelo et al., 2002), 34(Jain et al., 1999), 35(Kocar et al., 2010), 36(Carabante et al., 2009), 37(Carabante et al., 2010), 38(Manceau, 1995), 39(Waychunas et al., 1996), 40(Fuller et al., 1993), 41(Pierce & Moore, 1982), 42(Thirunavukkarasu et al., 2003b), 43(Benjamin et al., 1996), 44(Goldberg & Johnston, 2001), 45(Sherman & Randall, 2003), 46(Garcia-Sanchez et al., 2002), 47(Liao et al., 2011), 48(Burton et al., 2009), 49(Guo et al., 2007), 50(Waychunas et al., 2005), 51(Arai et al., 2004), 52(Su & Puls, 2008), 53(Nikolaidis et al., 2003), 54(Su, 2007), 55(Lackovic et al., 2000), 56(Su & Puls, 2001), 57(Farrell et al., 2001), 58(Vaishya & Gupta, 2003), 59(Chakraborty et al., 2011), 60(Partey et al., 2009), 61(Hsu et al., 2008), 62(Partey et al., 2008), 63(Zeng, 2004), 64(Joshi & Chaudhuri, 1996).*

			Arsenic(III)	Arsenic(V)
$Fe^{(III)}$	Goethite	α-FeOOH	1,2,3,4,5,6,7	3,4,5,6,7,8,9,10,11,12,13,14,15, 16,17
"	Akaganeite	β-FeOOH (+ Cl^- + H_2O) (Schwertmann & Cornell, 2000)		11
	GFH®	≈ β-FeOOH (+ Cl^- + H_2O)(Driehaus *et al.*, 1998)	18,19	18,19,20,21,22,23
"	Lepidocrocite	γ-FeOOH	3,5,24	3,5,11,12,24
"	Ferrihydrite	≈$Fe_5HO_8{\cdot}4H_2O$	25,26,27,28,29,30,31, 32,33,34	11,12,15, 27, 32,33,34,35,36,37, 38,39,40
"	Undefined Fe^{III} hydroxides	≈$Fe_xO_yH_{(2y-3x)}$	31,41,42,43,44	31,41,42, 44,45,46
"	Schwertmannite	$Fe_8O_8(OH)_x(SO_4)_y$	47,48	48
"	Hematite	α-Fe_2O_3	5,49	5,14,38,49,50,51
"	Maghemite	γ-Fe_2O_3	24	24
$Fe^{(II,III)}$	Magnetite	Fe_3O_4	24,29,52	24,52
$Fe^{(II)}$	Siderite	$FeCO_3$	49	49
$Fe^{(0)}$	Elemental iron	Fe	53,54,55,56	54,55,56,57
	Misc. Fe		3,58,59,60,61,62,63,64	3,15,58,59,60,61,62,63,64

1998) indicated that phosphate adsorbed almost as efficiently as arsenate. The noted interference is not as significant for arsenic(III) as for arsenic(V) (Zeng, 2004).

Since desorption is the reverse of the adsorption process, studies concerning this subject could also be used when assessing the relative adsorption competing strength of different species. The result of one such experiment support the idea that arsenate and phosphate adsorbs with equal strength (O'Reilly *et al.*, 2001), but an investigation where a dynamic FTIR-ATR system was used, estimated that a five-fold higher concentration of phosphate was required to desorb arsenate to the same extent as arsenate desorbs phosphate (Carabante *et al.*, 2010). One possible flaw with desorption studies is that some arsenate can be judged undesorbable, as noted for strong desorption solutions of sodium hydroxide (Benjamin *et al.*, 1996; Sun & Doner, 1996; Thirunavukkarasu *et al.*, 2003b). One study found partially undesorbable arsenate at a goethite surface but not on ferrihydrite and lepidocrocite (Pedersen *et al.*, 2006). The authors suggested that this is due to incorporation of arsenate into the goethite structure (Pedersen *et al.*, 2006).

2.12.3 Other factors

It is possible that arsenite on a ferrihydrite surface is oxidized to arsenate only in the presence of light and with a simultaneous release of iron(II) into the solution (Bhandari *et al.*, 2011). It has also been suggested that it may be oxidized via oxygen radicals from iron(II) mediated reactions with dissolved O_2 (Ona-Nguema *et al.*, 2010). Adsorption may be facilitated slightly by a temperature increase (Zeng, 2004). The effects of microbial activity in geological systems have been briefly discussed in a previous section.

2.12.4 Column capacity

Previous studies with columns are summarized in Table 2. These studies obtained very different results as the experimental conditions varied considerably. In addition to the variations that can be seen in Table 2, factors such as water chemistry and particle size differ between studies. Table 2 does not contain all important information but the purpose is rather to illustrate the spread in capacities. In many cases, the reported parameters have been calculated by this author from available information or read from figures. This can be the case for the capacity in $\mu g_{added}/cm^3_{adsorbent}$, the velocity and the empty bed contact time, EBCT. Where intervals have been given, average values have been used in the calculations. When authors reported breakthrough values, these are the ones used in Table 2.

Table 2. Studies on arsenic adsorption using columns with iron oxyhydroxides. Please note comments in text.

								Breakthrough		
Reference	Ads.	State	pH	C. µg/l	v. m/h	EBCT min		µg/l	Bed vol.	Cap. µg add. /cm³
(Thirunavukkarasu et al.,	GFH	As(III)	7.6	500	6.4	2.0	Tap	5	1260	**630**
2003a)	GFH	As(V)	7.6	500	6.4	2.0	Tap	5	1140	**570**
"	GFH	Mix.	7.6	169	6.4	1.4	Plant	5	910	**150**
(Driehaus et al..,1998)	GFH	As(V)	7.8	100-180	6-10		Tap	10	34000	**4800**
"	GFH	Mix.	7.8	21	7.6	0.4	Plant	10	37000	**780**
"	GFH	Mix.	8.2	16	5.7	0.5	Plant	10	32000	**510**
"	GFH	Mix.	7.6	15-20	15		Plant	10	85000	**1500**
(Westerhoff et al., 2005)	GFH	As(V)	8.8	51	23	2.6	Ground	5	1000	**51**
"	GFH	As(V)	7.6	14	11	5.0	Ground	5	38600	**540**
(Thirunavukkarasu et al.	oxide	As(III)	7.6	500	6.4	2.7	Tap	5	1403	**700**
2003b)	oxide	As(V)	7.6	500	6.4	2.7	Tap	5	1244	**620**
"	oxide	Mix.	7.4	177	6.4	1.0	Plant	5	1715	**300**
(Benjamin et al., 1996)	oxide	As(III)	3.5	ca75	-	5.0	Simul.	-	> 650	**> 49**
(Joshi & Chaudhuri, 1996)	oxide	As(III)	7.7	1000	0.6	50	Ground	10	184	**180**
	oxide	As(V)	7.7	1000	0.6	50	Ground	10	165	**170**
(Vaishya & Gupta, 2003)	oxide	mix	7.3	1000	1.6	7.7	Ground	5	51	**51**
	oxide	mix	7.3	1000	1.6	7.7	Ground	5	100	**100**
	oxide	mix	7.3	1000	1.6	7.7	Simul.	5	115	**120**
	oxide	mix	7.3	1000	1.6	7.7	Simul.	5	318	**320**
	oxide	mix	7.3	1000	1.6	7.7	Simul.	5	455	**460**
(Guo et al., 2007)	Mix	As(V)	7.3	500	0.1	68	Tap	5	2180	**1100**
"	Mix	As(V)	7.3	500	0.1	68	Tap	5	1168	**580**
"	Mix	As(V)	7.3	500	0.1	68	Tap	5	1744	**870**
"	Mix	As(V)	7.3	500	0.1	68	Tap	5	102	**51**
"	Mix	Mix.	7.3	500	0.1	68	Tap	5	1301	**650**
"	Mix	Mix.	7.3	200	0.2	47	Tap	5	116	**23**
"	Mix	Mix.	7.3	200	0.2	47	H_2O_2	5	439	**88**
(Nikolaidis et al., 2003)	Fe^0	As(III)	6.2	294	1.6	47	Landfill	20	8759	**2600**
"	Fe^0	As(III)	6.2	294	1.6	47	Landfill	20	7109	**2100**
"	Fe^0	As(III)	6.2	294	1.2	22	Landfill	20	6583	**1900**
"	Fe^0	As(III)	6.2	294	2.5	11	Landfill	20	4740	**1400**
"	Fe^0	As(III)	6.2	294	4.9	22	Landfill	20	>5705	**>1700**

Aware of the perils regarding over-interpretation of Table 2, some features can be pointed out:

- Arsenic(III) seems to adsorb to similar extent as arsenic(V) under similar conditions (Joshi & Chaudhuri, 1996; Thirunavukkarasu *et al.*, 2003a, 2003b)
- Alkaline pH appear to suppress adsorption (Driehaus *et al.*, 1998; Westerhoff *et al.*, 2005)
- There is no obvious and immediately noted change in breakthrough capacities following very short EBCT:s or very high velocities.
- No obvious relationship between inlet concentration and capacity is noted.
- In the same studies, different water qualities give quite different results (Driehaus *et al.*, 1998; Thirunavukkarasu *et al.*, 2003a, 2003b; Westerhoff *et al.*, 2005)

The studies in references (Thirunavukkarasu *et al.*, 2003a; Thirunavukkarasu *et al.*, 2003b) showed that iron oxyhydroxide coated sand and GFH® have similar adsorption capacities. Some studies indicate substantially higher capacities for GFH® (Driehaus *et al.*, 1998; Westerhoff *et al.*, 2005).

2.12.5 Time aspects and intraparticle diffusion

Batch experiments have usually been performed on rather long time scales but have also been used to show that both arsenic(III) and arsenic(V) species can be adsorbed to a considerable extent on the time-scale of minutes (Fuller *et al.*, 1993; Raven *et al.*, 1998). It has been proposed that the uptake of arsenic(V) species onto goethite occurs in two steps; one fast complex forming adsorption phase is followed by a buildup of surface precipitate on the adsorbed layer (Hongshao & Stanforth, 2001). The retention increases with time and suggested explanations are either formation of stronger complexes or migration into the material (Su & Puls, 2001). In another study the two observed time phases have been assigned either to carbonate desorption being a rate limiting process, or to a slow diffusion to less accessible sites (Carabante *et al.*, 2009). Yet another suggested cause is the existence of two different kinds of active adsorption surface sites (Pierce & Moore, 1982).

The high capacity for arsenic uptake by iron oxyhydroxides, could be due to large surface area of these materials (Fuller *et al.*, 1993; Nikolaidis *et al.*, 2003; Pierce & Moore, 1982). One study regarding adsorption of arsenic(V) species on GFH® suggest that intraparticle diffusion is rate limiting in that kind of water treatment systems (Badruzzaman *et al.*, 2004), and it may also explain regeneration of adsorption capacity following periods of downtime.

3 Aim

This project has one fundamental part and one more applied part. In the fundamental part, solutions of the weakly hydrated alkali metal ions were investigated with large angle X-ray scattering, LAXS, and with double difference infrared spectroscopy, DDIR. One goal is to improve ionic radii for alkali metal ions in aqueous solution, and in particular for the lighter ones. Such radii may differ somewhat from current literature values, which are frequently obtained from very constrained crystal structures. Literature data from the solid phase was screened, and the strong correlation between interatomic distances and coordination number was used to deduce correct hydration numbers for the alkali metal ions in aqueous solution. In order to achieve representative values for ionic radii in aqueous solution, only crystal structures in which the alkali metal ion are unconstrained and interacting with neutral oxygen atoms, have been used. Thereby, interfering lattice effects can be avoided. Furthermore, the alkali metal ions' effect on water structure has been studied with respect to their structure-making or structure breaking behavior.

The environmentally important arsenic oxyacid species were studied in solution with XAS spectroscopy, LAXS and DDIR. Obtained results were compared with available crystal structure data on the oxyacid species. The purpose was to reach insights in how bond distribution and structural behavior of these important species in the arsenic acid system is varied due to their protonation and deprotonation. It is quite likely that the phosphoric acid system behaves in a similar way as the investigated arsenic acid system. Reliable XANES edges for all protonation states of the arsenic acid system have been recorded. The purpose is to illustrate how the degree of protonation affects the XANES spectra for arsenic oxyacid species, and obtained spectra can also be used for future reference. The effect on water structures by the weak neutral oxyacids arsenous acid and orthotelluric acid have been investigated by DDIR.

The applied part of the project intends to improve knowledge about processes in which arsenic oxyacid species are removed from drinking water by adsorption to simple packed columns. Hopefully, knowledge gained can serve as a foundation for the development of a rapid small scale arsenic decontamination filter for use under primitive conditions in the northern rural part of Burkina Faso, or in other developing areas. The practical application is not within the scope of this project, although exchange students from the Swedish University of Agricultural Sciences are already in Burkina Faso for preliminary tests where real arsenic enriched tube well water is passed through columns similar to the ones used in this project.

More specifically, the applied part of the work investigates whether arsenic(III) and arsenic(V) adsorbs with sufficient rate for an online decontamination column to be feasible. The effects of pH on adsorption have been studied, and relative adsorption affinity of arsenic(III) and arsenic(V) estimated. The effects of present competitive species such as phosphate, hydrogen carbonate and fluoride have been studied as well, and it was discussed to what extent their presence in tube well water decreases adsorption of arsenic(III) and arsenic(V). Much of this has previously been investigated in batch experiments but a column setup is a better model of a true contamination unit, as for example, there is negligible build-up of hydroxide or oxonium ion concentrations from the adsorption reactions. Furthermore columns allow the use of lower, more realistic arsenic concentrations, as large volumes of water can be passed through the material. An adsorbent material has been prepared by coating quartz sand with ferrihydrite, and then used in columns for the removal of arsenic oxyacids. The effect of varying iron content and distribution on the grains of quartz sand have been controlled as well, and coating mineralogy have been checked. In addition to experiments with ferrihydrite coated sand, the industrial material GFH® have been tested to assess its suitability for arsenic removal on short time-scales. Towards the end of this thesis, practical considerations for a future up-scaling will be briefly discussed in connection to obtained results.

4 Experimental methods

The quantitative method used in the project has mainly been atomic absorption spectrophotometry, and it is complemented with several structural methods. Some are well known and widely used, while other are more specialized applications. A short summary of the main techniques follows below, as do descriptions of experimental methodologies used. For details about samples, see the experimental section of corresponding paper (I-IV).

4.1 Atomic absorption spectrophotometry

In atomic adsorption spectrophotometry, light in the UV-VIS range excites ground state valence electrons of atoms at certain specific wave lengths (Christian & Feldman, 1970). Reemission of light is unlikely to occur in direction of the incident light path and the intensity as measured by the detector is decreased. This might seem similar to the concept of UV-VIS spectrophotometry, but there are large and important differences. In UV-VIS spectrophotometry, it is the valence electrons of molecular orbitals that are excited while it in atomic absorption is the valence electrons of orbitals in neutral elemental atoms. In atomic absorption spectrophotometry atoms are vaporized using high temperature and most atoms are atomized to the neutral elemental form in the gas phase. The fraction of ionized atoms is negligible for most metals except the alkali and alkaline earth metals (Christian & Feldman, 1970). In the normal case, calibration curves are applicable even if made from solutions prepared from a different compound containing the same element (Christian & Feldman, 1970). The fact that measurements are performed in gas phase eliminates effects of the solvent. The wave lengths required for the excitation to certain valence states are very specific to the element, and light is absorbed only in very narrow wavelength intervals (Christian & Feldman,

1970). Therefore interference problems are unusual with this method (Harris, 2000).

The atomizer units could be either a flame or a graphite furnace. With the flame atomizer, a liquid solution is drawn from the sample jar, and atomized in a flame through which light passes. This atomizer handles higher concentrations than the graphite furnace. It is a quick and simple analysis method but often requires more sample solution.

With the graphite furnace atomizer, a drop of sample is transferred to a graphite tube which is electrically heated in an oxygen free environment. Light passes through the emitted gases containing the element of interest. Several heating steps are required for the controlled emission of the element in interest. A matrix modifier is frequently added to the sample to ensure that the element is not lost in the pyrolysis step prior to atomization (Harris, 2000). Absorbance is measured in the atomization step at high temperature. The graphite furnace atomizer is substantially more sensitive than the flame, primarily due to a longer residence time in the optical path (Harris, 2000).

The instrument manufacturer or analytical chemistry literature provides information about recommended conditions and parameters for analysis of a particular element, either with flame or graphite furnace atomizer. Such recommended settings might need to be slightly changed to suit the individual instrument. The atomic absorption spectrophotometer used for the work in these studies is shown in Figure 10.

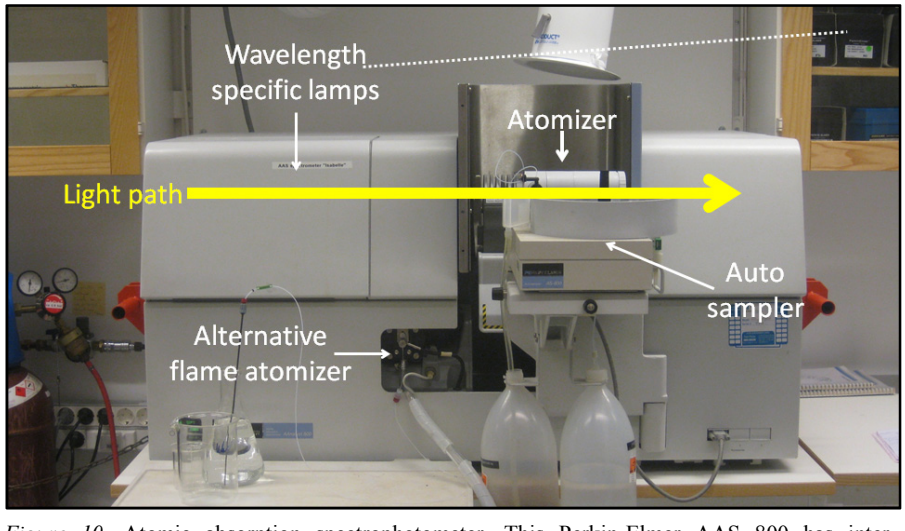

Figure 10. Atomic absorption spectrophotometer. This Perkin-Elmer AAS 800 has interchangeable graphite furnace and flame atomizers and is equipped with an autosampler. The instrument is run by PC-based software, WinLab32.

4.2 Double difference IR

Molecules absorb specific wavelengths of infrared light, depending on the molecular vibrations they perform. The possible vibrations a molecule is allowed to undergo depend on the symmetry of its molecular structure and may include symmetric and asymmetric stretching, wagging and scissoring. The absorption can be measured by the infrared spectroscopy technique, analogous to other spectroscopic techniques.

In a particular application of infrared spectroscopy, double difference infrared spectroscopy or DDIR, the O-D stretch is in focus. This bond absorbs infrared light at 2509 cm^{-1} in bulk water containing HDO. If the HDO participates in the hydration shell of an ion or molecule, this band is shifted to either higher or lower wavenumbers, Figure 11.

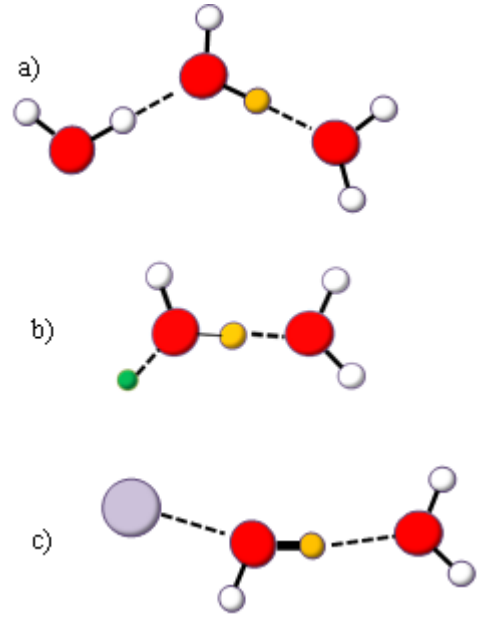

Figure 11: a) HDO molecule in bulk water - $\nu_{DO} = 2509$ cm^{-1}. b) HDO molecule in the hydration shell of a structure making ion - $\nu_{DO} < 2509$ cm^{-1} c) HDO molecule in the hydration shell of a structure breaking ion - $\nu_{DO} > 2509$ cm^{-1}.

Affected spectra for the solutions of interest are obtained by the following procedure: 1) Measure the spectrum for the solute in both H_2O and in 8% HDO(aq) for several concentrations including the pure solvents. 2) Subtract each H_2O spectrum from respective HDO spectrum, with a subtraction factor calculated as the fraction of molecules being H_2O in the HDO solution. This factor should be around 0.92-0.93 on a molar basis. 3) Multiply resulting spectra with the factor K, determined as $K=1/(C_{HDO} * L)$ where C_{HDO} is the concentration of HDO in the sample and L is the optical path length in the experiment. 4) Offset the local minimum value around 2750 cm^{-1} to zero in each spectrum. 5) Cut the spectra but keep local minima before and after main peak, e.g. in the region 2800-2000 cm^{-1}. 6) Open the set of spectra and check the validity of a linear assumption for the maximum height. If valid, calculate a concentration dependent derivative, $d\varepsilon/dm$, for the set of spectra.

So far, the method is rather straightforward, but now it is necessary to apply the *affected number*, N. In the development of the DDIR method, the affected number was previously thought to correspond to the number of molecules in the hydration shell, but is now defined as the number of spectroscopically

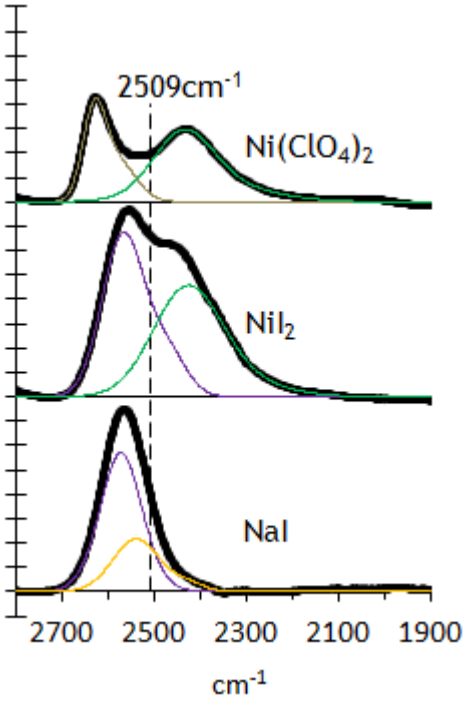

Figure 12: Affected DDIR spectra of three solutes. Brown represents the perchlorate ion at 2633 cm^{-1}, green the nickel ion at 2426 cm^{-1}, purple the iodide ion at 2568 cm^{-1} and yellow the sodium ion at 2539 cm^{-1}.

distinguishable molecules in the hydration shell. It does not exceed the hydration number.

To continue with the procedure: 7) Calculate a spectrum $\varepsilon_A = 1/(NM) \times d_\varepsilon/d_m + \varepsilon_B$ where N is the affected number, M is the mean molar mass of the ca 8% HDO solution (≈0.0181 kg/mol), d_ε/d_m is the derivative obtained in step No 6 and ε_B is the spectrum obtained in step No 5 for zero concentration. Repeat this point for several values of the affected number N. 8) For each possible affected number, reproduce the affected spectrum by fitting as few Gaussian peaks as possible. 9) Add the ε_B spectrum (zero concentration) to the spectrum, fixed at 2509 cm^{-1}, and attempt to fit again. If the added water peak remains with a substantial height, it means that the applied affected number is too large. The true affected number is the largest one with which the area of the added water peak shrinks to less than 0.5% of the total area. Rather large errors in N are usually required to change resulting affected spectra enough to substantially increase the risk of spectral misinterpretation.

The affected spectrum now represents the D-O stretch of HDO molecules in the hydration shell(s) of the solute and three examples are shown in Figure 12. In the figure, D-O stretches from anionic as well as cationic hydration can be seen. The position of the D-O stretch is affected proportionally to hydrogen bond energy (Badger & Bauer, 1937). Lower wave numbers mean a lower energy in the D-O vibrations, which correspond to stronger hydrogen bonds as shown in Figure 11b. High wave numbers show a high energy in the internal HO-D bond, corresponding to the formation of weaker hydrogen bonds as shown in Figure 11c. Therefore, the DDIR method can be used to evaluate whether constituents of the solute show a structure making or a structure breaking behaviour.

The method was first applied by the Lindgren group (Bergström *et al.*, 1991a, 1991b, 1992; Bergström & Lindgren, 1992; Eriksson *et al.*, 1984; Kristiansson *et al.*, 1984, 1988; Kristiansson & Lindgren, 1988, 1991) but has been further developed by the Stangret group (Stangret, 1988; Stangret & Gampe, 1999, 2002; Stangret & Kamieńska-Piotrowicz, 1997; Stangret & Kostrowicki, 1988; Śmiechowski *et al.*, 2004, 2009; Śmiechowski & Stangret, 2006, 2007a, 2007b).

4.3 Large angle X-ray scattering

The wave lengths of X-rays are on the same scale as the distances between neighboring atoms in a material, and this radiation can therefore be used to gain knowledge about interatomic distances. While there are straightforward and very accurate methods for structural determination of crystalline solids, other states of matter poses difficulties. This is the case for liquids, solutions and amorphous materials due to a comparatively low order. However, Large Angle X-ray scattering, LAXS, is one option.

A description of the equipment used for LAXS, Figure 13, is described in reference (Levy *et al.*, 1966) and descriptions of experimental setup and theory can be found elsewhere (Stålhandske *et al.*, 1997). In short, X-rays of a known wave length is irradiating the free surface of a sample solution and some of the light will be scattered in the direction of the detector. Some X-rays will be

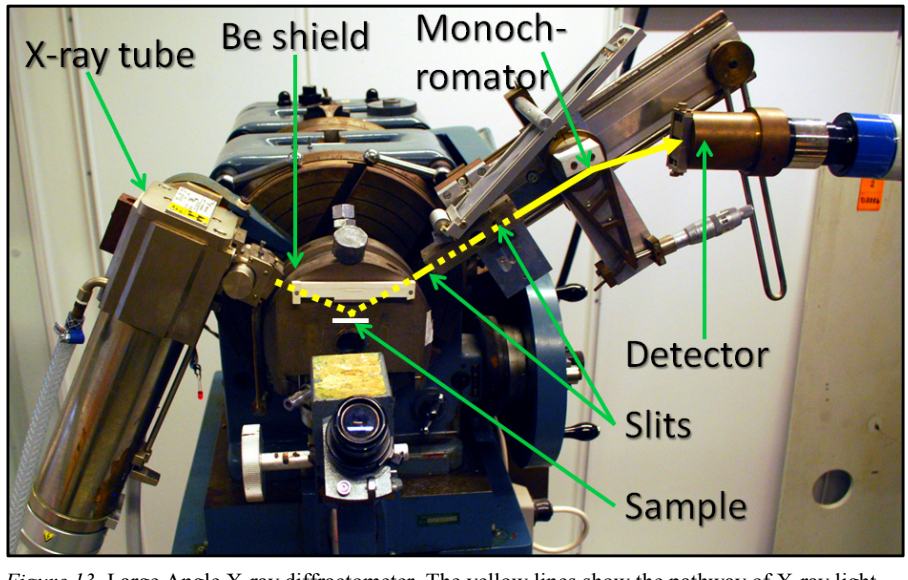

Figure 13. Large Angle X-ray diffractometer. The yellow lines show the pathway of X-ray light.

scattered by one atom while others are scattered twice (by adjacent atoms) before reaching the detector. $Mo_{K\alpha}$ X-ray radiation (λ=0.7107 Å) have been used in these experiments and measurements have been made in about 450 discrete points in the range $1 < \theta < 65°$, with a scattering angle of 2θ. The PTFE sample cup is placed in a compartment covered with a radiation shield with beryllium windows perpendicular to the X-ray pathway. Little X-ray interaction is expected from the electron poor Be material. Around 100 000 counts for each angle is collected and the required time measured. Data treatment is performed with the KURVLR program (Johansson & Sandström, 1973). X-ray scattering factors corrected for anamalous dispersion and Compton scattering (Cromer, 1969; Cromer & Mann, 1967) are used to compare with the experimental scattered intensitties for scaling the latter ones.

The method works by measuring the scattered intensities (counts per second) as a function of the scattering angle 2θ. A small contribution of atom-atom scattered X-rays will add to the counts from single atom scattering. In a hypothetical case where electrons in the solution are evenly distributed, detected counts per second would decrease by a smooth function with increasing angle θ. In a real sample the existence of atomic interactions causes an uneven electron distribution, where more electrons are found at more or less well-defined recurring distances. Exemplifying recurring distances with the arsenate ion, AsO_4^{3-}, they could be intra-molecular bonds (As-O), intra-molecular fixed distances (between two arsenate oxygen atoms) or well-defined intermolecular distances (from any arsenate atom to the oxygen atom of a hydrating water molecule). At certain values of θ, the contribution of atom-atom scattered X-rays will increase the total photon count, while at others it will decrease the total photon count. This can be explained by the probability of detectable scattering from one atom being a wave function of θ, and hence the probability of two-atom scattering is a combination of wave functions whose phases may either amplify or damp each other. This wave interference depends on the interatomic distances, since each of the original probability waves depend on the volumes electrons can occupy around a nucleus. Therefore, an increased photon count at a particular angle θ is proportional to increased electron density at a particular (average) distance.

A plausible model for the close environment of the ion or molecule of interest is built with coordinates corresponding to structural symmetries such as tetrahedrons, octahedrons or square antiprisms. The fit of the model to the experimental data are calculated in inverse space $s = (4\pi \sin\theta)/\lambda$ where λ is the applied wave length. It is shown in an intensity plot but values are also recalculated to a more easily comprehendible radial distribution function, RDF, through a Fourier transformation. Such functions are also shown in Papers I

and II, and their interpretations are discussed. A valid structural model give rise to a nice fit, and recurring distances in the solution are illustrated in the RDF. The distance between bulk water oxygen atoms is shown around 2.9 Å and sometimes this make it difficult to assign other relevant distances in this region. Distances of a reasonable structural interpretation can be refined with a least squares method, using the program STEPLR (Molund & Persson, 1985). The refinement occurs in the relevant range of $4 \leq s \leq 16$ Å^{-1}. Other parameters that can be refined are the number of distances for each unit as well as a temperature factor depending on the peak width thus the distance distribution. These two parameters have a very high correlation and to deduce hydration numbers merely by least-squares refinement is unfeasible. The LAXS method is independent of other methods of structural determination in solution, and therefore a good complementary method. All recurring distances in the solution can be found up to more than 10 Å, but required concentrations are often high. LAXS is also known as Wide Angle X-ray Scattering, WAXS.

4.4 X-ray absorption

In X-ray absorption spectroscopy, XAS, a sample is irradiated with X-rays and the absorbed light measured by gas filled ion chamber detectors. X-rays are electromagnetic radiation with wavelengths 10-5000 pm and may interact with matter in several ways. As the sample is irradiated, energy can be absorbed by inner core electrons which are exiceted either to a higher energy level or into the continuum. In the latter case, a photo electron has been formed. In addition, X-rays are diffracted by electrons elastically or inelastically and this will also appear as absorption to the spectroscopist, as the radiation direction is changed away from the straight path leading to the detector. These three processes are shown in Figure 14 and will from now on be referred to as absorption. Additional processes also occur: when an electron from higher energy levels fill the produced electron hole, excess energy is either emitted as a fluorescence X-ray or with another electron departing in addition to the photoelectron. Such electrons are

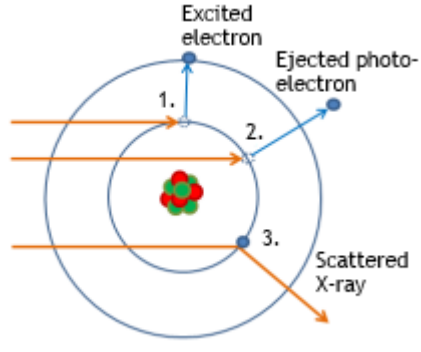

Figure 14: Schematic description of X-ray absorption processes. Orange arrows denote electromagnetic radiation and blue arrows denote electron particle-wave movement. 1) Electron excitation to higher energy level. 2) Excitation into continuum. 3) Scattering

called Auger electrons and contrary to photons, electrons have mass and carry kinetic energy. Departed photoelectrons as well as Auger electrons are usually soon replaced with electrons from the surroundings, and produced charges are short-lived. A more detailed description of these processes in connection to XAS spectroscopy can be found in (Jalilehvand, 2000).

XAS experiments are usually performed at a synchrotron light facility, where highly tunable and brilliant X-rays are produced. Electrons are travelling close to the speed of light in a large polygon storage ring, and X-rays are produced as magnetic fields force the electrons to bend their path, Figure 15. The produced X-rays are used in different experimental stations, and XAS spectroscopy represents one experimental application with primarily hard (short-wavelength) X-rays. An insertion device such as an undulator or a wiggler produce the light before the bending magnet in the storage ring, and it is then monochromatized in a cooled double crystal monochromator which can be finely controlled by piezo crystal technology. The X-ray radiation enters the hutch of the experimental station, passes a gas filled ionic chamber which measures the incident intensity. It penetrates the sample and is measured once again in a second ionic chamber. In hitting the sample, X-ray fluorescence is produced and measured in yet another detector orthogonally to the transmission line. Produced fluorescence is correlated to transmission mode absorption data, and any of the data sets may be used for further evaluation depending on their quality. The measurements are controlled from the beamline control room next to the hutch. The technique as well as the equipment is more complicated than described here but further information can be found elsewhere (Jalilehvand, 2000). All XAS measurements in this work have been performed at beam line I-811 of the MAXII synchrotron light facility, Lund, Sweden (Carlson *et al.*, 2006; Grehk & Nilsson, 2001).

In a typical X-ray absorption spectrum, absorption is plotted as a function of incoming radiation energy in electron volts. Absorption decreases with higher energy (shorter wavelength) until the energy is high enough to excite specific inner shell electrons into the continuum - to produce photoelectrons as exemplified by process No 2 in Figure 14. This is shown as a sharp rise of absorption in the spectrum - an absorption edge. By setting the energy range close to an absorption edge, it is usually possible to study the X-ray interactions of a particular element and disregard other components of the sample. This is one of the major advantages of the XAS technique. In Papers II and III, the arsenic and iron K-edges have been investigated. At the energy corresponding to such an edge, 1s electrons is ejected into the continuum.

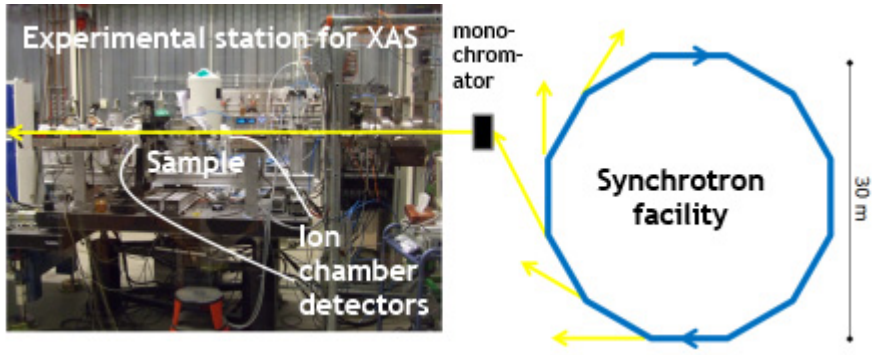

Figure 15. The I-811 beamline of the MAXII synchrotron light source at MAX-LAB, Sweden. The right part of the Figure is schematic. Blue arrows represent electrons travelling in the storage ring and yellow arrows represent emitted X-rays.

4.4.1 XANES

The XANES region of an XAS spectrum stretches from before the absorption edge and includes the following ≈50 eV. The physics behind this region in the spectrum is not fully understood but valuable information about the sample can be obtained anyway. It is often possible to determine the oxidation state of the studied element by observing the position of either absorption edge or white-line maximum (a sharp peak following the absorption edge for many elements). This is the case for arsenic in valence states +III and +V. The difference between different oxidation states can be several eV per change in oxidation number which is a lot considering the great repeatability and resolution of XAS spectra. It is also possible to gain information about electronic transitions and coordination figures of the particular species.

4.4.2 EXAFS

Considering energies above the XANES region of an XAS spectrum, a rippling shape is seen for any investigated species with a well-defined structure around the absorbing atom. These ripples carry structural information about the environment around the absorbing element. The origin is the photoelectron wave emerging upon exciting inner core electrons to a continuum, Figure 14. The energy of this photoelectron wave is $E\text{-}E_0$, and thus continuously increaseing during and experiment. The photoelectron wave can be backscattered by an atom in the vicinity of the absorbing atom and the backscattered wave interacts with the original photoelectron wave, Figure 16. The resulting wave will be either amplified or damped compared to the original one, depending on the interatomic distance and the wavelength of the photoelectron wave. An amplified photoelectron wave will in fact increase absorption by the

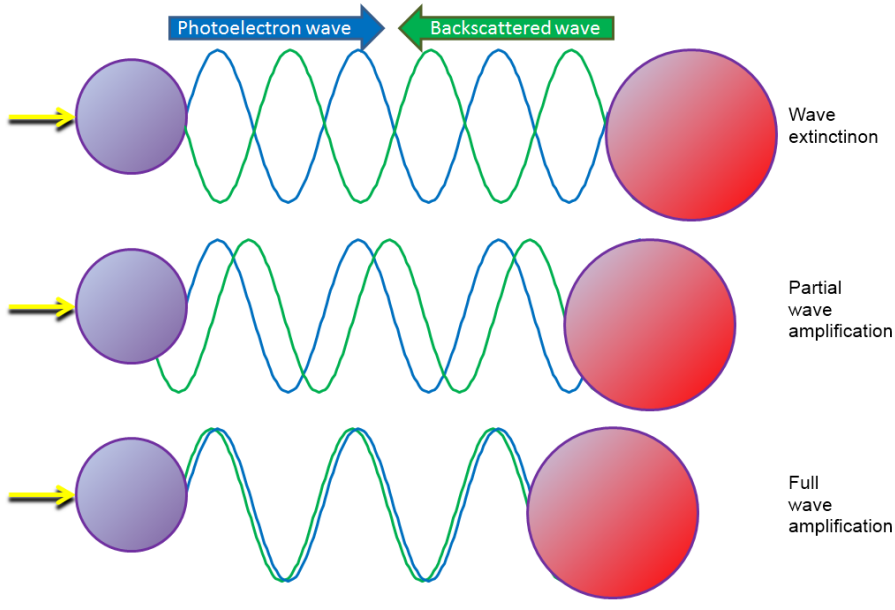

Figure 16. The photoelectron wave emitted from the absorbing atom may either be damped (top) or amplified (bottom) by the backscattered wave from a neighboring atom, depending on the wavelength/interatomic distance relationship. Yellow arrows denote incoming X-rays.

sample. Each energy level in eV represents a particular wave length, and thus it is possible to determine recurring distances for an atom of a particular element in any state of aggregation, in solution or adsorbed to a surface. The energy scale is converted in order to represent the photoelectron wavenumber in $Å^{-1}$ and the wave is weighted to increase the visibility of the high energy part.

4.5 Adsorbent preparation

The preparation of ferrihydrite was made in accordance with reference (Schwertmann & Cornell, 2000). The obtained suspension was centrifuged in 50 ml tubes for five minutes at $1700 \times g$. The supernatant was replaced with more suspension and centrifuged again. The centrifugation procedure was repeated another four times, each time replacing the supernatant with pure water. After the last centrifugation, water was filled to 37.5 ml, and the suspension was shaken for two hours. 12.5 ml quartz sand was added to the tubes, which were then shaken for 48 hours. The mixture was centrifuged at $2300 \times g$ in 40 minutes and the supernatant was discarded. The material was manually mixed and dried in a well-ventilated fume hood for two days. The material was then transferred to a beaker and carefully rinsed by hydrogravi-

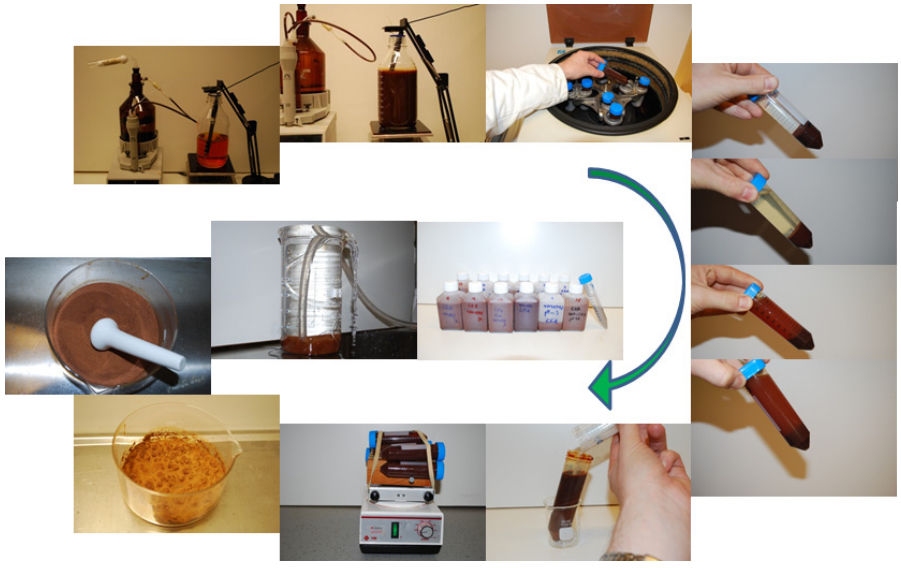

Figure 17. Overview of the adsorbent production. A Ferrihydrite suspension is produced, centrifuged and resuspended five times, shaken and left to air dry. Aggregates are gently separated and the resulting material is hydrogravimetrically cleaned before stored under water.

metry with deionized water for about 30 minutes. The color of the produced adsorbent is now red-brown, as opposed to the gray quartz sand, and the intensity of this color approximately reflect the iron content of the material. The material used for some of the tests has been prepared in a somewhat different way with higher ionic strength resulting in lower ferrihydrite coverage. The material has been stored under water to avoid loss of flakes due to drought. The adsorbent production cycle is illustrated in Figure 17.

4.6 Column setup

Water containing arsenic have been pumped to cylindrical ion exchange tubes containing either iron oxyhydroxide coated quartz sand or the commercial material GFH®, Figure 18. The water trickled through the column bed by gravity, and the pressure drop over the bed could be measured as the height of the water pillar above the bed. The inner diameter of the column was Ø15 mm and adsorbent was packed to a 75 mm pillar, following the recommendations of a height/diameter ratio of 5 (Nikolaidis *et al.*, 2003). The material is placed on top of 1 cm glass wool and 4 mm of Ø1mm glass beads. When GFH® was used, it was necessary to first clean the material hydrogravimetrically to prevent it from clogging the column. In a few experiments, only 1 cm of adsorbent was used, together with 6.5 cm of practically inert untreated quartz

sand. In the high velocity tests, the experimental setup was somewhat different. In these tests, sample water was sucked through the column by applying a vacuum at the effluent side.

Arsenic containing water was prepared by dissolving $NaAsO_2$ or $Na_2HAsO_4 \cdot 7H_2O$ in deionized water. Where pH has been altered, NaOH was used and the solution equilibrated with air for a number of days. During the experiments, pH was measured in the inlet storage tank to make sure that no substantial change took place. The experimental conditions of the different tests can be found in Papers III and IV. The experiments with competitors, as presented in Paper IV, were conducted in much the same was as described above but with additions of phosphate, hydrogen carbonate or fluoride in the inlet water.

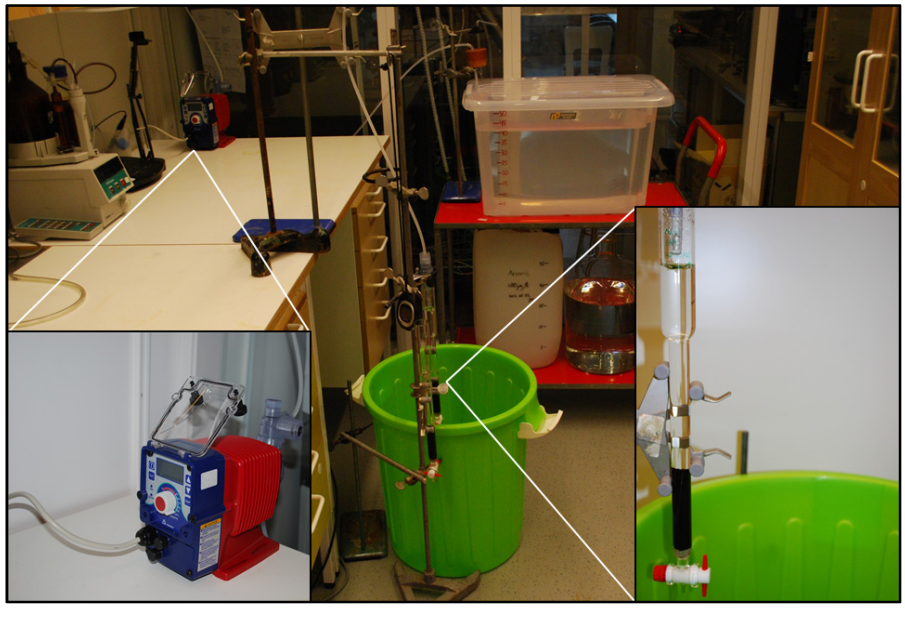

Figure 18. Setup for the column experiments. Water containing arsenic is pumped through a glass column containing adsorbent - in this case the commercial material GFH®.

5 Results and discussion

The results from manuscripts and published papers are summarized below, although with a different disposition. The fundamental research comes predominantly from Papers I and II, while most of the results from the applied part originate from Papers III and IV. When it comes to the applied work, I have taken the liberty to expand on the discussion of future practical implications, and perhaps somewhat on the expense of experimental details. Those can however be found in respective original paper and corresponding supplementary material files.

5.1 Fundamental research

Correct knowledge about ionic radii and hydration number of common ions in aqueous solution is important from a fundamental point of view, and may improve models in many scientific fields such as cell membrane transport or studies of capillary forces. The values from Shannon's work (Shannon, 1976) is frequently used, without considering whether these data obtained for highly polarizing crystal structures such as oxides also are applicable in aqueous solution. Ions and molecules in water do affect the structure of the liquid water bulk (Marcus, 2009; Rodnikova, 2003), and it might be useful for everyone working with aqueous solutions to estimate the degree of this interaction. This is especially true when it comes to very common ions such as the alkali metal ions or environmentally important molecules or ions such as the arsenic oxyacid species. Interatomic distances in the crystal phase can facilitate the understanding of the behavior of the corresponding species in aqueous solution. The relevance of fundamental research is often questioned. Not everyone find knowledge valuable for its own sake but fundamental research often aids its applied equivalent. A wise scientist once said to this author:

> "Many engineers attempting to build houses would benefit from knowing the dimensions of the bricks"

5.1.1 Alkali metal ions

In Paper I, improved ionic radii for weakly hydrated lithium, sodium and potassium ions was proposed by screening a large number of crystal structures in databases (Allen, 2002; *Inorganic Crystal Structure Database*, 2009). Great care has been taken to include only hydrates or other complexes with neutral oxygen ligand atoms, in order to study the kind of weak hydration expected for alkali metal ions in aqueous solution. Comparing these crystal structures with experiments, it can be seen that metal-oxygen distances are about 0.02 Å longer for sodium and 0.01 Å longer for potassium in aqueous solution. The rubidium and cesium ions do not crystallize with full coordination shells of weakly interacting neutral ligands. In the discussion of coordination in solution, the most stable coordination state of the distribution is the one deduced. Relevant structures as well as a discussion of that concept are found in Paper I and its supplementary material.

Regarding the lithium ion, a crystal structure survey show that the relevant lithium structures, as defined above, exists either as four-coordinated metal ions in tetrahedral structures, or as six-coordinated metal ions in linear chains where each ion is in near-octahedral coordination. From Table 3 it can be seen that metal-oxygen distances differs to a large extent between four- and six-coordinated lithium. The difference between four-coordinated hydrates and an expanded group containing structures with other neutral monodentate ligands is negligible. Distances from neutron scattering (Ohtomo & Arakawa, 1979) and computer modeling (Bouazizi & Nasr, 2007; Loeffler & Rode, 2002; Rudolph *et al.*, 1995) indicated that the aqueous lithium ion does indeed exist in a four-coordinated state.

Relevant crystal structures of the sodium ion are summarized in Table 4 and similarly with the lithium ion, different choices of (relevant) ligands result in similar metal-oxygen distances. The experimental value for sodium in aqueous solution suggests that the ion exist in six-coordination. The obtained radius of 1.07 Å is longer than the listed Shannon value (Shannon, 1976). As discussed in the last section of 2.5.2, the use of strongly polarizing ligands make Shannon's value less suitable for representing a sodium ion in aqueous solution. Shannon's alternative radius extraction on page 761 of his paper (Shannon, 1976) is in better agreement with our obtained value, although still based on many structures poorly representable for aqueous solution.

As for the potassium ion, it is necessary to make use of tetrahydrofuran (THF) solvates to determine the ionic radius. The ion does not crystallize with full shells of other neutral monodentate oxygen binding ligands. The small cyclical ether tetrahydrofuran have a different electronic structure than other

Table 3. *Li^+ structures for coordination numbers 4 and 6. Except for THF and 1,2-Dimethoxyethane solvates, no ether structures are shown. Categories have been sorted in order of importance and categories in bold are summarizing all structures above, i.e. neutral homoleptic solvates in four-coordination include the 36 structures of neutral homoleptic hydrates and the additional 30 structures of neutral homoleptic non-hydrates. The category with grey background has been chosen for the evaluation of Li^+ radius.*

	CN =	4		CN =	6	
Description	Number Obs.	d_{M-O} (Å)	Stddev (Å)	Number Obs.	d_{M-O} (Å)	Stddev (Å)
Neutral, homoleptic, nonbridging hydr.	24	1.936	0.016	0		
Neutral, homoleptic, bridging hydrates	12	1.954	0.010	10	2.132	0.010
Neutral homoleptic hydrates	**36**	**1.942**	**0.017**	**10**	**2.132**	**0.010**
Neutral homoleptic, non-hydrate	30	1.939	0.025	0		
Neutral homoleptic solvates	**66**	**1.941**	**0.021**	**10**	**2.132**	**0.010**
Neutral heteroleptic monodentate	14	1.943	0.018	0		
Neutral monodentate	**80**	**1.941**	**0.020**	**10**	**2.132**	**0.010**
Neutral multidentate	3	1.916	0.018	0		
Neutral	**83**	**1.940**	**0.021**	**10**	**2.132**	**0.010**
THF-solvates	242	1.918	0.013	3	2.169	0.006
1,2-Dimethoxyethane	0			75	2.134	0.015

Table 4. *Na^+ structures for coordination numbers 5 and 6. Except for THF and 1,2-Dimethoxyethane solvates, no ether structures are shown. Categories have been sorted in order of importance and categories in bold are summarizing all structures above, i.e. neutral homoleptic solvates in six-coordination include the 45 structures of neutral homoleptic hydrates and the additional 4 structures of neutral homoleptic non-hydrates. The category with grey background has been chosen for the evaluation of Na^+ radius.*

	CN =	5		CN =	6	
Description	Number Obs.	d_{M-O} (Å)	Stddev (Å)	Number Obs.	d_{M-O} (Å)	Stddev (Å)
Neutral, homoleptic, nonbridging hydr.	2	2.340	0.006	6	2.412	0.042
Neutral, homoleptic, bridging hydrates	7	2.379	0.012	39	2.415	0.026
Neutral homoleptic hydrates	**9**	**2.370**	**0.020**	**45**	**2.415**	**0.028**
Neutral homoleptic, non-hydrate	4	2.341	0.028	4	2.392	0.027
Neutral homoleptic solvates	**13**	**2.361**	**0.026**	**49**	**2.413**	**0.028**
Neutral heteroleptic monodentate	8	2.352	0.029	9	2.407	0.022
Neutral monodentate	**21**	**2.358**	**0.027**	**58**	**2.412**	**0.027**
Neutral multidentate	2	2.341	0.021	5	2.399	0.046
Neutral	**23**	**2.356**	**0.026**	**63**	**2.411**	**0.029**
THF-solvates	11	2.324	0.017	36	2.395	0.030
1,2-Dimethoxyethane				26	2.377	0.039

molecules with neutral oxygen ligand atoms, and thus a deviating size (Lundberg *et al.*, 2010). It is therefore necessary to first determine the radius of the THF oxygen, which can be done by subtracting the radii of lithium or sodium from Li-O_{THF} and Na-O_{THF} distances respectively:

Four-coordinated lithium

$r_{OTHF} = d_{Li\text{-}OTHF} - r_{Li+} =$ 1.918 Å - 0.601 Å = 1.317 Å ≈ 1.32Å

Six-coordinated sodium

$r_{OTHF} = d_{Na\text{-}OTHF} - r_{Na+} =$ 2.395 - 1.072 Å = 1.323 Å ≈ 1.32 Å

This radius can now be used to deduce to the potassium ion radius in six- and seven-coordination by subtraction from K-O_{THF} distances.

Proposed ionic radii are summarized in Table 5, where those of cesium and rubidium only have values from aqueous solution and that of francium is estimated by two approaches similar to the previously applied (Ahrens, 1952) but using more recent radii for metal ions, with a preference for those determined in aqueous solution (Paper I; Lindqvist-Reis *et al.*, 2006; Lundberg *et al.*, 2010; Persson *et al.*, 1995; Persson, 2010; Torapava *et al.*, 2009). The estimation is further decribed in appendix II. The determination of coordination numbers of rubidium and cesium, not to mention francium, is difficult due to the lack of relevant crystal structures. In Paper I, coordination numbers of eight were suggested for both ions, but the uncertainty is much higher than for the smaller alkali metal ions.

By plotting ionic radii as obtained from solution against their primary quantum number, the graph in Figure 19 is obtained. The values for Li^+ have been taken from the crystal structure database search and corrected with +0.02 Å to better represent a value in aqueous solution. Without suggesting a physical significance, it is interesting to note that the ionic radii for lithium to cesium can be modeled with a simple second degree polynomial. Without lock-

Table 5. *Proposed ionic radii in Å for the alkali metal ions. Denotion (s) represent a value from crystal structures, (aq) is determined in aqueous solution and (est) is estimated.*

	4-coord.	5-coord.	6-coord.	7-coord.	~8-coord.
Li^+	0.60(s)		0.79(s)		
Na^+		1.02(s)	1.07(s)/1.09(aq)		
K^+			1.38(s)	1.46(s)/1.47(aq)	
Rb^+					1.64(aq)
Cs^+					1.73(aq)
Fr^+					~1.79(est)

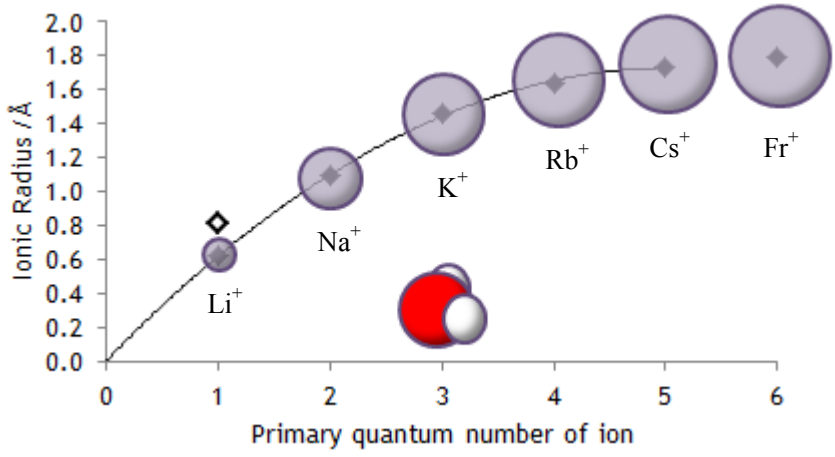

Figure 19. Proposed ionic radii as a function of the primary quantum number of the alkali metal ions, based on experimentally measured M-O distances. The Fr^+ radius is estimated. For Li^+, the values from the database crystal structure survey have been used, after adding 0.02 Å to better simulate aqueous solution. Six-coordinated Li^+ is shown for comparison as an open diamond. The different sizes of alkali metal ions are also visualized and compared to a water molecule.

ing the intercept, the trend line is extrapolated to origin, where a hypothetical electron free proton would be located. This occurs however only if the value for four-coordinated lithium is used. The value of the francium ion appears to be somewhat high when comparing to the shape of the curve, but this ion is on the other hand the only one with inner shell f-electrons. It requires more than a dash of imagination to discern a similar effect for the rubidium and cesium ions, being the first ions with inner shell d-electrons. The difference in radii for the larger alkali metal ions appear small, but as surface area and volume are second and third degree polynomial functions of r, the relative difference in charge density will be larger. Measurements in the aprotic solvent dimethyl sulfoxide, DMSO, confirmed the radii in aqueous solution. No well-defined solvation shell was observed around the iodide ion in DMSO.

The effect on water structure from alkali metal ions

In Paper I, the weak hydration of alkali metal ions was illustrated by use of double difference infrared spectroscopy, DDIR. Lithium was the only ion for which a second hydration shell could be discerned. The sodium, potassium, rubidium and cesium ions all gave rise to very similar affected spectra in solutions of the iodide salts, underlining a similar hydration behavior for these ions. Lithium iodide is not sufficiently soluble to be studied, but tests with lithium and sodium perchlorate solutions indicate that the lithium ion has a very different hydration. The alkali iodide spectra could be interpreted as if the

small cationic contribution declines down through group one, being extinguished when arriving to cesium iodide. However, the intensity of the cationic peaks appeared low in comparison with the iodide anion, probably due to insufficient peak separation. With this ambiguity remaining, over-interpretation of the alkali iodide spectra must be avoided.

It can be seen in the spectrum of a sodium perchlorate solution that the sodium ion behaves as a structure breaker. More specifically, the sodium perchlorate solution spectrum shows that HDO molecules in the hydration shell of a sodium ion are less affected by their environment, than HDO molecules in the bulk. This is not intuitive considering the presumed longer reorientation times of water molecules in the hydration shell of a sodium ion as compared to a molecule in the bulk (Marcus, 2009; Rodnikova, 2003). To say that molecules are less affected by their environment than HDO molecules in the bulk is not the same as claiming that the interaction with the ion is weaker than the interaction between two bulk molecules. An O-D oscillator in the bulk may be affected from three directions - two from the oxygen side and one from the deuterium side. Geometrical limitations might restrict the interactions of the hydration shell HDO molecule to only two directions - towards the ion and from the deuterium.

The results of Paper I are in general agreement with previous DDIR on alkali hexaflurophosphates (Smiechowski *et al.*, 2004) but interpretations differ slightly. For example, the authors in that study consider the coexistence of four- and six-coordinated lithium. No such indication can be seen when comparing our spectra at different concentrations. Also, the large difference in metal-oxygen distances for four- and six-coordinated lithium, Tables 3 or 5, makes it appear unlikely that the existence of both coordination states simultaneously would be energetically identical.

It has been suggested that the boundary between negative hydration and hydrophobic hydration is a hypothetical univalent ion with a 3.3 Å radius (Rodnikova, 2003). This would suggest that the francium ion is a structure breaker in the same way as the other larger alkali metal ions.

5.1.2 Orthotelluric acid, arsenous acid and arsenic acid species

Structural properties of species from the arsenic oxyacid systems have been reported in Paper II, along with studies on orthotelluric acid, $Te(OH)_6$. In an investigation with XANES, inorganic white line maxima differed by 4.0 eV for arsenic oxyacid species with the same charge but different oxidation state, Table 6. The shapes of the spectra were almost identical within an oxidation state. The neutral species $As(OH)_3$ and H_3AsO_4 deviate slightly, with a barely visible smoothening in the shape. XANES spectra for the organic arsenate

MMA^V and DMA^V present as $CH_3AsO_3^{2-}$ and $(CH_3)_2AsO(OH)$, respectively, were also produced. White line maxima are observed at slightly lower values, about 1 eV, than those of inorganic arsenic(V) species, as shown in Table 6. Shape also differs for these organic oxyacids, being somewhat less well-defined and with lower relative white line intensity.

Table 6. *White line maxima in eV for arsenic oxyacid species in varied states of protonation. *Literature data from (Smith* et al*., 2005b); ** Reported value for trivalent arsenic was obtained at pH 9, and thus speciation is unclear (Figure 6). MMA^V refers to $CH_3AsO_3^{2-}$ and DMA^V refers to $(CH_3)_2AsO(OH)$. Both decimals of the peak positions are probably not valid, but shown to highlight the small deviation in difference.*

Species	Peak	Literature*	Species	Peak	Literature*	Diff V-III
H_3AsO_4	11875.54		$As(OH)_3$	11871.53	11871.7**	4.01
$H_2AsO_4^-$	11875.22	11875.3	$AsO(OH)_2^-$	11871.22		4.00
$HAsO_4^{2-}$	11875.26					
AsO_4^{3-}	11875.43		AsO_3^{3-}	11871.43		4.00
Mean As^V	**11875.36**		**Mean As^{III}**	**11871.39**		
MMA^V	11874.4	11874.1				
DMA^V	11874.6	11873.3				

Interatomic distances

Interatomic distances in solution can be obtained by extracting the EXAFS wave from the XAS data. A geometrical model is built and data analysis performed with the program packages EXAFSPAK (George & Pickering, 2003) and GNXAS (Filipponi & Di Cicco, 1995). The influence from different scattering paths with respect to phase and amplitude are calculated by the FEFF7 program (Zabinsky *et al.*, 1995). The model is refined with respect to scattering path length, amplitude and energy until theoretical waves agree with the measured ones.

The phases of EXAFS waves are quite different between the two oxidation states. Species of different protonation state within the same oxidation state, however, are very much in phase. This is not unexpected, considering the previously mentioned similarity of XANES spectra. The resolution of the EXAFS technique does not allow differentiation between protonated and unprotonated oxygen atoms but waves in phase indicate the same average As-O distance within an oxidation state. The EXAFS waves for the organic species MMA^V and DMA^V are out of phase due to the presence of both As-O and As-C bond distances, where the latter are about 0.18 Å longer, Paper II.

The difference in average As-O bond length between inorganic arsenic(V) and arsenic(III) species turns out to be 0.10 Å as calculated for each

protonation state. The organic arsenic(V) species have very much the same average intramolecular As-O distance (1.71 Å) as the inorganic ones, independently of the number of methyl groups. The average As-C distance (1.89 Å) was also independent of the number of methyl groups. Within an oxidation state, all As-O bond lengths are very similar. Intramolecular As-O distances are shown in Table 7 together with data from the crystal structure database survey. Results for $As(OH)_3$ have been compared with an oversaturated 0.5 M solution obtained from As_2O_3, as shown in the supporting material of article II. The spectra are identical and there are no indications of species such as As_4O_6 or $As_3O_3(OH)_3$ as suggested by (Tossell, 1997).

A thorough investigation of As-O bond distances in crystals containing species from the arsenic acid system have been made by searching the databases CSD (Allen, 2002) and ICSD (*Inorganic Crystal Structure Database*, 2009). The four As-O distances have been sorted in increasing order for each of the four species AsO_4^{3-}, $HAsO_4^{2-}$, $H_2AsO_4^-$ and H_3AsO_4. This is shown in Figure 20 and average values are given in Table 7. Structures failing Grubbs' statistical test for outliers have been excluded from calculations not to incriminate them of necessarily being wrong, but to facilitate a general interpretation. Such structures are shown as crosses in Figure 20. The As-O bond length depends on whether the oxygen atom binds a hydrogen atom or not. The bond from arsenic to non-protonated oxygen atoms is shorter, both for charged and uncharged oxygen atoms.

The fully deprotonated arsenate ion, AsO_4^{3-}, have similar bond lengths for the occurring four distances, reflecting its symmetrical shape (upper left part of Figure 20). As all oxygen atoms are deprotonated, they all fall on the short distance level. The $HAsO_4^{2-}$ ion has one protonated oxygen atom and it can be seen in upper right part of Figure 20 that it is substantially longer than the other

Table 7. *Results for the crystal structure database search regarding inorganic arsenic(V) oxyacid species. The long level represent the three longest As-O distances for H_3AsO_4, the two longest As-O distances for $H_2AsO_4^-$ and the longest distance for $HAsO_4^{2-}$. Other As-O distances fall on the short level. The last column show the As-O distances as determined in aqueous solution.*

	No of crystal structures	Short/Å	Long/Å	Average/Å	Stdev/Å	Experiment (aq) /Å
H_3AsO_4	10	1.641	1.686	**1.674**	0.009	**1.703**
$H_2AsO_4^-$	38	1.655	1.708	**1.681**	0.004	**1.707**
$HAsO_4^{2-}$	10	1.670	1.736	**1.687**	0.005	**1.708**
AsO_4^{3-}	9	1.674	-	**1.674**	0.012	**1.706**
$As(OH)_3$						**1.802**
$AsO(OH)_2^-$						**1.801**
AsO_3^{3-}						**1.798**

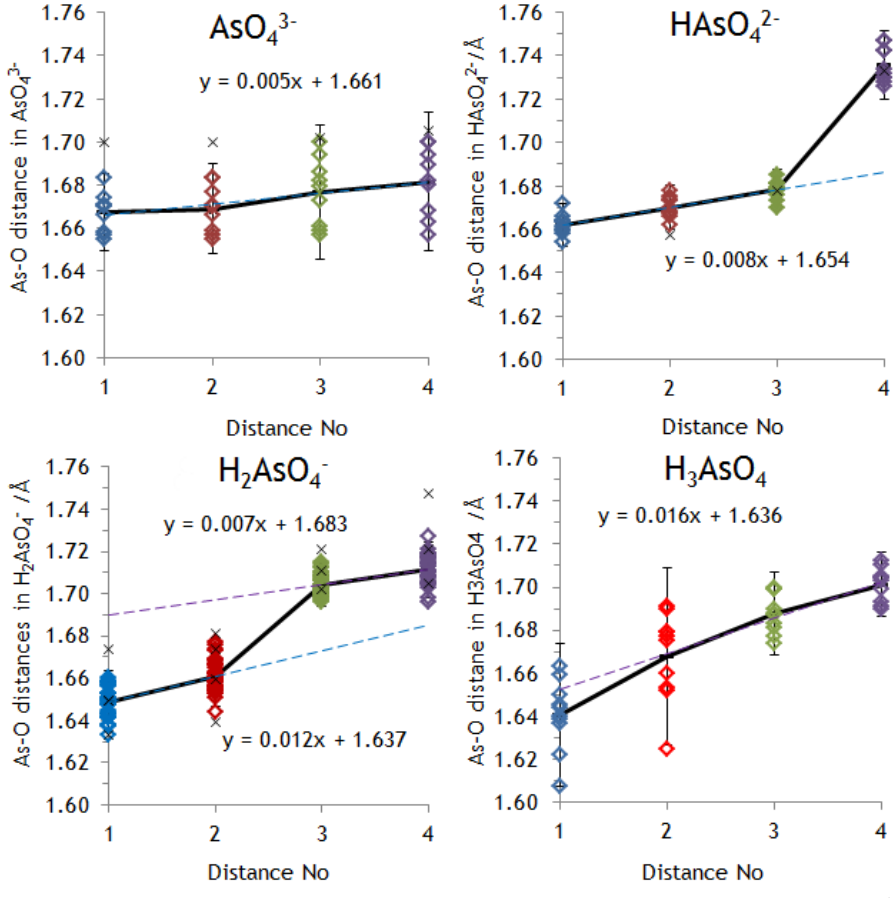

Figure 20. The four As-O distances obtained for a number of crystal structures containing AsO_4^{3-} (upper left), $HAsO_4^{2-}$ (upper right), $H_2AsO_4^-$ (lower left) and H_3AsO_4 (lower right) species. Distances are sorted as shortest (blue), second shortest (red), second longest (green) and longest (purple). Structures failing a recursive Grubbs' test for outliers are shown as crosses. In these cases, all distances of a structure have been excluded if one failed the test. The black line connects average values for each distance. A blue dashed line show the trend for short level distances and a purple dashed line show the trend for long level distances.

distances. Moving on to $H_2AsO_4^-$, two distances fall on the long (protonated) level and two on the short level. The difference between the two obtained trend lines connecting averages is about 0.03-0.04 Å. The structures of H_3AsO_4 have three atoms on the long level, although the difference towards the short level is much less pronounced than for the other species. The slopes of the long level trend lines increase 0.005 to 0.008 to 0.012 with increasing protonation, Figure 20. Similarly, the short level trend lines increase from 0.007 to 0.016 with increasing protonation. It can also be seen that the standard deviation is substantially lower for $HAsO_4^{2-}$ and $H_2AsO_4^-$, reflecting the relative stability of

these crystallized compounds in comparison with species dominating on very low or high pH. References for the crystal structures can be found in Paper II.

Perhaps somewhat counter-intuitive, Table 7 shows that even though structures on both the longer and shorter distance level increases with increasing charge, they are weighted together to give approximately the same average As-O bond length. The system appears to compensate a high deviation from the mean from of one As-O distance by allowing the other distances to deviate less. More information about all referenced structures can be found in the supporting material of Paper II.

The resolution of the EXAFS method is not sufficient to differentiate between short and long level bonds in aqueous solution, but the average seems to be rather independent of the species' charge. The experimentally determined As-O distances in solution are about 0.02-0.03 Å longer than the average of corresponding crystal structures, Table 7. This is in agreement with observations of other anions such as perchlorate (Jalilehvand *et al.*, 2001) sulfate (Vchirawongkwin *et al.*, 2007) and sulfite (Eklund *et al.*, 2012).

It was not possible to deduce As-O bond angles in the AsO_3^{3-} and $As(OH)_3$ species from EXAFS data as the influence of the As-O-O scattering path was negligible in comparison to intramolecular bond distances. The distance between the arsenous acid oxygen atoms would have to be determined with some degree of certainty in order to extract such angles. In one relevant crystal structure, intermolecular angles are 104.8°, 98.5° and 100.3°with an average of 101.2°, where the largest value represent the angle between charged oxygen atoms with shorter bond distance (Sheldrick & Häusler, 1987). Bond lengths have also been determined for the arsenic(V) species AsO_4^{3-} and for the arsenic(III) species $AsO(OH)_2^-$ by large angle X-ray scattering, LAXS, as shown in Paper II. The value for the former is in excellent agreement with EXAFS results and the value for the latter show only a minor deviation. By comparing recurring distances as determined by LAXS, As-O-(H)O angles of 120 and 122º (Figure 21) can be calculated by the cosine theorem for AsO_4^{3-} and $AsO(OH)_2^-$ respectively. This is an indication that two water molecules on average are bound to each oxygen atom. One drawback of this calculation is that the O···(H)-O distances are uncertain due to their proximity to bulk water O-O distances. Nevertheless, the obtained angles differ substantially from the 109.5º representing three-coordination and the 180º representing one-coordination. Neither the LAXS nor EXAFS data contained signs of water interactions with the As lone pair of arsenic(III) species. A recent computer simulation of the sulfite ion indicate interesting features of the lone pair but support the absence of well-defined electrostatic interactions with water (Eklund *et al.*, 2012).

There is a lack of relevant crystal structures containing the arsenite ion. When trivalent arsenic is present with low charge density cations, it appears to prefer crystallization as linear chain meta-arsenite ions, $[AsO_2^-]_n$ rather than as ortho-arsenite, AsO_3^{3-}. The latter form appears when counter ions have high charge density. However, high charge density also causes high lattice energies, making the compounds unsuitable for comparison with aqueous solution regarding bond lengths and angles.

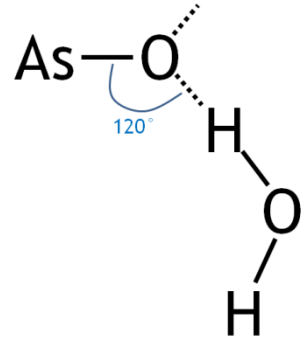

Figure 21 As-O-(H)O angle.

Similarly to the case with inorganic arsenic(V) species, a crystal structure database search of organic species have been performed and differentiation between structures on the forms $RAsO(OH)_2$ and $R_2AsO(OH)$ have been made. Similarly to the survey of inorganic arsenic(V) oxyacid species, two distinct As-O distance levels can be seen for $RAsO(OH)_2$. Average distances were 0.02 Å shorter than found in aqueous solutions of $CH_3AsO_3^{2-}$ and $(CH_3)_2AsO(OH)$.

The Te-O distances in orthotelluric acid, $Te(OH)_6$, have been determined by LAXS. It is advantageous to determine the structure of neutral species, as counter ions are absent. The octahedral structure shown in Figure 22 was confirmed and a Te-O distance of 1.940 Å was determined. This is similar to previous work in aqueous solution (Andersson *et al.*, 1981), and about 0.02 Å longer than in solid phase as determined by crystallography or solid phase EXAFS in referenced studies from Paper II.

The number of water molecules hydrating the atoms of the oxyacid is related to the hybridisation of these atoms. Pure sp^3 hybridisation represents a tetrahedral structure around the atom with 109.5° angles, while sp^2 represents a trigonal planar structure with 120° angles. The Te-O-H oxygen atoms are affected by the covalently bound hydrogen atoms but also by primarily electrostatic bonds of hydrating water molecules. Obtained distances from LAXS can be used to calculate angles between the tellurium atom, the hydroxyl oxygen and hydrating oxygen atom. This angle is found to be 118.6°, indicating that approximately two water molecules are bound to each hydroxyl group. Analogous to $AsO(OH)_2^-$, a possible flaw with this reasoning is that the position of the covalently bound hydroxyl hydrogen may set a specific angle, making it harder to deduce true hydration numbers. Nevertheless, the number is far from the 109.5° of a tetrahedral angle. Would the Te-O-H angle be the determining factor, an angle close to 112° would be expected as indicated in the crystal structures referred to in Paper II.

Effect on water structure

As there is no counter ion for the neutral orthotelluric acid, it is particularly advantageous to study this species with the DDIR technique. The resulting affected spectrum will only depend on the HDO molecules in the hydration shell of the $Te(OH)_6$ molecule. It could be seen that HDO in the hydration shell of telluric acid are more affected by their environment than bulk molecules. In other words, orthotelluric acid is a weak structure maker.

Being an acid, the hydroxyl dipole should have a larger charge separation than an ordinary water dipole, which would explain why water molecules form stronger bonds to the $Te(OH)_6$ molecule than to another water molecule in solution. In fact this reasoning can be used to argue that the hydroxyl groups of all neutral oxyacids are structure makers. Other parts of such molecules may still be hydrophobic though. The increased charge separation of the hydroxyl group relative to a water molecule, should affect the hydrogen side more if considering a relative change in electron density. Therefore, the hydrogen side of the hydroxyl group, rather than the oxygen side, should be more likely to be hydrated, Figure 22. It has to be kept in mind though, that these species are still weakly hydrated and the distributions of hydration numbers as well as O/H hydration sites are likely to be large. Both $Te(OH)_6$ and $As(OH)_3$ are weakly acidic oxyacids, neutral over a wide range. Therefore it is possible that the former can be used as a model compound for the latter.

Arsenous acid is less soluble in water than telluric acid as $As_2O_3(s)$ may precipitate at a concentration around 0.2 $mol \cdot dm^{-3}$ (Puigdomenech, 2004, 2009). Due to this lower concentration, the affected spectrum has low S/N ratio and is less certain, as shown in the supporting material of Paper II. Even if the affected number is presumed to be wrong, Paper II, the observation that the spectrum have the same general shape as $Te(OH)_6$ is probably correct. This indicates that the species have a similar effect on the water structure, despite the presence of a lone pair in arsenous acid, which presumably is surrounded by a clathrate like structure of water molecules. The derivatives with respect to concentration is very similar for $Te(OH)_6$ and $As(OH)_3$ and as they are obtained from raw

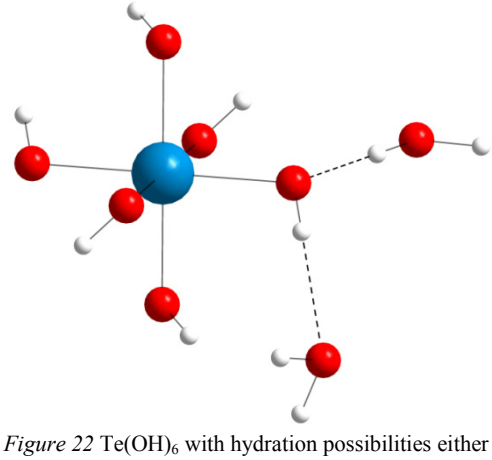

Figure 22 $Te(OH)_6$ with hydration possibilities either at the hydroxyl oxygen or at the hydroxyl hydrogen.

data, they do not depend on a chosen affected number. Analogous with the discussion about $Te(OH)_6$, hydration at hydroxyl hydrogen atoms should be favored. Arsenous acid is an even weaker acid than telluric acid with respect to the first acid dissociation constant and charge separation on hydroxyl atoms should be smaller.

5.2 Applied research

This work can be seen as start of a larger project, with the long term goal to develop a cheap and efficient cleaning method for tube-well drinking water in northern Burkina Faso. For the success of such a method, it is necessary that it is fast and sufficiently efficient to be easily manageable. A low-technology solution is preferred considering the sometime rough conditions in the area of interest. One solution could be an adsorption column with a bed of course particles, through which water is rapidly filtered by gravity. The principles behind the adsorption of arsenic oxyacid species onto iron oxyhydroxide based adsorbents have been studied in Papers III-IV with respect to parameters such as time, pH and competing ions.

5.2.1 Adsorbents

Among inorganic arsenic adsorbing materials, the iron oxyhydroxides are probably the best ones, considering efficiency, availability and non-toxicity. Arsenic can also react with sulfur atoms of proteins and therefore organic materials can be considered for arsenic removal (Fox *et al.*, 2012; Teixeira & Ciminelli, 2005). However, such adsorbents are perhaps more suitable for waste water treatment, as the microbial activity of wet organic material may be unhealthy for humans.

Our investigation in Paper III as well as previous studies show that iron oxyhydroxide based column adsorbents would be a possible choice in a full scale decontamination filter. As much as one would like to use the large surface area of tiny iron oxyhydroxide particles in suspensions, it is not a feasible approach for a system out of lab scale. Sand particles coated with iron oxyhydroxides can be considered, as can current commercial agents such as GFH®. Yet an option is adsorbents produced from local available materials such as iron rich clays.

Coated sand

Many of the laboratory columns in the project were filled with sand covered by ferrihydrite. The actual mineralogy of the coating was confirmed by Fe K-edge EXAFS. By comparing EXAFS spectra of known minerals, it is possible to

determine mineralogy for an unknown sample even if the matrix is unsuitable for other analyses. Analyzing a sample which had been aged for almost a year indicated a partial change in mineralogy, and this could affect results of different tests with the same material. Iron content could be measured by dissolution in hydrochloric acid and subsequent AAS measurements. Different routes of coating turned out to give rather different results as far as iron content was concerned. Scanning electron microscopy has been applied to the samples of coated sand, Figures 23-24. The grain shown in Figure 23 is a sample of somewhat lower coating, chosen to also show the grain surface next to the coating flakes. More images can be seen in the supplementary material of Paper III. Energy Dispersive Spectroscopy, EDS, connected to the scanning electron microscope showed a substantially increased iron content not only in the coating flakes but also on the seemingly uncovered area next to the flakes. This explains why arsenic removal is not proportional to iron content, Paper III.

If some kind of iron oxyhydroxide coated material would be utilized in a full scale application in Burkina Faso, the setup of a larger coating facility is probably required. Sand is locally available and required chemicals such as iron(III) nitrate and alkali hydroxides are cheap. However, the substantial work required to produce a laboratory batch of ferrihydrite coated sand would multiply when considering the amounts required for the wells of northern Burkina Faso. While mixing the chemicals is straight forward, the challenge would be to find a convenient way to lower the ionic strength to promote iron oxyhydroxide coverage. The laboratory method of several sequences of centrifugation is not suitable for up-scaling. Unfortunately the experiments have shown that too high ionic strength is detrimental for ferrihydrite coverage. One possible solution that should be evaluated is to replace hydrogravimetrical cleaning by a gentle flow of water through the newly installed column. In a best case scenario, this would allow arsenic species to adsorb also to non-coating aggregates of ferrihydrite, and hence increase capacity. If the aggregates clog the column however, this solution is not suitable.

GFH®

The commercial adsorbent GFH® can be considered as well. One drawback is a fairly high price. In a report from 2008, the price is said to be $7-14 per kilogram (Kumar *et al.*, 2008). Yet, as can be seen in Paper III and in previous studies, Table 2, the material is a very efficient adsorbent under certain conditions and could be an alternative to locally produced adsorbents. The material is however mainly produced for drinking water plants where larger quantities are used in serially connected reactors (Siemens, 2013). The flow in

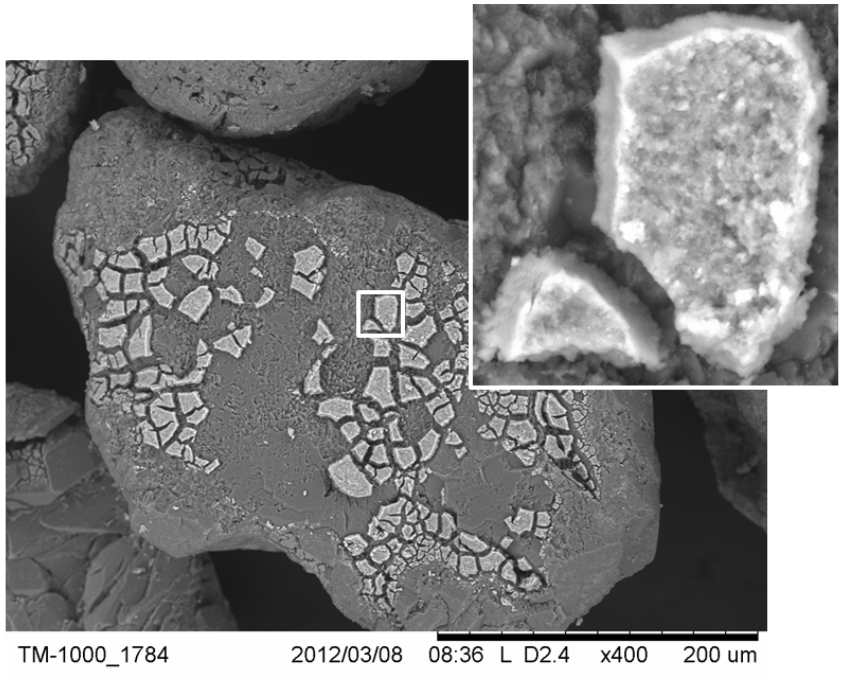

Figure 23. Grain of quartz sand partly covered with an iron oxyhydroxide coating. The scale is shown in the right bottom corner and the iron content have been determined to 2.0 mg/g.

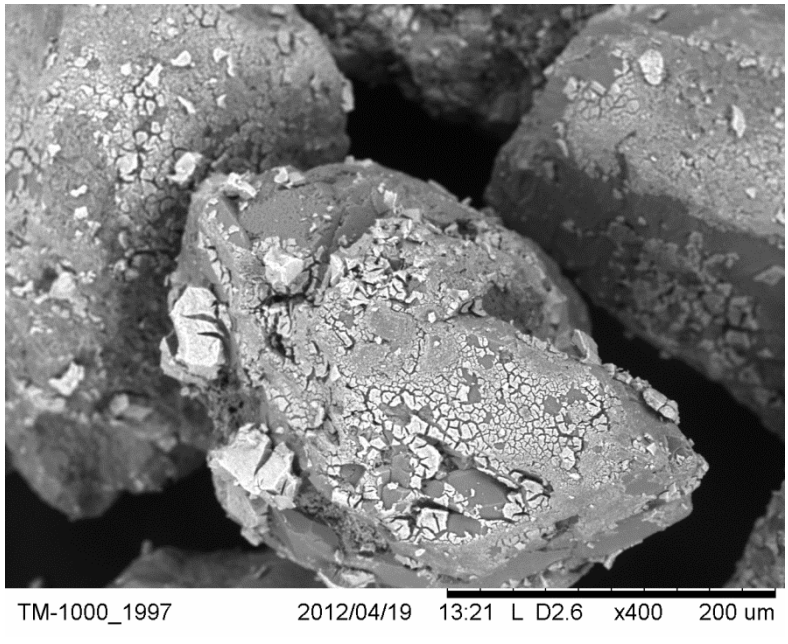

Figure 24. Coated grain of quartz sand in a sample with an iron content of 7.9 mg/g.

such reactors is low to avoid bed compaction. In the experiments of Paper III, it was necessary to rinse the material hydrogravimetrically to avoid clogging the column. Even so, pressure drop over the column increased and eventually became fairly high, as measured in mm water pillar above the bed.

The risk for bed compression should be addressed if GFH® is to be applied as an adsorbent in the problematic wells of northern Burkina Faso. This could perhaps be done by ensuring a fairly slow flow. Concerns might be exaggerated as a larger inlet area and lower flow velocity are likely in an up-scaled column.

In Paper III, the low crystallinity of GFH® was confirmed by EXAFS spectroscopy. It could possibly be an intermediate of akaganeite and ferrihydrite, although the EXAFS spectra of these minerals are quite similar. By thermogravimetric analysis, a previously reported moisture content of 46% was confirmed, and the effect of porosity was illustrated in the slow removal of water. Due to porosity, the migration of arsenic species into the bulk of the material may take some time. The relocation may continue also in periods of downtime and GFH® appears to regenerate its adsorption capacity when the column is not operational (Paper III, Westerhoff *et al.*, 2005).

Local clays

In a best case scenario, iron rich clays of local origin could be used as adsorbents to address the problem of drinking water arsenic contamination in the northern parts of Burkina Faso. At the University of Ouagadougou, a substantial knowledge about these local clays has been gathered. The University cooperates with the brick industry, and the chemical laboratory is equipped with firing furnaces and other relevant apparatuses. These local clays have previously been investigated as possible adsorbents of cationic contaminants (Pare *et al.*, 2012; 2013). Values of pH_{pzc} are rather high, 6.8-9.5, and EDS analysis also promise high iron content on the surface.

Clay consists of very fine particles, and using them directly in a column would either clog the column or substantially reduce the flow of water. An attempt was made to adsorb arsenic on bricks made out of the clay burned at 950°C without addition of manganese dioxide, MnO_2. The bricks were manually crushed and sieved into fractions whereof the grains between 0.25 and 2.0 mm were used as an adsorbent in a column. This material did not show any substantial capacity to adsorb arsenic, but it is possible that particles were to course and EBCT to short. As the fraction below 250 µm is very fine, it is unlikely to give good flow properties in a column. A fraction between 250 and 500 mm would be desirable, but a lot of work is involved in crushing enough brick material into such a well-defined range. Yet another possibility is to dope

larger pieces of local clay with iron oxyhydoxides and hopefully improve adsorption capacity. To this date, experiments have not been performed, but it is likely that a low ionic strength is crucial, as in the coating of sand particles discussed above and in Paper III.

5.2.2 Local water chemistry

Arsenic concentrations as well as other parameters may vary to a large extent between different wells, even if they are geographically close to each other (Smedley *et al.*, 2007; Some *et al.*, 2012). Authorities have closed some wells with very high arsenic concentration, although similar or higher concentrations have been measured in wells that remain open. Since water is a scarce resource in the area, it is only with great reluctance wells are closed. Upon the closing of a well, the pump handle or pedal is removed, Figure 25.

Figure 25. A closed well with arsenic concentration exceeding 150 $\mu g \cdot dm^{-3}$

Speciation and pH

Conditions in northern Burkina Faso is rather oxic and studies show that almost all of the arsenic in the problem area is speciated as arsenic(V) (Smedley *et al.*, 2007). The pH range in tube wells stretches from 5.8 to 7.8, although median pH values are neutral (Smedley *et al.*, 2007). Results from the column tests in Paper III underline the importance of pH when considering adsorption of arsenic(V) upon iron oxyhydroxides. Adsorption capacities have been defined as µg added arsenic per cubic centimeter adsorbent until breakthrough occurs, in short $\mu gAs_{added}/cm^3_{adsorbent}$. Column breakthroughs for different pH is illustrated in the upper left panel of Figure 26, and it can be seen that arsenic(V) adsorption capacities decreases substantially with increasing pH, while adsorption of arsenic(III) is largely unaffected. This is in

line with a more negative surface charge at higher pH, repelling the anionic arsenate species but not the neutral $As(OH)_3$. Batch experiments in Paper III indicated a somewhat faster adsorption of arsenic(III) compared to arsenic(V), and this have been noted before (Raven *et al.*, 1998). The lone pair of arsenous acid probably lack interactions with water as discussed in Paper II, and as previously shown for sulfite (Eklund *et al.*, 2012). Weakly hydrated ions generally move faster through a solution (Li & Gregory, 1974) and it is quite possible that the need for diffusion into porosities allows the more weakly hydrated $As(OH)_3$ to faster reach many available adsorption sites.

The pH of deionized water is somewhat acidic due to dissolved carbon dioxide, and sodium hydroxide has been added to achieve pH around 6.5. It is difficult to achieve a stable neutral pH in this kind of solutions without using a buffer, which in itself would disturb the adsorption system. As pH first increases to the alkaline side before stabilizing after a few days, it is likely that the solutions contained substantial amounts of hydrogen carbonate. It cannot be excluded that, in addition to the effect of higher hydroxide ion concentrations, the prevalence of hydrogen carbonate could also contribute to the reduction in arsenate adsorption at higher pH.

Column studies with water plant water around pH 7.6 showed a similar adsorption behavior for arsenic(III) and arsenic(V) (Thirunavukkarasu *et al.*, 2003a, 2003b). The fact that adsorption capacity differs to such a large degree depending on pH, is one of the reasons why estimating the adsorption capacity in a pilot filter is complicated. Another one is the eventual presence of competing species.

Phosphate content

In a previous investigation, phosphorus concentrations stretches from < 20 to 282 $\mu g \cdot dm^{-3}$ with a median of 26 $\mu g \cdot dm^{-3}$(Smedley *et al.*, 2007), although there are indications of several hundred $\mu g \cdot dm^{-3}$ in many wells nearby (*unconfirmed*).

In the experiments of Paper IV, phosphate is added to the columns with ferrihydrite coated sand together with arsenate. It was shown that phosphate adsorbs to roughly the same extent as arsenate does, illustrated in the upper right part of Figure 26. That is, an equimolar addition of phosphate gives about half of the arsenate adsorption as compared to the phosphate free case. The same is true when phosphate is added together with arsenous acid, $As(OH)_3$. It is notable that even though arsenic adsorption is decreased by roughly 50% upon equimolar addition of phosphate, the reduction differs in absolute numbers. In the phosphate+arsenic(V) case, arsenic adsorption reduction was 129 $\mu g_{added} \cdot cm^{-3}{}_{adsorbent}$ while it in the phosphate+arsenic(III) case was 75

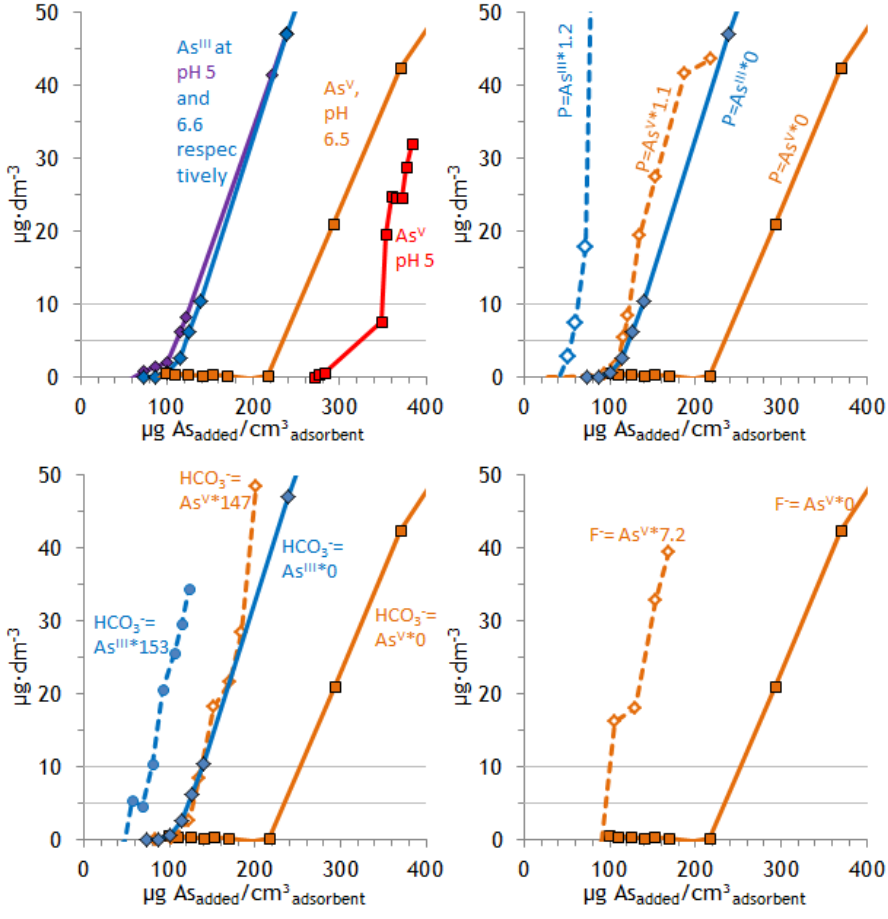

Figure 26. Arsenic(III) and arsenic(V) breakthrough curves for different pH and competitors, as stated in the graphs. Where not stated otherwise, pH is close to 6.5. For a more complete discussion, see Paper III and IV.

$\mu g_{added} \cdot cm^{-3}{}_{adsorbent}$. This could either be due to increased phosphate adsorption relative to the phosphate+arsenate(V) case, due to lower utilization of available surface groups or by a combination. Arsenic(V) adsorption is affected by pH (and indirectly by surface charge) to a higher degree than arsenic(III) adsorption, as seen in the upper left part of Figure 26. The surface charge may differ substantially between a fresh ferrihydrite surface, a ferrihydrite surface approaching arsenic(V) saturation and a surface approaching arsenic(III) saturation. Adsorption of both arsenic(III) and arsenic(V) reduces surface charge (Jain *et al.*, 1999), which should mean that the negativly charged arsenic(V) anions would be more negatively affected than the neutral arsenous acid molecules as saturation is approached. While it has not been tested, it is

reasonable to think that the phosphate oxyanions would be affected in much the same way as arsenate oxyanions.

In judging adsorption competitor efficiency, these column experiments have an advantage over batch experiments: with short empty bed contact times, adsorption will dominate over slower sorption processes such as the build-up of surface precipitate and mineral formation. In Table 8, data from the tests are given. The first column shows the molar ratio of phosphorus to arsenic. The second show observed arsenic adsorption capacities as µg added per cubic centimeter of adsorbent. The third column is the hypothetical total adsorption, if the competitor is an equally efficient adsorptive as arsenic. It is calculated by taking the value in the former column and multiply it with (1+P:As). Finally, sorption limiting units, or SLU, is a measure of the competitor adsorption strength, and calculated by dividing the arsenic adsorption capacity of a reference solution with the value obtained in the third column. A value close to 1 means that the competitor has similar adsorption strength as arsenic while a value substantially below 1 means that the competitor has less sorption strength, and a value substantially above 1 means that the competitor is a better adsorptive, Paper IV.

In a full scale decontamination filter, it is not possible to remove arsenate without simultaneous removal of phosphate, as the adsorption behavior of the two species is too similar. This is essentially a waste of precious adsorption sites, but probably a waste that has to be accepted.

Table 8. *Competitor experiments with phosphate presented together with reference samples without phosphate. P:As is the amount of phosphate compared to arsenic on a molar basis. The next column is the adsorption capacity measured as µg added arsenic per cubic centimeter of adsorbent, until breakthrough occurs. The As+P column is the former column multiplied with (1+P:As). SLU*, sorption limiting units, is a measure of the competitor strength, see text above.*

	P:As	As $\mu g_{add}/cm^3_{ads}$	As+P (as As) $\mu g_{add}/cm^3_{ads}$	SLU*
As(V)	1.1	123	257	0.98
As(V)	0	253		
As(III)	1.2	63	140	0.98
As(III)	0	137		

Hydrogen carbonate content

In Paper IV it could be seen that hydrogen carbonate is not at all is as efficient as arsenic(V) or arsenic(III) in adsorbing to ferrihydrite coated sand, and the breakthrough curves are shown in the lower left panel of Figure 26. Although valid only under a certain set of conditions, the obtained SLU value was as low as 0.01. However, when this is seen in the light of the high concentrations of

hydrogen carbonate that can occur in nature, it is clear that hydrogen carbonate can be a fierce competitor for adsorption sites. In batch experiments with ferrihydrite suspensions, a lower adsorption reducing effect from hydrogen carbonate was noticed in comparison with column experiments, indicating that kinetic hindrance of hydrogen carbonate desorption could be responsible for the observed decrease in arsenic adsorption on the column. This could however not be confirmed in batch experiments with ferrihydrite coated sand. In the investigation by Smedley *et al.*, hydrogen carbonate content in Burkina Faso stretched from 25 to 346 $mg \cdot dm^{-3}$ with a median of 191 $mg \cdot dm^{-3}$ (Smedley *et al.*, 2007). If the SLU values obtained are valid under real conditions, i.e. if there is no kinetic effect to be improved by longer empty bed contact times, it would mean a substantial reduction in arsenic adsorption capacity.

Fluoride content

The fluoride ion is a small and hard anion (Pearson, 1963), isoelectric with the hydroxide ion. It is therefore plausible that it forms strong inner sphere surface complexes. Tests in Paper IV gave an SLU value of 0.31, proposing an intermediate adsorption affinity between phosphate and hydrogen carbonate. The arsenate breakthrough curve is shown in the lower right part of Figure 26. While fluoride content in the tube well water of northern Burkina Faso is by no means extreme or even particularly high, it can be noted that the highest concentration was found together with the highest arsenate concentration (Smedley *et al.*, 2007). While no particular correlation was seen for the majority of samples, it is worth considering the fact that iron forms strong water soluble complexes with fluoride. Comparisons between ~1 h batch experiments and ~48 s column experiments indicated that the decrease in arsenate adsorption observed in column tests may have kinetic causes. In fact adsorption capacity in batch tests with ferrihydrite coated sand appeared to increase somewhat due to the addition of fluoride, Paper IV. One possibility is that the presence of fluoride causes a more dynamic surface situation where iron ions of the surface is in equilibrium with soluble iron-fluoride complexes, and thereby facilitates migration into the bulk material.

5.2.3 Additional sorption behavior

In addition to the adsorption studied in column experiments, it is possible that the porous material GFH® show additional sorption behavior. Batch experiments have been performed in which GFH® was shaken together with solutions of arsenic(V) or arsenic(III). Before addition of the arsenic solutions, pH was adjusted with potassium hydroxide or nitric acid to obtain a pH varying over a range relevant for drinking water. pH was also measued after the samp-

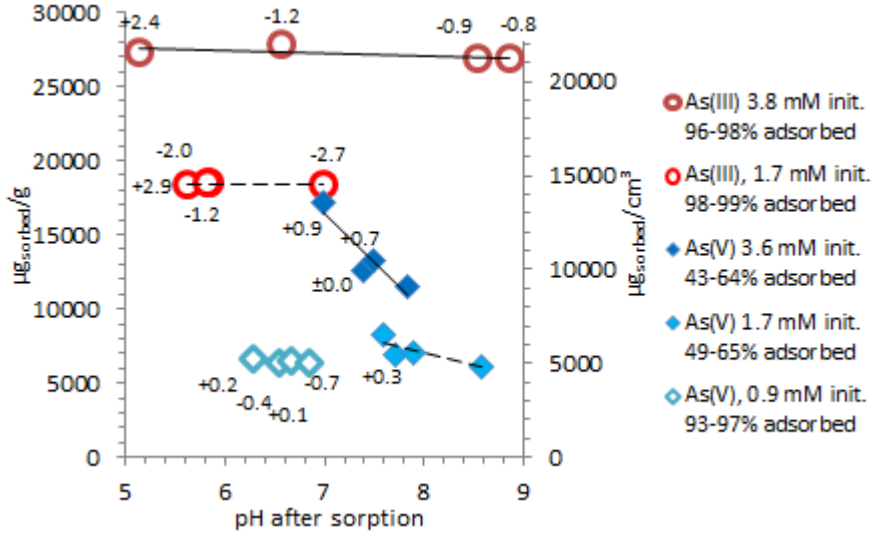

Figure 27. Batch experiments in which GFH® have been shaken together with solutions of arsenic(V) or arsenic(III). Diamonds represent arsenic(V) while circles represent arenic(III). Open markers represent samples where sorption was more than 90%, which is unfortunate from an interpretations perspective. The pH scale refers to the pH after sorption reactions. Numbers written next to sample points informs about the change in pH during the sorption reactions, i.e. in the upper left sample pH increased 2.4 units from 2.8 to 5.2.

les was shaken for 16 h. After centrifugation, arsenic content was measured by Atomic Absorption Spectrophotometry - Graphite Furnace, and results are shown in Figure 27. In several of the measurement series, very high percental sorption was obtained and the ratio between arsenic solution and the amount of adsorbent have apparently been mis-estimated. The amount of sorbed arsenic is shown as function of pH, and presented both as $\mu g_{sorbed}/g_{adsorbent}$ and as $\mu g_{sorbed}/cm^3_{adsorbent}$, with a GFH® density of 0.79 g/cm³.

While the pH scale referes to pH after reactions, the general shape of the graph remains the same if plotting against initial pH, although distributed over a wider range. It can be seen that the amount of arsenic sorbed is much higher than have been observed in columns, Paper III and Table 2. Thus the potential is also greater than indicated by columns. The higher capacity could be explained by other sorption phenomena such as surface precipitation, or it might be an effect of species migrating into the porous structure of GFH®. It is worth to notice that arsenic(III) appear to be sorbed to a much greater extent under these conditions. One possible explanation might be a greater mobility of arsenic(III), allowing it to better distribute over the entire surface - including pores - within the time of the reaction.

5.2.4 Practical consideration

The difference between laboratory experiments and a pilot or full scale column is large, but the design of the latter should build upon the conclusions reached in the laboratory. The purpose of this section is not to design a pilot or full scale column, but perhaps to identify issues to be addressed in such a task.

A chief or eldest is usually the front figure of small as well as large villages in northern Burkina Faso. Official as well as unofficial contacts with the village go via this leader, and his approval and commitment is of utmost importance for any drinking water decontamination project in the area. In a full scale implementation situation, the task of maintaining the columns or changing adsorbent would presumably be delegated by the chief to a responsible person in the village.

Desired operation conditions

It is crucial to design decontamination units in such a way that they gain a social acceptance in the rural villages of interest. Such acceptance is likely to be reached only if the system is simple to use and easy to maintain. The daily work of Burkinabe farmers does not need to be further complicated by sophisticated and time consuming water routines. Furthermore, very technically advanced solutions are likely to fail, if not due to economic reasons, then due to maintenance problems.

The adsorbent material must be efficient enough to allow operations for a substantial amount of time, in order to not be a nuisance to the maintenance man. Perhaps a month could be a goal to aim for. The changing of material should be fairly straightforward, preferable as easy as changing a cassette with adsorbent. A strong man should be able to lift and handle the cassette without extreme effort, as well as moving it a few hundred meters with the help of a wheel barrow. These requirements could probably be fulfilled with a cassette weight of maximum 30 kg. It should be kept in mind that the wet weight substantially exceeds the dry weight.

In order to save adsorption capacity of the adsorbent, it is desirable to only clean water that is actually used for drinking and cooking. Water used for personal hygiene should not be lead through the decontamination column. It should be kept in mind that the adverse health effects of arsenic in low concentrations develop during consumption of water for a long time, and the risks regarding skin contact are likely small. Much adsorbent capacity can be saved if water for farm animals can be extracted without decontamination. Much arsenic is excreted from animals through feces and urine or is accumulated in the hair of animals (Bera *et al.*, 2010; Datta *et al.*, 2010) due to protein sulfur. Arsenic excreted through urine and feces is partly metabolized

to organic forms (Datta *et al.*, 2010; Tseng, 2009). Unmetabolized inorganic arsenic have been found in milk (Datta *et al.*, 2010) but this route of exposure to humans is likely small compared to direct consumption of drinking water. In any case, the decontamination unit should be easy to connect and disconnect.

Flow and time parameters

Adsorption capacity is promoted by a large surface area, which is equivalent with small particles of the adsorbent. However, too small particle size will decrease the flow rate through the column, and possibly clog it altogether. It is likely that one of the biggest challenges of an up-scaling project will be the choice of sufficiently large adsorbents particles, without losing too much adsorption capacity. Before constructing a full scale decontamination unit, it should be considered how long additional waiting time that is acceptable. If the required time to extract 10 liters of water is 2 minutes today, is an additional 2 minutes acceptable? If longer times are required, can changed working routines be accepted by the farmers? Such changes in working routines could concern a greater cooperation between water fetchers or maybe an intermediate storage time in the unit – pump first and extract later. While there are solutions, the best probability of success for this project, is with a system which from a practical point of view involves as few complications as possible compared to the current situation.

In the experiments of Paper III, pressure drop over the column was measured as the height of the overlying water pillar. The approximate conversion to Pascal is achieved by assuming a water density of 1 $kg \cdot dm^{-3}$ and multiplying the value in mm Water pillar with 9.81 N/kg. A higher pressure from the water pillar corresponds to a higher speed through the column, but too high pressure makes the column overflow. The following relationship is valid for flow through a bed of spherical particles, and approximate through a bed of non-spherical particles (Coulson *et al.*, 1991):

$$u_c = \frac{1}{180} \cdot \frac{e^3}{(1-e^2)} \cdot \frac{-\Delta P d^2}{\mu l} \qquad \text{(Eq. 6)}$$

The superficial (apparent) velocity (m/s) through the column is denoted u_c and e is the fractional voidage – the proportion of the bed not occupied by solid material. The pressure drop is $-\Delta P$ as measured in Pascal, μ is the viscosity in $kg \cdot m^{-1} \cdot s^{-1}$and l is the length of the column in meters. The diameter of the particles in meters is denoted d, and for non-spherical particles this can be seen as the Sauter mean diameter, d_s. The Sauter mean diameter is defined as the diameter of a sphere with the same surface area as the mean surface area of the

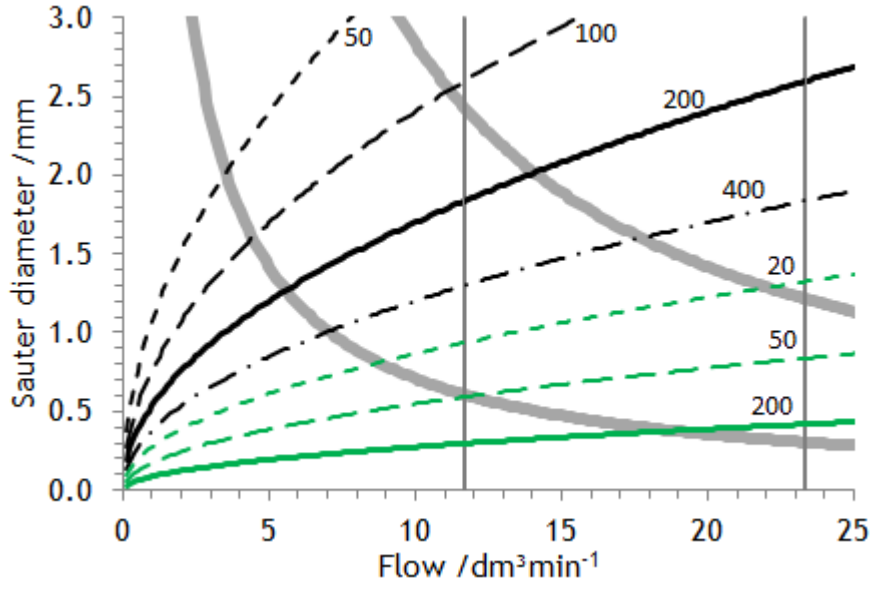

Figure 28. Relationship between adsorbent particle diameter and flow, for a particular hypothetical column as described in the text. Black lines represent a material with a fractional voidage of 0.41 and green lines a material with a fractional voidage of 0.76. Labels next to black and green lines refer to pressure loss over the column, as measured in mm water pillar. Vertical grey lines delimit an approximate depth-dependent range of flows for a Vergnet hand pump (Vergnet Hydro, 2013). Thick grey curves represent a Reynolds number of 10 (left) and 40 (right) respectively.

particles. This relationship can now be used to estimate the required particle size to fit certain desirable conditions. In Figure 28, the relationship between flow and adsorbent particle diameter according to previous equation is shown for a *particular* hypothetical full scale column. The calculations are based on an 81 cm rectangular column with a cross section area of 14.4 x 14.4 cm which corresponds to a length/hydraulic diameter ratio of 5. The viscosity of the water have been set to 0.000958 $kg \cdot m^{-1} \cdot s^{-1}$, intrapolated to 22° C from (Weast, 1975). Black curves in Figure 28 represent a material with a fractional porosity of 0.41, as in the quartz sand experiments of Paper III. Green lines represent a material with a fractional voidage of 0.76 – the suggested porosity of GFH® (Saha *et al.*, 2005). As a comparison it can be mentioned that a random loose-packing of spheres give a fractional voidage of ~0.45 and a random close-packing result in a fractional voidage of no less than 0.366 (Song *et al.*, 2008). A perfect close-packing of spheres give a fractional voidage of about 0.26 (Zong, 1999). Approximate diameters used in the tests can also be compared with Figure 28: The ferrihydrite coated quartz sand was of approximate size 0.3 mm (Figure 23 and Paper III), GFH® in the range of 0.2-2.0 mm (Driehaus

et al., 1998) and the tested brick fraction of size 0.25-2.0 mm. The relationships may be less valid for a broad size distribution, and for deviation from laminar flow. A flow through a bed of particles is considered laminar if the Reynolds number is less than 10, and fully turbulent if the flow is 2000 or more (Rhodes, 2008). In Figure 28, Reynolds-number limits for 10 and 40 respectively are shown as thick grey curves, and according to the following equation (Rhodes, 2008):

$$Re = \frac{d_p \cdot u_c \cdot \rho_{H2O}}{\mu(1-e)} \qquad \text{(Eq. 7)}$$

Symbols are the same as in as in previous formula and ρ_{H2O} is the density of water in $kg \cdot m^{-3}$.

Column experiments in Paper III showed that very short empty bed contact times were enough for substantial arsenic adsorption. The EBCT was on sub-minute scale in most tests, and in some cases as low as a few seconds. This does not mean that an equilibrium state has been reached, but neither is such a condition necessary for the current purpose of drinking water decontamination. Batch experiments showed that even with very high concentrations, almost all arsenic was sorbed after 10-25 minutes. Even while adsorption is a fast process, other sorption processes such as surface precipitate buildup and possible incorporation into the material may require longer time. Comparisions between normal length columns (five times diameter) and miniature columns (0.7 times diameter) showed that time is not completely unimportant for the capacity as measured in grams added arsenic per cubic centimeter of adsorbent before breakthrough occurs. Yet, even such a small column resulted in a comparatively fair capacity.

Columns with GFH® showed very good adsorption capacity but also a pressure drop increasing with time, Paper III. It is possible that this problem is caused by the bed support – glass wool in the experiments of Paper III. As previously noted it was also necessary to clean the GFH® hydrogravimetrically prior to use, to prevent the column from clogging. This is not required in large scale water plants. Increases in pressure drops were observed in some but not all of the coated quartz sand columns. This indicates that it is a problem for specific rather than general conditions, and a particular too compact bed support may be responsible. More bed volumes were treated in the GFH® columns, which may explain a higher increase in pressure loss.

Dimensions and design

Even if the experiments in Papers III and IV were performed in laboratory scale, it is important to discuss the construction of a full scale column. The construction of such a device is outside the scope of this project, but several thoughts and considerations will be presented below. The schematic setups in Figure 29 are only two of many possibilities. A filter internal to the pump would be complicated and expensive to install in all the affected wells. Furthermore, it would probably be complicated to change the adsorbent unit. Perhaps the most convincing reason to not install the filter inside the pump is the substantial (and perhaps impregnable) increase in pressure drop which would make collecting water a hard work. Water collection is frequently a duty of women and children and should not be made harder than necessary. Remaining is the solution that water moves through the filter by gravity. The adsorbent particle size required for this to happen within a reasonable time was discussed in previous section and Figure 28.

The height of the wellhead put limits on the possible height of adsorbent. A vertically mounted reasonable size adsorbent unit below the wellhead would leave little room for a collection vessel, such as the yellow can carried by the woman in Figure 30. The prospect of an eventual prolongation of the pump effluent tube depends on the lifting principle of the pump, but in many cases it will not be possible due to physical reasons. Therefore, a horizontal column such as the one shown to the left in Figure 29 should be considered in order to

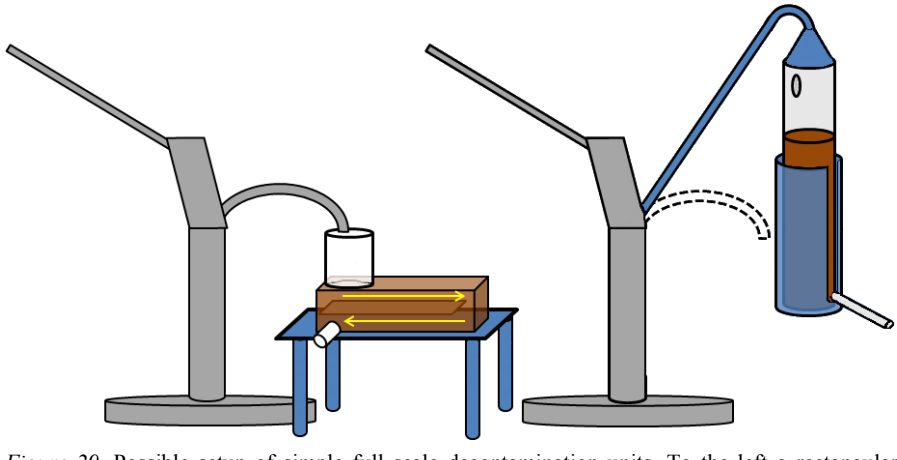

Figure 29. Possible setup of simple full scale decontamination units. To the left a rectangular horizontal column with an inner plane as discussed in the text. To the right a solution with a prolonged wellhead. The latter may no longer be possible to pump manually due to physical limitations of the lifting principle.

Figure 30: Water fetching in Lilgomdé village

save space vertically. Other constructions than the one shown is of course possible, but the shortage of vertical space should be kept in mind when designing the column. The expected life span of a 16.8 dm^3 column as a function of adsorption capacity is shown in Figure 31. This volume of the column unit is the same as previously discussed in connection with Figure 28. Filled with quartz sand as the one used in the columns of Paper III, the dry adsorbent weight would be around 22 kg and the wet adsorbent weight ca 32 kg. If the column is filled with GFH® instead, the weights decrease to about 14 and ca 25 kg respectively, calculated by dry and wet densities of 0.8 and 1.5 $kg \cdot dm^{-3}$. If it is required that the unit lasts for 30 days, the adsorbent capacity for the discussed column should be at least 357 $\mu g_{add} \cdot dm^{-3}_{adsorbent}$, with an influent concentration of 100 $\mu g \cdot dm^{-3}$ and a daily extraction of 2 cubic meters. Under ideal conditions, this could almost be achieved with ferrihydrite coated sand in the tests of Paper III, but to account for higher pH and competing ions, the substantially better adsorbent GFH® may better fit the requirements.

To further compact the adsorption unit, a possible engineering solution could be to equip the unit with an inner plane, as shown in Figure 29, to make the water travel though a longer tube unit, without taking up too much horizontal space. The possibility of vertical inner planes should also be considered. Any horizontal column must be throughly tested, to make sure that water is sufficiently dispersed through the column. In any case, adsorption units should be carefully filled for the first time, as there is a risk that air bubbles are trapped in the column. This risk could possibly be avoided by filling the column for the first time in a vertical position. Another possibility to consider is to let the top of the unit be a lid to to be closed after the filling of the column. In that case, the column could be water filled first and loaded with

adsobent afterwards, which would eliminate the risk of trapping air inside before the first use. If it turns out that the column unit dries up between uses, it might be necessary to close the effluent tube between collections. In the laboratory experiments of Papers III and IV, the bed support was Ø1 mm glass beads on glass wool. In a full scale application, a rather coarse filter such as a piece of plastic mosquito net might be suitable to stop adsorbent from ending up in the collected water. If that does happen anyway to a minor extent, no adverse health effects is to be expected as iron(III) is not dangerous in reasonable amounts and there should be very little arsenic near the effluent tube of a newly filled column. As previously mentioned, it would be desirable to be able to quickly disconnect the adsorption unit. One way to facilitate this is to equip the unit support table with wheels, not shown in Figure 29. Another possibility is to simply connect a valve to the well head, for the opportunity to collect non-filtered water through a wide hose.

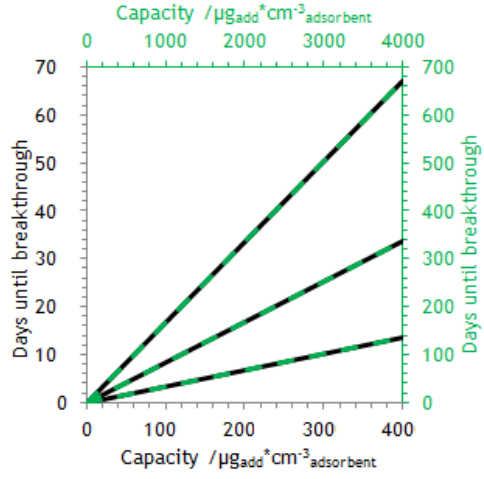

Figure 31: Time until breakthrough as a function of adsorbent capacity, for a 16.8 dm^3 column, shown on two different scales. The middle curve represent an inlet concentration of 100 $\mu g \cdot dm^{-3}$ and a daily use of 2 m^3. In the top line case, the inlet concentration decreased to 50 $\mu g \cdot dm^{-3}$ OR the daily use deceased to 1 m^3. In the bottom line case, inlet concentration increased to 250 $\mu g \cdot dm^{-3}$ OR the daily use increased to 5 m^3.

One of the greatest advantages with tube wells is that the problem of microbiological hazards in surface water and dug wells can be avoided. It would be utterly bad if a poorly designed or used adsorption unit would bring back this problem. Therefore the adsorption unit should be an almost closed system, where only necessary replacement air is let in through a filter equipped opening in the top of the column. Not shown in Figure 29, is a cover necessary to prevent contamination through the inlet hole. A thick plastic bag would be enough to protect the unit from bird droppings and similar large contaminants. If it is judged necessary to protect the unit also from air-borne bacteria, a more sophisticated cover needs to be designed. This might be to an exaggeration, considering the low population density in rural conditions. In a best case scenario, the temperature of the adsorption unit would be far from 37°C to discourage the growth of microorganisms flourishing in the human body. One

approach would be to isolate the adsorption unit to keep the temperature of tube well water. Another one, is to do the opposite – keeping the adsorbent in a thin walled transparent container which would quickly be warmed up in the sun, and then alternate with cooler temperatures during water collection or nighttime. Both approaches may pose difficulties.

Used material

An iron oxyhydroxide based adsorbent could hypothetically be regenerated by a strong hydroxide solution. Attempts have been made to regenerate ferrihydrite coated quartz columns by rinsing with 0.1 $mol \cdot dm^{-3}$ KOH but this caused high amounts of iron to dissolve and flow through the column decreased. Column regeneration has been achieved before (Thirunavukkarasu *et al.*, 2003a, 2003b) but in any case the handling of strong hydroxide solution is not likely to be suitable for a full scale application in the affected villages.

Used GFH® is typically disposed in ordinary landfill as it satisfactorily passes a Toxicity Characteristic Leaching Procedure, TCLP. However, the appropriateness of this have been questioned, as the mildly alkaline, anaerobic conditions of mature landfills may host a microbial community able to reduce the arsenic bearing iron(III) based adsorbent (Ghosh *et al.*, 2006). The disposal of GFH® or other iron(III) based adsorbents in Burkina Faso would preferably be done under oxygen rich conditions to avoid the potential risks of mineral reduction. It is also recommended that the pile of waste is separate from ordinary municipal waste, in order to limit the supply of organic electron donating compounds.

Additional effects on water

The iron concentration of the effluent have only been a few $\mu g \cdot dm^{-3}$ in the laboratory experiments, Paper III. This can be compared to a non-enforceable EPA standard of 300 $\mu g \cdot dm^{-3}$. Iron is not harmful at that level either, but may affect taste and color. In fact, it is an essential element which humans require in doses of 10-50 mg/day.

The removal of ordinary mineral ions such as sodium, potassium, halogenides and nitrate will not happen as these low charge density ions resist chemisorption. Furthermore the low concentrations with which they exist as balancing ions in the diffuse layer is negligible in comparison to their total concentrations. Neither is a substantial removal of nutrients such as calcium and magnesium likely. It is possible that others such as zinc and manganese ions is removed to some extent, but food rather than drinking water is the major source of most nutrients.

As discussed in section 2.11.1, the adsorption of arsenate species could result in a slight increase in pH and that of arsenous acid usually decreases pH unless the solution was alkaline to begin with. These effects are negligible for humans, considering the wide pH range that exists in foods.

Suggested continuous research

Laboratory experiments performed in Sweden can be seen as a pre-study to form the basis for a more practical continuation of the project. It is time to move into a stage, which can only be performed in Burkina Faso. The reason is the large amounts of native water required for the upcoming experiments, which are unrealistic to transport abroad. Fortunately, there is a deep knowledge about water management and chemistry within the Ouagadougou group, and further help can if necessary be received from the Swedish team.

Three phases can be imagined, Figure 32, whereof the first can be called preparatory. Small scale laboratory experiments would be performed at the University of Ouagadougou, but with large quantities of water fetched from the problematic area of northern Burkina Faso. These experiments would have many similarities to those performed in Papers III and IV. Perhaps it is also possible to assess the suitability of spent adsorbent disposal by measuring lea-

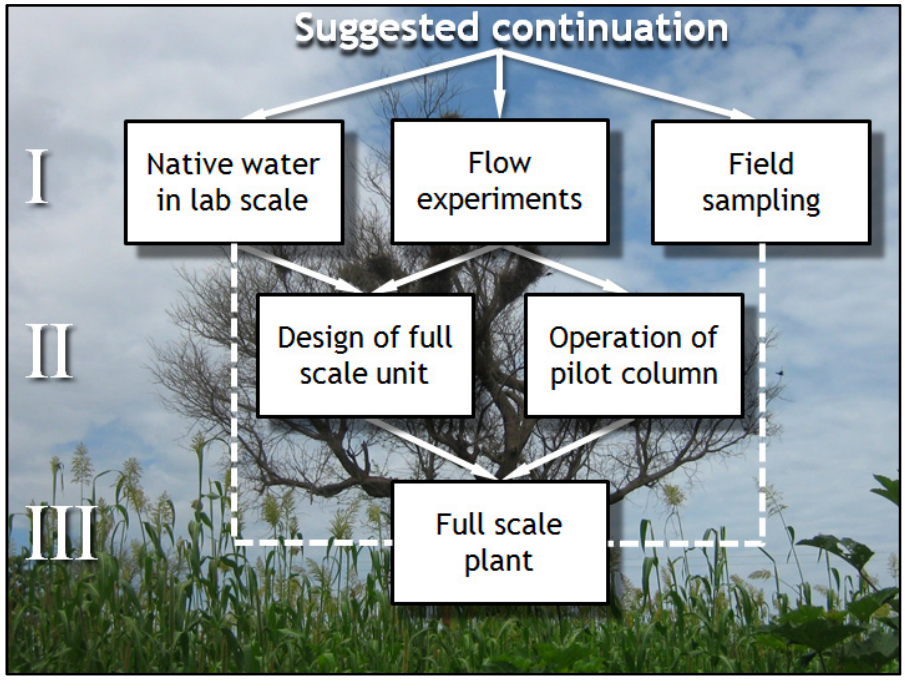

Figure 32. Three suggested phases for continuation of the project, further described in the text.

ched arsenic from laboratory scale piles. Simultaneously, experiments with flow should be performed on materials of different particle size. In order to determine factors such as residence time, flow velocity and dispersion, no particular requirements is needed for the water. In fact ordinary tap water can be used and reused for these purposes. Another factor that can be studied at this stage is the rate of drying for material inside a container. It would also be appropriate to perform additional field sampling during phase I, for example to measure the occurrence of arsenic in milk from animals consuming arsenic enriched water. In these tests it is important to choose old animals as arsenic build-up through drinking water takes time. The testing must be done on animals which do drink the tube-well water and not the unaffected water from dug wells or from surface water. As animals consume tube-well water only during the dry season, a reasonable time point for sampling would be at the later stage of the Burkina Faso dry season. If one of these animals is to be slaughtered, it could be interesting to measure arsenic in the meat. A previous investigation did not find any trace of arsenic in vegetables, although these were mainly watered with water from dug wells (Some *et al.*, 2012). In studies from other parts of the world it has been found that much arsenic taken up by plants is accumulated in the roots (Huq, 2006; Marin *et al.*, 1992; Smith *et al.*, 2008), which could mean that eventual risks are likely to be related to root crops. If judged necessary, possible further testing of plants should focus on such vegetables. Arsenic(V), dominating in the areas of interest (Smedley *et al.*, 2007), might be less bioavailable than arsenic(III) (Marin *et al.*, 1992).

Once completing phase I, hopefully preferences for adsorbent material and adsorbent particle size have crystallized. In phase II, the pilot phase, a larger pilot column can be run at the Ouagadougou laboratory facility. If too large amounts of arsenic enriched water are needed, it might be necessary to simulate water by addition of arsenic to ordinary tap water. Simultaneously as this happens, it is time to start the design of a full scale decontamination unit. Without preconceptions and with an open mind, matters discussed in 5.2.3 should be taken into consideration.

A well with high arsenic concentration, such as the one shown in Figure 33, could be used in phase III when it is time to install the first full scale decontamination unit. This could be done at an already closed well such as the one in Figure 25, although this would require substantial extra work or an automatized sampling system. In the case the full scale column would be set up at an open well, locals should be instructed to disconnect the unit when collecting water for drinking. This precaution would be done in order to make sure that the unit will not host any harmful microbial communities. It would not be responsible to open the unit for public use until such microbiological tests have

Figure 33. Wells are often located close to the fields and not necessarily in the village center

been run. As an alternative, a well which is used exclusively for other purposes can be chosen. For the building of any full scale decontamination plant, it is necessary to have the consent of the village chief. There is a local awareness of the problem and hopefully such permission will be granted. As the affected villages in the Yatenga province is located quite some distance from Ouagadougou, it might be necessary to base MSc or PhD students in the village during phase III.

Some personal reflections

Clean water should be accessible to everyone, and hopefully there is - somewhere - enough will and money to proceed in constructing full scale decontamination plants, despite the apparent challenges. The challenges are partly of fundamental character: is there sufficient adsorption capacity, is the material safe from a microbial point of view, can it be safely disposed of? Furthermore there are also a number of attitudes to be challenged. While batch experiments are less time consuming than column experiments, they don't give the results which are truly needed. While the production of scientific Papers may be faster with laboratory experiments, the most interesting and useful results are more likely to come from field experiments. I realize there is good reason why much research is conducted the way it is, and I do not acquit myself from similar approaches. Still, scientists should not be like the man who lost his home key and refuses to search outside the illuminated area below the lamp post.

Would it turn out that the approach with well-based decontamination units does not work well, it can be considered whether units on household level may be an alternative (Hussam & Munir, 2007). It is possible that the arsenic problem could also be relieved by a more complete mapping of arsenic concentrations, and where there are big differences appoint only certain wells in the village as suitable for human consumption. This might be the fastest way to decrease human intake of arsenic, although hardly a final solution. As there are indications that a large fraction of bioavailable arsenic is concentrated in the roots of plants (Huq, 2006; Marin *et al.*, 1992; Smith *et al.*, 2008), the results of such a mapping might also be taken into consideration when farmers choose which crop to plant and where.

Some tend to come up with very sophisticated technical ideas, but forget the people which will implement and use them on a daily basis. I believe that any idea which substantially complicates daily work in the village is unlikely to work out well. Despite being well-informed, the farming population of the Yatenga province would presumably risk chronical arsenic poisoning to keep reasonable working routines. This is not unlike how Europeans risk death by eating too much sugar or riding bicycles without helmets.

5.2.5 Preliminary Burkina Faso results

Days before the printing of this thesis, preliminary results from exchange M.Sc students Lundin and Öckerman arrived from Africa. In their studies, GFH® columns have been treated with naturally arsenic enriched tube well water by a similar methodology as described in this thesis. It has to be kept in mind that these results are not yet fully evaluated, and readers are advised to consult the upcoming project report (Lundin & Öckermann, *Unpublished*).

Lundin and Öckerman notice a large positive effect from longer EBCT, both when changed by increasing the amount of adsorbent and when changed by decreasing flow. Considering the small dependence indicated in high flow velocity tests, Paper III, it is likely that desorption kinetics play a major role. This is good news considering that a full scale column is likely to have longer EBCT than laboratory scale columns. A capacity of about 460 $\mu g_{added} \cdot dm^{-3}$ could be achieved in these lab scale experiments with realistic flow conditions and with natural water. Experiments were performed with a fairly high pH tube well water (pH ≈ 7.5) which increased further to (pH ≈ 7.9) before the start of experiments, presumably due to the reaction $HCO_3^- \rightarrow CO_2(g) + OH^-$. It was also seen that material interactions caused the effluent pH to vary with a sharp decrease in the beginning of the experiment followed by a slower readjustment to the inlet pH. No major hindrances for the development of a full scale method based on iron oxyhydroxide adsorption were encountered.

6 Conclusions

Ionic radii corresponding to common coordination numbers for the alkali metal ions have been derived. These are more representative than frequently used literature data, considering the ions in aqueous solution. It has also been confirmed that the lithium ion is a structure making ion while potassium, rubidium and cesium ions are structure breakers. Molecules in the hydration shell of a sodium ion are less affected by their environment than corresponding molecules in the bulk, even though they are thought to have a longer reorientation time than bulk molecules. It would be satisfying if these results, and perhaps particularly the sodium ion radius, could improve biological and biochemical models regarding aqueous solution, for example in connection to ion transport in membranes, capillaries or porous materials.

XANES spectra for arsenic(V) species of different protonation show great similarity, and EXAFS investigations of As-O distances underline their structural similarity. The same can be said about arsenic(III) species with different degree of protonation. White line maxima in the XANES spectra differs with 4 eV for species in oxidation states +III and +V. A crystal structure database search of different arsenate species revealed that even though there is a difference between distances to non-protonated and protonated oxygen atoms, the average distance in the different species remain approximately the same. Arsenic(III) usually do not crystallize as orthoarsenite, AsO_3^{3-}, in the presence of low charge density cations. Instead linear metaarsenite, $[AsO_2^-]_n$, chain units are formed, not relevant for the comparison with aqueous solution. It has been seen that orthotelluric acid is a weak structure maker and much indicate that the same is true for arsenous acid.

Adsorption of arsenic oxyacid species onto iron oxyhydroxide based adsorbents has been studied in column experiments. It has been observed that adsorption occurs on a fast time scale for both arsenic(III) and arsenic(V). The adsorption capacity for arsenic(V), measured as added arsenic before column

breakthrough, decreases substantially with increasing pH. A similar effect for arsenic(III) cannot be observed. Comparisons with batch experiments indicate that the adsorption of arsenic(III) is somewhat faster than the adsorption of arsenic(V). The presence of competitors also affects arsenic adsorption to a large extent. Surface affinity is greatest for phosphate but hydrogen carbonate exists at such concentrations that it is likely to be a significant competitor. Despite having substantially lower surface affinity, it promotes a faster breakthrough at levels far below the ones found in natural water. Therefore it might constitute one of the most severe complications in the use of iron oxyhydroxide based column adsorbents for arsenic. Fluoride ions have less surface affinity than phosphate but much higher than hydrogen carbonate. In some water chemistry situations, fluoride may also substanially affect arsenic adsorption to iron oxyhydroxide based column adsorbents.

Adsorbents were produced by coating quartz sand with ferrihydrite and the mineralogy of the coated material was confirmed by EXAFS. Adsorption capacity is not directly proportional against iron content of the material. The coating consisted partly of larger flakes and partly of a thin layer of adsorbed iron. Adsorption capacity was to some extent regenerated when making pauses in operation, as has been noted before. This support the possibility that adsorptives migrates into the bulk material. The commercial material GFH® has also been tested, showing very good capacity. The material is said to be poorly crystalline akaganeite and this is partly confirmed by EXAFS measurements. The structural features of akaganeite and ferrihydrite is similar and GFH® may contain an intermediate, although the main observation is its poor crystallinity. Unfortunately, attempts to adsorb arsenate upon bricks made from iron containing clay turned out to be futile.

Some practical considerations of a column up-scaling in Burkina Faso have been discussed, underlining the importance of sufficient flow velocity which is related to particle size. The importance of easy installation and operation has been discussed. This work does not propose a final solution to the problems in the Yatenga province of Burkina Faso, although several matters of consideration have been pointed out. These include but are not limited to the demand for vertical and horizontal space at the pump, the risks of microbial growth and the handling of adsorbent material before and after use. A possible scheme for continued research in Burkina Faso is lined out, partially based on the experiences of the performed laboratory experiments.

Experiments with natural water and GFH® columns have been performed by M.Sc. exchange students in Burkina Faso, and preliminary results confirm the potential of the material for arsenic decontamination in low-tech applications.

7 References

Acharyya, S. K., Chakraborty, P., Lahiri, S., Raymahashay, B., Guha, S. & Bhowmik, A. (1999). Arsenic poisoning in the Ganges delta. *Nature* 401(6753), 545–545.

Ahrens, L. (1952). The Use of Ionization Potentials .1. Ionic Radii of the Elements. *Geochimica et Cosmochimica Acta* 2(3), 155–169.

Ahsan, H., Perrin, M., Rahman, A., Parvez, F., Stute, M., Zheng, Y., Milton, A. H., Brandt-Rauf, P., van Geen, A. & Graziano, J. (2000). Associations between drinking water and urinary arsenic levels and skin lesions in Bangladesh. *Journal of Occupational and Environmental Medicine* 42(12), 1195–1201.

Allen, F. H. (2002). The Cambridge Structural Database: a quarter of a million crystal structures and rising. *Acta Crystallographica Section B* 58, 380–388.

Andersson, E., Lindqvist, O. & Yamaguchi, T. (1981). An X-ray diffraction study on the structure of telluric acid $Te(OH)_6$ in aqueous solution. *Acta Chemica Scandinavica Series a-Physical and Inorganic Chemistry* 35(8), 591–597.

Appelo, C. A. J., Van der Weiden, M. J. J., Tournassat, C. & Charlet, L. (2002). Surface complexation of ferrous iron and carbonate on ferrihydrite and the mobilization of arsenic. *Environmental Science & Technology* 36(14), 3096–3103.

Arai, Y., Sparks, D. L. & Davis, J. A. (2004). Effects of dissolved carbonate on arsenate adsorption and surface speciation at the hematite-water interface. *Environmental Science & Technology* 38(3), 817–824.

Asgari, A. R., Vaezi, F., Nasseri, S., Dördelmann, O., Mahvi, A. H. & Fard, E. D. (2008). Removal of Hexavalent Chromium from Drinking Water by Granular Ferric Hydroxide. *Iranian Journal of Environmental Health Science & Engineering* 5(4), 277–282.

Audi, G., Bersillon, O., Blachot, J. & Wapstra, A. H. (2003). The NUBASE evaluation of nuclear and decay properties. *Nuclear Physics A* 729(1), 3–128.

Averbuch-Pouchot, M. & Durif, A. (1989). Determination of the hydrogen-bond scheme in the adduct telluric acid-urea-$Te(OH)_6.2CO(NH_2)_2$. *Comptes Rendus De L Academie Des Sciences Serie Ii* 309(1), 25–28.

Averbuch-Pouchot, M. & Durif, A. (1990). Crystal-Chemistry of TRIS(ethylene-diammonium) cycklohexaphosphate tellurate dihydrate. *Acta Crystallographica Section C-Crystal Structure Communications* 46, 2236–2238.

Averbuch-Pouchot, M. & Schulke, U. (1996). Preparation and crystal structure of guanidinium cyclododecaphosphate telluric acid hydrate: $[C(NH_2)_3]_{12}P_{12}O_{36}$ center dot $12Te(OH)_6$ center dot $24H_2O$. *Zeitschrift Fur Anorganische Und Allgemeine Chemie* 622(11), 1997–2002.

Averbuch-Pouchot, M. T. (1988). Crystal-structure of a new telluric acid adduct - $Te(OH)_6.2(CH_3NHCH_2COOH)$. *Zeitschrift Fur Kristallographie* 183(1-4), 285–291.

Avery, S. (1995). Microbial Interactions with Cesium - Implications for Biotechnology. *Journal of Chemical Technology and Biotechnology* 62(1), 3–16.

Azam, S. S., Hofer, T. S., Randolf, B. R. & Rode, B. M. (2009). Hydration of Sodium(I) and Potassium(I) Revisited: A Comparative QM/MM and QMCF MD Simulation Study of Weakly Hydrated Ions. *Journal of Physical Chemistry A* 113(9), 1827–1834.

Badger, R. M. & Bauer, S. H. (1937). Spectroscopic Studies of the Hydrogen Bond. II. The Shift of the O-H Vibrational Frequency in the Formation of the Hydrogen Bond. *The Journal of Chemical Physics* 5(11), 839–851.

Badruzzaman, M., Westerhoff, P. & Knappe, D. (2004). Intraparticle diffusion and adsorption of arsenate onto granular ferric hydroxide (GFH). *Water Research* 38(18), 4002–4012.

Banerjee, K., Amy, G. L., Prevost, M., Nour, S., Jekel, M., Gallagher, P. M. & Blumenschein, C. D. (2008). Kinetic and thermodynamic aspects of adsorption of arsenic onto granular ferric hydroxide (GFH). *Water Research* 42(13), 3371–3378.

Bates, M. N., Rey, O. A., Biggs, M. L., Hopenhayn, C., Moore, L. E., Kalman, D., Steinmaus, C. & Smith, A. H. (2004). Case-control study of bladder cancer and exposure to arsenic in Argentina. *American Journal of Epidemiology* 159(4), 381–389.

Beattie, J., Best, S., Skelton, B. & White, A. (1981). Structural Studies on the Cesium Alums, $CsM^{III}[SO_4]_2*12H_2O$. *Journal of the Chemical Society-Dalton Transactions* (10), 2105–2111.

Benjamin, M. M., Sletten, R. S., Bailey, R. P. & Bennett, T. (1996). Sorption and filtration of metals using iron-oxide-coated sand. *Water Research* 30(11), 2609–2620.

Bentley, R. & Chasteen, T. G. (2002). Arsenic Curiosa and Humanity. *The Chemical Educator* 7(2), 51–60.

Bera, A. K., Rana, T., Das, S., Bhattacharya, D., Bandyopadhyay, S., Pan, D., De, S., Samanta, S., Chowdhury, A. N., Mondal, T. K. & Das, S. K. (2010). Ground water arsenic contamination in West Bengal, India: A risk of sub-clinical toxicity in cattle as evident by correlation between arsenic exposure, excretion and deposition. *Toxicology and Industrial Health* 26(10), 709–716.

Bergström, P. A. & Lindgren, J. (1992). Infrared study on the hydration of Mn^{2+}, Fe^{2+}, Co^{2+}, Nd^{3+}, Dy^{3+} and Yb^{3+} in dilute aqueous solution. *Inorganic Chemistry* 31(8), 1529–1533.

Bergström, P. A., Lindgren, J. & Kristiansson, O. (1991a). An IR study of the hydration of ClO_4^-, NO_3^-, I^-, Br^-, Cl^- and SO_4^{2-} anions in aqueous solution. *Journal of Physical Chemistry* 95(22), 8575–8580.

Bergström, P. A., Lindgren, J., Read, M. & Sandström, M. (1991b). Infrared spectroscopic evidence for 2nd sphere hydration in aqueous solutions of Al^{3+}, Cr^{3+} and Rh^{3+}. *Journal of Physical Chemistry* 95(20), 7650–7655.

Bergström, P. A., Lindgren, J., Sandström, M. & Zhou, Y. X. (1992). Infrared spectroscopic study on the hydration of mercury(II), cadmium(II) and zinc(II) in aqueous solution and in the hexahydrated perchlorate salts. *Inorganic Chemistry* 31(1), 150–152.

Bhandari, N., Reeder, R. J. & Strongin, D. R. (2011). Photoinduced Oxidation of Arsenite to Arsenate on Ferrihydrite. *Environmental Science & Technology* 45(7), 2783–2789.

Bhattacharya, P., Welch, A. H., Stollenwerk, K. G., McLaughlin, M. J., Bundschuh, J. & Panaullah, G. (2007). Arsenic in the environment: Biology and Chemistry. *Science of the Total Environment* 379(2-3), 109–120.

Bissen, M. & Frimmel, F. H. (2003). Arsenic - a review. Part II: Oxidation of arsenic and its removal in water treatment. *Acta Hydrochimica Et Hydrobiologica* 31(2), 97–107.

van den Bogaard, A. E. & Stobberingh, E. E. (1999). Antibiotic usage in animals - Impact on bacterial resistance and public health. *Drugs* 58(4), 589–607.

Bosi, P., Felici, R., Rongoni, E. & Sacchetti, F. (1984). On the Structure of Alkali-Halide Solutions .2. Neutron and X-Ray-Diffraction. *Nuovo Cimento Della Societa Italiana Di Fisica D-Condensed Matter Atomic Molecular and Chemical Physics Fluids Plasmas Biophysics* 3(6), 1029–1038.

Bouazizi, S. & Nasr, S. (2007). Local order in aqueous lithium chloride solutions as studied by X-ray scattering and molecular dynamics simulations. *Journal of Molecular Structure* 837(1-3), 206–213.

Bowell, R. J. (1994). Sorption of arsenic by iron-oxides and oxyhydroxides in soils. *Applied Geochemistry* 9(3), 279–286.

Buchner, R. & Hefter, G. (2009). Interactions and dynamics in electrolyte solutions by dielectric spectroscopy. *Physical Chemistry Chemical Physics* 11(40), 8984–8999.
Calderón, J., Navarro, M. E., Jimenez-Capdeville, M. E., Santos-Diaz, M. A., Golden, A., Rodriguez-Levya, I., Borja-Aburto, V. & Diaz-Barriga, F. (2001). Exposure to arsenic and lead and neuropsychological development in Mexican children. *Environmental Research* 85(2), 69–76.
Carabante, I., Grahn, M., Holmgren, A. & Hedlund, J. (2010). In situ ATR-FTIR studies on the competitive adsorption of arsenate and phosphate on ferrihydrite. *Journal of Colloid and Interface Science* 351(2), 523–531.
Carabante, I., Grahn, M., Holmgren, A., Kumpiene, J. & Hedlund, J. (2009). Adsorption of As (V) on iron oxide nanoparticle films studied by in situ ATR-FTIR spectroscopy. *Colloids and Surfaces a-Physicochemical and Engineering Aspects* 346(1-3), 106–113.
Carlson, S., Clausén, M., Gridneva, L., Sommarin, B. & Svensson, C. (2006). XAFS experiments at beamline I811, MAX-lab synchrotron source, Sweden. *Journal of Synchrotron Radiation* 13, 359–364.
Chakraborty, S., Bardelli, F., Mullet, M., Greneche, J.-M., Varma, S., Ehrhardt, J.-J., Banerjee, D. & Charlet, L. (2011). Spectroscopic studies of arsenic retention onto biotite. *Chemical Geology* 281(1-2), 83–92.
Chen, R. X., Smith, B. W., Winefordner, J. D., Tu, M. S., Kertulis, G. & Ma, L. Q. (2004). Arsenic speciation in Chinese brake fern by ion-pair high-performance liquid chromatography-inductively coupled plasma mass spectroscopy. *Analytica Chimica Acta* 504(2), 199–207.
Chiou, H.-Y., Chiou, S.-T., Hsu, Y.-H., Chou, Y.-L., Tseng, C-H., Wei, M.-L. & Chen, C.-J. (2001). Incidence of transitional cell carcinoma and arsenic in drinking water: A follow-up study of 8,102 residents in an arseniasis-endemic area in northeastern Taiwan. *American Journal of Epidemiology* 153(5), 411–418.
Chizhik, V. I., Mikhailov, V. I. & Su, P. C. (1987). NMR relaxation data on the microstructure of aqueous solutions of alkali-metal salts and hydroxides. *Theoretical and Experimental Chemistry* 22(4), 480–483.
Christian, G. D. & Feldman, F. J. (1970). *Atomic absorption spectroscopy. Applications in agriculture, biology and medicine*. New York: Wiley-Interscience.
Cisarova, I., Podlahova, J. & Podlaha, J. (1995). Crystal-structure of the adduct hexahydroxotelluric-acid-disodium-ethylenediaminetetraacetate-water(1/1/2). *Collection of Czechoslovak Chemical Communications* 60(5), 820–828.
Coker, V. S., Gault, A. G., Pearce, C. I., van der Laan, G., Telling, N. D., Charnock, J. M., Polya, D. A. & Lloyd, J. R. (2006). XAS and XMCD evidence for species-dependent partitioning of arsenic during microbial reduction of ferrihydrite to magnetite. *Environmental Science & Technology* 40(24), 7745–7750.
Coulson, J., Richardson, J., Backhurst, J. & Harker, J. (1991). Chapter 4: Flow of fluids through granular beds and packed columns. *Particle Technology & Separation Processes*. 4th. ed. Bath: Butterworth Heinemann. (Chemical Engineering). ISBN 0 7506 2942 8.
Cromer, D. (1969). Compton scattering factors for aspherical free atoms. *Journal of Chemical Physics* 50(11), 4857–4859.
Cromer, D. & Mann, J. (1967). Compton scattering factors for spherically symmetric free atoms. *Journal of Chemical Physics* 47(6), 1892–1894.
Cruickshank, D. W. J. (1964). Refinements of structures containing bonds between Si, P, S or Cl and O or N. II. $Na_4P_2O_7.10H_2O$. *Acta Crystallographica* 17(6), 672–673.
Czarnecki, G. L. & Baker, D. H. (1984). Feed Additive Interactions in the Chicken: Reduction of Tissue Copper Deposition by Dietary Roxarsone in Healthy and in Eimeria acervulina-lnfected or Eimeria tenella-lnfected Chicks. *Poultry Science* 63(7), 1412–1418.
D'Angelo, P. & Persson, I. (2004). Structure of the hydrated and dimethyl sulfoxide solvated rubidium ions in solution. *Inorganic Chemistry* 43(11), 3543–3549.
Datta, B. K., Mishra, A., Singh, A., Sar, T. K., Sarkar, S., Bhatacharya, A., Chakraborty, A. K. & Mandal, T. K. (2010). Chronic arsenicosis in cattle with special reference to its metabolism in arsenic endemic village of Nadia district West Bengal India. *Science of the Total Environment* 409(2), 284–288.

Davis, J. & Kent, D. (1990). *Surface Complexation Modeling in Aqueous Geochemistry*.(Hochella, M. & White, A., Eds.) Washington: Mineralogical Soc America. ISBN 0-939950-28-6.

Driehaus, W., Jekel, M. & Hildebrandt, U. (1998). Granular ferric hydroxide - a new adsorbent for the removal of arsenic from natural water. *Journal of Water Services Research and Technology-Aqua* 47(1), 30–35.

Driess, M., Merz, K. & Rowlings, R. (2001). Orthotelluric acid as substitute for crystal-water: Syntheses and crystal structure of the co-crystallate [$Te(OH)_6$ center dot 2 adenine center dot 4 H_2O] and the disodium ditellurate(VI) aggregate {[$Te_2O_2(OH)_6(ONa)_2]_2$[NaOH center dot 12.5 H_2O]}. *Zeitschrift Fur Anorganische Und Allgemeine Chemie* 627(2), 213–217.

Du, H., Rasaiah, J. C. & Miller, J. D. (2007). Structural and dynamic properties of concentrated alkali halide solutions: A molecular dynamics simulation study. *Journal of Physical Chemistry B* 111(1), 209–217.

Dutton, W. & Cooper, W. (1966). Oxides and oxyacids of tellurium. *Chemical Reviews* 66(6), 657–675.

Dzombak, D. A. & Morel, F. (1990). *Surface complexation modeling: hydrous ferric oxide*. Wiley-Interscience.

Eklund, L., Hofer, T. S., Pribil, A. B., Rode, B. M. & Persson, I. (2012). On the structure and dynamics of the hydrated sulfite ion in aqueous solution – an ab initio QMCF MD simulation and large angle X-ray scattering study. *Dalton Transactions* 41(17), 5209–5216.

Elias, M., Wellner, A., Goldin-Azulay, K., Chabriere, E., Vorholt, J. A., Erb, T. J. & Tawfik, D. S. (2012). The molecular basis of phosphate discrimination in arsenate-rich environments. *Nature*.

Ellison, H., Healy, E. & Edwards, J. (1962). Polyol-tellurate complex formation reaction 1. Thermodynamics of telluric acid ionization and of complex formation. *Journal of the American Chemical Society* 84(10), 1820–1824.

Erb, T. J., Kiefer, P., Hattendorf, B., Guenther, D. & Vorholt, J. A. (2012). GFAJ-1 Is an Arsenate-Resistant, Phosphate-Dependent Organism. *Science* 337(6093), 467–470.

Eriksson, A., Kristiansson, O. & Lindgren, J. (1984). Hydration of ions in aqueous-solution studied by IR spectroscopy. *Journal of Molecular Structure* 114(MAR), 455–458.

Farquhar, M., Charnock, J., Livens, F. & Vaughan, D. (2002). Mechanisms of arsenic uptake from aqueous solution by interaction with goethite, lepidocrocite, mackinawite, and pyrite: An X-ray absorption spectroscopy study. *Environmental Science & Technology* 36(8), 1757–1762.

Farrell, J., Wang, J. P., O'Day, P. & Conklin, M. (2001). Electrochemical and spectroscopic study of arsenate removal from water using zero-valent iron media. *Environmental Science & Technology* 35(10), 2026–2032.

Fendorf, S., Eick, M. J., Grossl, P. & Sparks, D. L. (1997). Arsenate and chromate retention mechanisms on goethite .1. Surface structure. *Environmental Science & Technology* 31(2), 315–320.

Ferreccio, C., González, C., Milosavjlevic, V., Marshall, G., Sancha, A. M. & Smith, A. H. (2000). Lung cancer and arsenic concentrations in drinking water in Chile. *Epidemiology* 11(6), 673–679.

Filipponi, A. & Di Cicco, A. (1995). X-ray-absorption spectroscopy and n-body distribution functions in condensed matter .2. Data analysis and applications. *Physical Review B* 52(21), 15135–15149.

Fortes, A. D., Wood, I. G., Grigoriev, D., Alfredsson, M., Kipfstuhl, S., Knight, K. S. & Smith, R. I. (2004). No evidence for large-scale proton ordering in Antarctic ice from powder neutron diffraction. *Journal of Chemical Physics* 120(24), 11376–11379.

Fox, D. I., Pichler, T., Yeh, D. H. & Alcantar, N. A. (2012). Removing Heavy Metals in Water: The Interaction of Cactus Mucilage and Arsenate (As (V)). *Environmental Science & Technology* 46(8), 4553–4559.

Fuller, C. C., Davis, J. A. & Waychunas, G. (1993). Surface-Chemistry of ferrihydrite .2. Kinetics of arsenate adsorption and coprecipitation. *Geochimica et Cosmochimica Acta* 57(10), 2271–2282.

Gahn, H. (1800). Förgiftning af arsenik, lyckligen botad. *Kongl. Vetenskaps Academiens Handlingar* XXI, 71–73.

George, G. N. & Pickering, I. J. (2003). *EXAFSPAK - A suite of Comuter Programs for Analysis of X-ray absorption spectra*. Stanford CA: SSRL.

Ghosh, A., Mukiibi, M., Sáez, A. E. & Ela, W. P. (2006). Leaching of arsenic from granular ferric hydroxide residuals under mature landfill conditions. *Environmental Science & Technology* 40(19), 6070–6075.

Goldberg, S. & Johnston, C. T. (2001). Mechanisms of arsenic adsorption on amorphous oxides evaluated using macroscopic measurements, vibrational spectroscopy, and surface complexation modeling. *Journal of Colloid and Interface Science* 234(1), 204–216.

Grafe, M., Eick, M. J. & Grossl, P. (2001). Adsorption of arsenate (V) and arsenite (III) on goethite in the presence and absence of dissolved organic carbon. *Soil Science Society of America Journal* 65(6), 1680–1687.

Greenwood, N. N. & Earnshaw, A. (1997). *Chemistry of the Elements*. 2nd. ed. Butterworth Heinemann. ISBN 978-0-7506-3365-9.

Grehk, T. M. & Nilsson, P. O. (2001). The design of the material science beamline, I811, at MAX-II. *Nuclear Instruments & Methods in Physics Research Section a-Accelerators Spectrometers Detectors and Associated Equipment* 467, 635–638.

Guan, X.-H., Wang, J. & Chusuei, C. C. (2008). Removal of arsenic from water using granular ferric hydroxide: Macroscopic and microscopic studies. *Journal of Hazardous Materials* 156(1-3), 178–185.

Guha Mazumder, D. N., Haque, R., Ghosh, N., De, B. K., Santra, A., Chakraborti, D. & Smith, A. H. (2000). Arsenic in drinking water and the prevalence of respiratory effects in West Bengal, India. *International Journal of Epidemiology* 29(6), 1047–1052.

Guo, H., Stüben, D. & Berner, Z. (2007). Arsenic removal from water using natural iron mineral-quartz sand columns. *Science of the Total Environment* 377(2-3), 142–151.

Gurney, R. W. (1953). Chapter 10. *Ionic processes in solution*. New York: McGraw-Hill.

Gustafsson, J. (2003). Modelling molybdate and tungstate adsorption to ferrihydrite. *Chemical Geology* 200(1-2), 105–115.

Hall, A. H. (2002). Chronic arsenic poisoning. *Toxicology Letters* 128(1-3), 69–72.

Harris, D. C. (2000). *Quantitative Chemical Analysis*. 5th. ed. W.H. Freeman and Company. ISBN 0-7167-2881-8.

Heinje, G., Luck, W. & Heinzinger, K. (1987). Molecular-Dynamics Simulation of an Aqueous $NaClO_4$ Solution. *Journal of Physical Chemistry* 91(2), 331–338.

Helm, L. & Merbach, A. E. (1999). Water exchange on metal ions: experiments and simulations. *Coordination Chemistry Reviews* 187, 151–181.

Herbel, M. & Fendorf, S. (2005). Transformation and transport of arsenic within ferric hydroxide coated sands upon dissimilatory reducing bacterial activity. In: O´Day, P. A., Vlassopoulos, D., Meng, Z., & Benning, L. G. (Eds.) *Advances in Arsenic Research: Integration of Experimental and Observational Studies and Implications for Mitigation*. pp 77–90. Washington: Amer Chemical Soc. ISBN 0-8412-3913-4.

Herbel, M. & Fendorf, S. (2006). Biogeochemical processes controlling the speciation and transport of arsenic within iron coated sands. *Chemical Geology* 228(1-3), 16–32.

Hernández-Cobos, J., Vargas, M. C., Ramírez-Solis, A. & Ortega-Blake, I. (2010). Aqueous solvation of $As(OH)_3$: A Monte Carlo study with flexible polarizable classical interaction potentials. *Journal of Chemical Physics* 133(11), 114501–1 –114501–9.

Hiemstra, T. & van Riemsdijk, W. H. (1996). A surface structural approach to ion adsorption: The charge distribution (CD) model. *Journal of Colloid and Interface Science* 179(2), 488–508.

Hofer, T. S., Randolf, B. R. & Rode, B. M. (2005). Structure-breaking effects of solvated Rb(I) in dilute aqueous solution - An ab initio QM/MM MD approach. *Journal of Computational Chemistry* 26(9), 949–956.

Hongshao, Z. & Stanforth, R. (2001). Competitive adsorption of phosphate and arsenate on goethite. *Environmental Science and Technology* 35(24), 4753–4757.
Hsu, J.-C., Lin, C.-J., Liao, C.-H. & Chen, S.-T. (2008). Removal of As(V) and As(III) by reclaimed iron-oxide coated sands. *Journal of Hazardous Materials* 153(1-2), 817–826.
Hughes, M. F., Beck, B. D., Chen, Y., Lewis, A. S. & Thomas, D. J. (2011). Arsenic Exposure and Toxicology: A Historical Perspective. *Toxicological Sciences* 123(2), 305–332.
Huheey, J. E., Keiter, E. A. & Keiter, R. L. (1993). *Inorganic Chemistry - Principles of structure and reactivity*. 4th. ed. New York: Harper Collins. ISBN 0-06-042995.
Huq, S. M. I. (2006). Arsenic contamination in food-chain: transfer of arsenic into food materials through groundwater irrigation. *Journal of health, population and nutrition* 24(3), 305.
Hussam, A. & Munir, A. K. M. (2007). A simple and effective arsenic filter based on composite iron matrix: Development and deployment studies for groundwater of Bangladesh. *Journal of Environmental Science and Health Part a-Toxic/Hazardous Substances & Environmental Engineering* 42(12), 1869–1878.
Ilczyszyn, M., Lis, T., Baran, J. & Ratajczak, H. (1992). Structure and IR-spectra of the solid complex of bis(betaine) telluric acid. *Journal of Molecular Structure* 265(3-4), 293–310.
Inorganic Crystal Structure Database (2009). Karlsruhe: FIZ.
Jain, A., Raven, K. & Loeppert, R. (1999). Arsenite and arsenate adsorption on ferrihydrite: Surface charge reduction and net OH^- release stoichiometry. *Environmental Science & Technology* 33(8), 1179–1184.
Jakariya, M., Vahter, M., Rahman, M., Wahed, M. A., Hore, S. K., Bhattacharya, P., Jacks, G. & Persson, L. Å. (2007). Screening of arsenic in tubewell water with field test kits: Evaluation of the method from public health perspective. *Science of the Total Environment* 379(2-3), 167–175.
Jalilehvand, F. (2000). *Structure of Hydrated Ions and Cyanide Complexes by X-ray Absorption Spectroscopy*. Diss. Stockholm: Royal Institute of Technology.
Jalilehvand, F., Spångberg, D., Lindqvist-Reis, P., Hermansson, K., Persson, I. & Sandström, M. (2001). Hydration of the calcium ion. An EXAFS, large-angle X-ray scattering, and molecular dynamics simulation study. *Journal of the American Chemical Society* 123(3), 431–441.
Jansen, E., Kyek, A., Schäfer, W. & Schwertmann, U. (2002). The structure of six-line ferrihydrite. *Applied Physics a-Materials Science & Processing* 74, S1004–S1006.
Jessen, S., Larsen, F., Koch, C. & Arvin, E. (2005). Sorption and desorption of arsenic to ferrihydrite in a sand filter. *Environmental Science & Technology* 39(20), 8045–8051.
Johansson, G. & Sandström, M. (1973). Computer Programs for the Analysis of Data on X-ray Diffraction by Liquids. *Chem. Scr.* 4, 195–198.
Joshi, A. & Chaudhuri, M. (1996). Removal of arsenic from ground water by iron oxide-coated sand. *Journal of Environmental Engineering-Asce* 122(8), 769–771.
Kapaj, S., Peterson, H., Liber, K. & Bhattacharya, P. (2006). Human health effects from chronic arsenic poisoning- A review. *Journal of Environmental Science and Health Part a-Toxic/Hazardous Substances & Environmental Engineering* 41(10), 2399–2428.
Khare, V., Mullet, M., Hanna, K., Blumers, M., Abdelmoula, M., Klingelhöfer, G. & Ruby, C. (2008). Comparative studies of ferric green rust and ferrihydrite coated sand: Role of synthesis routes. *Solid State Sciences* 10(10), 1342–1351.
Kocar, B. D., Borch, T. & Fendorf, S. (2010). Arsenic repartitioning during biogenic sulfidization and transformation of ferrihydrite. *Geochimica et Cosmochimica Acta* 74(3), 980–994.
Konopik, N. & Leberl, O. (1949). Dissoziationskonstanten sehr schwacher Säuren. *Monatshefte Fur Chemie* 80(5), 655–669.
Korte, N. & Fernando, Q. (1991). A Review of Arsenic(III) in Groundwater. *Critical Reviews in Environmental Control* 21(1), 1–39.
Krakowiak, J., Lundberg, D. & Persson, I. (2012). A Coordination Chemistry Study of Hydrated and Solvated Cationic Vanadium Ions in Oxidation States plus III, plus IV, and plus V in Solution and Solid State. *Inorganic Chemistry* 51(18), 9598–9609.

Kristiansson, O., Eriksson, A. & Lindgren, J. (1984). Hydration of ions in aqueous solution studied by infrared-spectroscopy. 2. Application. *Acta Chemica Scandivavica Series A - Physical and inorganic chemistry* 38(8), 613–618.

Kristiansson, O. & Lindgren, J. (1988). On the hydration of the F^- anion in aqueous-solution. *Journal of Molecular Structure* 177, 537–541.

Kristiansson, O. & Lindgren, J. (1991). Infrared spectroscopic studies of concentrated aqueous - electrolyte solutions. *Journal of Physical Chemistry* 95(3), 1488–1493.

Kristiansson, O., Lindgren, J. & de Villepin, J. (1988). A quantitative infrared spectroscopic method for the study of the hydration of ions in aqueous solutions. *Journal of Physical Chemistry* 92(9), 2680–2685.

Kristiansson, O., Persson, I., Bobicz, D. & Xu, D. W. (2003). A structural study of the hydrated and the dimethylsulfoxide, N,N ’-dimethylpropyleneurea, acetonitrile, pyridine and N,N-dimethylthioformamide solvated nickel(II) ion in solution and solid state. *Inorganica Chimica Acta* 344, 15–27.

Kubozono, Y., Hirano, A., Maeda, H., Kashino, S., Emura, S. & Ishida, H. (1994). An Exafs Investigation of Local-Structure Around Rb+ in Aqueous-Solution. *Zeitschrift Fur Naturforschung Section a-a Journal of Physical Sciences* 49(6), 727–729.

Kumar, A., Bucciarelli-Tieger, R. H. & Gurian, P. L. (2008). Cost-effectiveness of Arenic Adsorbents. *Proceedings of American Water Works Association, Annual Conference and Exposition*, 2008. American Water Works Association.

Kunz, W. (2010). Specific ion effects in colloidal and biological systems. *Current Opinion in Colloid & Interface Science* 15(1-2), 34–39.

Lane, N. (2003). *Oxygen: The molecule that made the world*. Oxford University Press. ISBN 0198607830.

Lee, M. Y., Bae, O. N., Chung, S. M., Kang, K. T., Lee, J. Y. & Chung, J. H. (2002). Enhancement of platelet aggregation and thrombus formation by arsenic in drinking water: A contributing factor to cardiovascular disease. *Toxicology and Applied Pharmacology* 179(2), 83–88.

Levason, W., Oldroyd, R. D. & Webster, M. (1994). Extended X-ray absorption fine structure studies of transition-metal periodate and tellurate complexes. Crystal structure of $Rb_2Na_4[OsO_2(H_2TeO_6)_2]\cdot 16H_2O$. *Journal of the Chemical Society, Dalton Transactions* (20), 2983–2988.

Levy, H., Danford, M. & Narten, A. (1966). *Data Collection and Evaluation with an X-ray Diffractometer Designed for the Study of Liquid Structure*. Oak Ridge: Oak Ridge National Laboratory. (ORNL-3960).

Li, Y. & Gregory, S. (1974). Diffusion of Ions in Sea-Water and in Deep-Sea Sediments. *Geochimica et Cosmochimica Acta* 38(5), 703–714.

Liao, Y., Liang, J. & Zhou, L. (2011). Adsorptive removal of As(III) by biogenic schwertmannite from simulated As-contaminated groundwater. *Chemosphere* 83(3), 295–301.

Lindqvist-Reis, P., Persson, I. & Sandström, M. (2006). The hydration of the scandium(III) ion in aqueous solution and crystalline hydrates studied by XAFS spectroscopy, large-angle X-ray scattering and crystallography. *Dalton Transactions* (32), 3868–3878.

Loeffler, H. H. & Rode, B. M. (2002). The hydration structure of the lithium ion. *Journal of Chemical Physics* 117(1), 110–117.

Loehr, T. & Plane, R. (1968). Raman spectra and structures of arsenious acid and arsenites in aqueous solution. *Inorganic Chemistry* 7(9), 1708–1714.

Loring, J. S., Sandström, M. H., Noren, K. & Persson, P. (2009). Rethinking Arsenate Coordination at the Surface of Goethite. *Chemistry-a European Journal* 15(20), 5063–5072.

Lundberg, D., Eriksson, L., D’Angelo, P. & Persson, I. (2007a). A structural study of the N,N-dimethylpropyleneurea solvated zinc(II) and cadmium(II) ions in solution and crystalline state. *Journal of Molecular Liquids* 131, 105–112.

Lundberg, D., Persson, I., Eriksson, L., D’Angelo, P. & De Panfilis, S. (2010). Structural Study of the N,N ’-Dimethylpropyleneurea Solvated Lanthanoid(III) Ions in Solution and Solid State with an Analysis of the Ionic Radii of Lanthanoid(III) Ions. *Inorganic Chemistry* 49(10), 4420–4432.

Lundberg, D., Ullström, A.-S., D'Angelo, P. & Persson, I. (2007b). A structural study of the hydrated and the dimethylsulfoxide, N,N ᾽-dimethylpropyleneurea, and N,N-dimethylthioformaraide solvated iron(II) and iron(III) ions in solution and solid state. *Inorganica Chimica Acta* 360(6), 1809–1818.
Lundin E. & Öckerman H. (*Unpublished*), Project report, Swedish University of Agricultural Sciences / Uppsala University - International Science Program
Maeda, M. & Ohtaki, H. (1975). X-Ray-Diffraction Study of a Concentrated Aqueous Sodium Iodide Solution. *Bulletin of the Chemical Society of Japan* 48(12), 3755–3756.
Mamindy-Pajany, Y., Hurel, C., Marmier, N. & Romeo, M. (2009). Arsenic adsorption onto hematite and goethite. *Comptes Rendus Chimie* 12(8), 876–881.
Manceau, A. (1995). The mechanism of anion adsorption on iron-oxides - Evidence for the bonding of arsenate tetrahedra on free $Fe(O,OH)_6$ edges. *Geochimica et Cosmochimica Acta* 59(17), 3647–3653.
Mancinelli, R., Botti, A., Bruni, F., Ricci, M. A. & Soper, A. K. (2007). Hydration of sodium, potassium, and chloride ions in solution and the concept of structure maker/breaker. *Journal of Physical Chemistry B* 111(48), 13570–13577.
Manning, B., Fendorf, S., Bostick, B. & Suarez, D. (2002a). Arsenic(III) oxidation and arsenic(V) adsorption reactions on synthetic birnessite. *Environmental Science & Technology* 36(5), 976–981.
Manning, B., Fendorf, S. & Goldberg, S. (1998). Surface structures and stability of arsenic(III) on goethite: Spectroscopic evidence for inner-sphere complexes. *Environmental Science & Technology* 32(16), 2383–2388.
Manning, B. & Goldberg, S. (1996). Modeling competitive adsorption of arsenate with phosphate and molybdate on oxide minerals. *Soil Science Society of America Journal* 60(1), 121–131.
Manning, B. & Goldberg, S. (1997). Adsorption and stability of arsenic(III) at the clay mineral-water interface. *Environmental Science & Technology* 31(7), 2005–2011.
Manning, B., Hunt, M., Amrhein, C. & Yarmoff, J. (2002b). Arsenic(III) and Arsenic(V) reactions with zerovalent iron corrosion products. *Environmental Science & Technology* 36(24), 5455–5461.
Marcus, Y. (2009). Effect of Ions on the Structure of Water: Structure Making and Breaking. *Chemical Reviews* 109(3), 1346–1370.
Marin, A.R., Masscheleyn, P.H. & Patrick, W.H. (1992). The Influence of Chemical Form and Concentration of Arsenic on Rice Growth and Tissue Arsenic Concentration. *Plant and Soil* 139(2), 175–183.
Mile, V., Pusztai, L., Dominguez, H. & Pizio, O. (2009). Understanding the Structure of Aqueous Cesium Chloride Solutions by Combining Diffraction Experiments, Molecular Dynamics Simulations, and Reverse Monte Carlo Modeling. *Journal of Physical Chemistry B* 113(31), 10760–10769.
Milton, A. H. & Rahman, M. (2002). Respiratory effects and arsenic contaminated well water in Bangladesh. *International Journal of Environmental Health Research* 12(2), 175–179.
Milton, A. H., Smith, W., Rahman, B., Hasan, Z., Kulsum, U., Dear, K., Rakibuddin, M. & Ali, A. (2005). Chronic arsenic exposure and adverse pregnancy outcomes in Bangladesh. *Epidemiology* 16(1), 82–86.
Molund, M. & Persson, I. (1985). STEPLR - A program for refinements of data on X-ray-scattering by liquids. *Chemica Scripta* 25(2), 197–197.
Myneni, S., Traina, S., Waychunas, G. & Logan, T. (1998). Experimental and theoretical vibrational spectroscopic evaluation of arsenate coordination in aqueous solutions, solids, and at mineral-water interfaces. *Geochimica et Cosmochimica Acta* 62(19-20), 3285–3300.
Ni Dhubhghaill, O. & Sadler, P. (1991). The Structure and Reactivity of Arsenic Compounds - Biological-Activity and Drug Design. *Structure and Bonding* 78, 129–190.
Nikolaidis, N., Dobbs, G. & Lackovic, J. (2003). Arsenic removal by zero-valent iron: field, laboratory and modeling studies. *Water Research* 37(6), 1417–1425.

Nikologorskaya, E. L., Kuznetsov, V. V., Grechin, O. V. & Trostin, V. N. (2000). X-ray diffraction study of anion hydration in solutions of potassium halides. *Russian Journal of Inorganic Chemistry* 45(11), 1759–1766.

Nilsson, A. & Pettersson, L. G. M. (2011). Perspective on the structure of liquid water. *Chemical Physics* 389(1–3), 1–34.

Novikov, A. G., Rodnikova, M. N., Savostin, V. V. & Sobolev, O. V. (1999). The study of hydration effects in aqueous solutions of LiCl and CsCl by inelastic neutron scattering. *Journal of Molecular Liquids* 82(1-2), 83–104.

Näslund, J., Persson, I. & Sandström, M. (2000). Solvation of the bismuth(III) ion by water, dimethyl sulfoxide, N,N ’-dimethylpropyleneurea, and N,N-dimethylthioformamide. An EXAFS, large-angle X-ray scattering, and crystallographic structural study. *Inorganic Chemistry* 39(18), 4012–4021.

O’Reilly, S., Strawn, D. & Sparks, D. (2001). Residence time effects on arsenate adsorption/desorption mechanisms on goethite. *Soil Science Society of America Journal* 65(1), 67–77.

Ohkubo, T., Konishi, T., Hattori, Y., Kanoh, H., Fujikawa, T. & Kaneko, K. (2002). Restricted hydration structures of Rb and Br ions confined in slit-shaped carbon nanospace. *Journal of the American Chemical Society* 124(40), 11860–11861.

Ohtaki, H. & Fukushima, N. (1992). A Structural Study of Saturated Aqueous-Solutions of Some Alkali-Halides. *Journal of Solution Chemistry* 21(1), 23–38.

Ohtomo, N. & Arakawa, K. (1979). Neutron-Diffraction Study of Aqueous Ionic-Solutions .1. Aqueous-Solutions of Lithium-Chloride and Cesium-Chloride. *Bulletin of the Chemical Society of Japan* 52(10), 2755–2759.

Ohtomo, N. & Arakawa, K. (1980). Neutron Diffraction Study of Aqueous Ionic-Solutions .2. Aqueous Solutions of Sodium Chloride and Potassium Chloride. *Bulletin of the Chemical Society of Japan* 53(7), 1789–1794.

Omta, A. W., Kropman, M. F., Woutersen, S. & Bakker, H. J. (2003). Negligible effect of ions on the hydrogen-bond structure in liquid water. *Science* 301(5631), 347–349.

Ona-Nguema, G., Morin, G., Wang, Y., Foster, A. L., Juillot, F., Calas, G. & Brown, G. E. (2010). XANES Evidence for Rapid Arsenic(III) Oxidation at Magnetite and Ferrihydrite Surfaces by Dissolved O_2 via Fe^{2+}-Mediated Reactions. *Environmental Science & Technology* 44(14), 5416–5422.

Oremland, R. S. & Stolz, J. F. (2003). The ecology of arsenic. *Science* 300(5621), 939–944.

Palinkas, G., Radnai, T. & Hajdu, F. (1980). Ion-Solvent and Solvent-Solvent Interactions - X-Ray Study of Aqueous Alkali Chloride Solutions. *Zeitschrift Fur Naturforschung Section a-a Journal of Physical Sciences* 35(1), 107–114.

Pare, S., Persson, I., Guel, B. & Lundberg, D. (2013). Trivalent Chromium removal from Aqueous solution using Raw Natural Mixed Clay from Burkina Faso. *International Research Journal of Environment Sciences* 2, 30–37.

Pare, S., Persson, I., Guel, B., Lundberg, D., Zerbo, L., Kam, S. & Traoré, K. (2012). Heavy metal removal from aqueous solutions by sorption using natural clays from Burkina Faso. *African Journal of Biotechnology* 11(45), 10395–10406.

Partey, F., Norman, D. I., Ndur, S. & Nartey, R. (2009). Mechanism of arsenic sorption onto laterite iron concretions. *Colloids and Surfaces a-Physicochemical and Engineering Aspects* 337(1-3), 164–172.

Partey, F., Norman, D., Ndur, S. & Nartey, R. (2008). Arsenic sorption onto laterite iron concretions: Temperature effect. *Journal of Colloid and Interface Science* 321(2), 493–500.

Pearson, R. (1963). Hard and soft acids and bases. *Journal of the American Chemical Society* 85(22), 3533–&.

Pedersen, H. D., Postma, D. & Jakobsen, R. (2006). Release of arsenic associated with the reduction and transformation of iron oxides. *Geochimica et Cosmochimica Acta* 70(16), 4116–4129.

Penczek, S., Kubisa, P. & Matyjaszewski, K. (1980). Cationic Ring-Opening Polymerization of Heterocyclic Monomers .1. Mechanisms. *Advances in Polymer Science* 37, 1–144.

Persson, I. (2010). Hydrated metal ions in aqueous solution: How regular are their structures? *Pure and Applied Chemistry* 82(10), 1901–1917.
Persson, I., Lyczko, K., Lundberg, D., Eriksson, L. & Płaczek, A. (2011). Coordination Chemistry Study of Hydrated and Solvated Lead(II) Ions in Solution and Solid State. *Inorganic Chemistry* 50(3), 1058–1072.
Persson, I., Sandström, M., Yokoyama, H. & Chaudhry, M. (1995). Structure of the Solvated Strontium and Barium Ions in Aqueous, Dimethyl-Sulfoxide and Pyridine Solution, and Crystal-Structure of Strontium and Barium Hydroxide Octahydrate. *Zeitschrift Fur Naturforschung Section a-a Journal of Physical Sciences* 50(1), 21–37.
Pierce, M. & Moore, C. (1982). Adsorption of arsenite and arsenate on amorphous iron hydroxide. *Water Research* 16(7), 1247–1253.
Puigdomenech, I. (2004). *Hydrochemical Equilibrium-Constant Database*.
Puigdomenech, I. (2009). *Medusa*.
Qui, D., Lambertandron, B. & Boucherle, J. (1987). Neutron refinement of telluric acid glycine (1/2) monohydrate. *Acta Crystallographica Section C-Crystal Structure Communications* 43, 907–909.
Qui, D., Vicat, J. & Durif, A. (1984). Structure of telluric acid glycine (1-2) monohydrate, $Te(OH)_6.2C_2H_5NO_2.H_2O$, at 120K and determination of hydrogen positions. *Acta Crystallographica Section C-Crystal Structure Communications* 40(JAN), 181–184.
Rahman, M. M., Mandal, B. K., Chowdhury, T. R., Sengupta, M. K., Chowdhury, U. K., Lodh, D., Chanda, C. R., Basu, G. K., Mukherjee, S. C., Saha, K. C. & Chakraborti, D. (2003). Arsenic groundwater contamination and sufferings of people in North 24-Parganas, one of the nine arsenic affected districts of West bengal, India. *Journal of Environmental Science and Health Part a-Toxic/Hazardous Substances & Environmental Engineering* 38(1), 25–59.
Ralph, S. J. (2008). Arsenic-Based Antineoplastic Drugs and Their Mechanisms of Action. *Metal-Based Drugs* 2008, 1–13.
Ramos, S., Barnes, A. C., Neilson, G. W. & Capitan, M. J. (2000). Anomalous X-ray diffraction studies of hydration effects in concentrated aqueous electrolyte solutions. *Chemical Physics* 258(2-3), 171–180.
Raposo, J., Sanz, J., Zuloaga, O., Olazabal, M. & Madariaga, J. (2002). The thermodynamic model of inorganic arsenic species in aqueous solutions - Potentiometric study of the hydrolitic equilibrium of arsenic acid. *Talanta* 57(5), 849–857.
Raven, K. P., Jain, A. & Loeppert, R. H. (1998). Arsenite and arsenate adsorption on ferrihydrite: Kinetics, equilibrium, and adsorption envelopes. *Environmental Science & Technology* 32(3), 344–349.
Reaves, M. L., Sinha, S., Rabinowitz, J. D., Kruglyak, L. & Redfield, R. J. (2012). Absence of Detectable Arsenate in DNA from Arsenate-Grown GFAJ-1 Cells. *Science* 337(6093), 470–473.
Rhodes, M. (2008). Fluid flow through a packed bed of particles. *Introduction to particle technology*. 2nd. ed. John Wiley & Sons, Ltd. eISBN: 9780470727119.
Rodnikova, M. N. (2003). Negative hydration of ions. *Russian Journal of Electrochemistry* 39(2), 192–197.
Rosdahl, J., Persson, I., Lars, K. & Stahl, K. (2004). On the solvation of the mercury(I) ion. A structural, vibration spectroscopic and quantum chemical study. *Inorganica Chimica Acta* 357(9), 2624–2634.
Rossman, T. G. (2003). Mechanism of arsenic carcinogenesis: an integrated approach. *Mutation Research-Fundamental and Molecular Mechanisms of Mutagenesis* 533(1-2), 37–65.
Rossman, T. G., Uddin, A. N. & Burns, F. J. (2004). Evidence that arsenite acts as a cocarcinogen in skin cancer. *Toxicology and Applied Pharmacology* 198(3), 394–404.
Rudolph, W., Brooker, M. & Pye, C. (1995). Hydration of Lithium Ion in Aqueous-Solution. *Journal of Physical Chemistry* 99(11), 3793–3797.
Rönnow, C. (1778). Rön som utvisa, at Arsenicum icke allenast är et Botemedel emot Kräftan, utan ock dess egenteliga motgift; och at alla Mercurialia äro deremot ganska skadeliga. *Kongl. Vetenskaps Academiens Handlingar* XXXIX, 146–166.

Saha, B., Bains, R. & Greenwood, F. (2005). Physicochemical characterization of granular ferric hydroxide (GFH) for arsenic(V) sorption from water. *Separation Science and Technology* 40(14), 2909–2932.
San-Román, M. L., Hernández-Cobos, J., Saint-Martin, H. & Ortega-Blake, I. (2009). A theoretical study of the hydration of Rb^+ by Monte Carlo simulations with refined ab initio-based model potentials. *Theoretical Chemistry Accounts* 126(3-4), 197–211.
Scheele, C. W. (1778). Tilredningssättet af en ny grön färg. *Kongl. Vetenskaps Academiens Handlingar* XXXIX, 327–328.
Schwenk, C. F., Hofer, T. S. & Rode, B. M. (2004). "Structure breaking" effect of hydrated Cs^+. *Journal of Physical Chemistry A* 108(9), 1509–1514.
Schwertmann, U. & Cornell, R. (2000). *Iron Oxides in the Laboratory*. 2nd. ed. Wiley-VCH.
Shannon, R. (1976). Revised Effective Ionic-Radii and Systematic Studies of Interatomic Distances in Halides and Chalcogenides. *Acta Crystallographica Section A* 32(SEP1), 751–767.
Shannon, R. & Prewitt, C. (1969). Effective Ionic Radii in Oxides and Fluorides. *Acta Crystallographica Section B-Structural Crystallography and Crystal Chemistry* B 25, 925–&.
Sheldrick, W. & Häusler, H. (1987). Zur Kenntnis von Natriumarseniten im Dreistoffsystem Na_2O-As_2O_3-H_2O bei 6°C. *Zeitschrift Fur Anorganische Und Allgemeine Chemie* 549(6), 177–186.
Sherman, D. & Randall, S. (2003). Surface complexation of arsenie(V) to iron(III) (hydr)oxides: Structural mechanism from ab initio molecular geometries and EXAFS spectroscopy. *Geochimica et Cosmochimica Acta* 67(22), 4223–4230.
Siemens. *GFH Media for Arsenic Removal*. [online] (2013-03-07). Available from: http://www.water.siemens.com/SiteCollectionDocuments/Product_Lines/General_Filter_Products/Brochures/GF-GFH-BR-0709.29.pdf.
Smedley, P. L. & Kinniburgh, D. (2002). A review of the source, behaviour and distribution of arsenic in natural waters. *Applied Geochemistry* 17(5), 517–568.
Smedley, P. L., Knudsen, J. & Maiga, D. (2007). Arsenic in groundwater from mineralised Proterozoic basement rocks of Burkina Faso. *Applied Geochemistry* 22(5), 1074–1092.
Śmiechowski, M., Gojlo, E. & Stangret, J. (2004). Ionic hydration in $LiPF_6$, $NaPF_6$, and KPF_6 aqueous solutions derived from infrared HDO spectra. *Journal of Physical Chemistry B* 108(40), 15938–15943.
Śmiechowski, M., Gojlo, E. & Stangret, J. (2009). Systematic Study of Hydration Patterns of Phosphoric(V) Acid and Its Mono-, Di-, and Tripotassium Salts in Aqueous Solution. *Journal of Physical Chemistry B* 113(21), 7650–7661.
Śmiechowski, M. & Stangret, J. (2006). Proton hydration in aqueous solution: Fourier transform infrared studies of HDO spectra. *Journal of Chemical Physics* 125(20).
Śmiechowski, M. & Stangret, J. (2007a). Hydroxide ion hydration in aqueous solutions. *Journal of Physical Chemistry A* 111(15), 2889–2897.
Śmiechowski, M. & Stangret, J. (2007b). Molecular picture of hydroxide anion hydration in aqueous solutions studied by FT-IR ATR spectroscopy. *Journal of Molecular Structure* 834, 239–248.
Smirnov, P. R. & Trostin, V. N. (2006). Structure of the nearest surrounding of the Li^+ ion in aqueous solutions of its salts. *Russian Journal of General Chemistry* 76(2), 175–182.
Smirnov, P. R. & Trostin, V. N. (2007a). Structure of the nearest surrounding of the Na^+ ion in aqueous solutions of its salts. *Russian Journal of General Chemistry* 77(5), 844–850.
Smirnov, P. R. & Trostin, V. N. (2007b). Structures of the nearest surroundings of the K^+, Rb^+ and Cs^+ ions in aqueous solutions of their salts. *Russian Journal of General Chemistry* 77(12), 2101–2107.
Smith, A. H., Lingas, E. O. & Rahman, M. (2000). Contamination of drinking-water by arsenic in Bangladesh: a public health emergency. *Bulletin of the World Health Organization* 78(9), 1093–1103.
Smith, E., Juhasz, A. L. & Weber, J. (2008). Arsenic uptake and speciation in vegetables grown under greenhouse conditions. *Environmental Geochemistry and Health* 31(S1), 125–132.

Smith, J. D., Cappa, C. D., Wilson, K. R., Cohen, R. C., Geissler, P. L. & Saykally, R. J. (2005a). Unified description of temperature-dependent hydrogen-bond rearrangements in liquid water. *Proceedings of the National Academy of Sciences of the United States of America* 102(40), 14171–14174.

Smith, P. G., Koch, I., Gordon, R. A., Mandoli, D. F., Chapman, B. D. & Reimer, K. J. (2005b). X-ray absorption near-edge structure analysis of arsenic species for application to biological environmental samples. *Environmental Science & Technology* 39(1), 248–254.

Some, I. T., Sakira, A. K., Ouédraogo, M., Ouédraogo, T. Z., Traoré, A., Sondo, B. & Guissou, P. I. (2012). Arsenic levels in tube-wells water, food, residents' urine and the prevalence of skin lesions in Yatenga province, Burkina Faso. *Interdisciplinary Toxicology* 5(1), 38–41.

Song, C., Wang, P. & Makse, H. A. (2008). A phase diagram for jammed matter. *Nature* 453(7195), 629–632.

Soper, A. K. & Weckström, K. (2006). Ion solvation and water structure in potassium halide aqueous solutions. *Biophysical Chemistry* 124(3), 180–191.

Sperlich, A., Werner, A., Genz, A., Amy, G., Worch, E. & Jekel, M. (2005). Breakthrough behavior of granular ferric hydroxide (GFH) fixed-bed adsorption filters: modeling and experimental approaches. *Water Research* 39(6), 1190–1198.

Stachowicz, M., Hiemstra, T. & van Riemsdijk, W. H. (2006). Surface speciation of As(III) and As(V) in relation to charge distribution. *Journal of Colloid and Interface Science* 302(1), 62–75.

Stachowicz, M., Hiemstra, T. & van Riemsdijk, W. H. (2007). Arsenic-bicarbonate interaction on goethite particles. *Environmental Science & Technology* 41(16), 5620–5625.

Stangret, J. (1988). Solute-affected vibrational-spectra of water in $Ca(ClO_4)_2$ aqueous solutions. *Spectroscopy Letters* 21(5), 369–381.

Stangret, J. & Gampe, T. (1999). Hydration sphere of tetrabutylammonium cation. FTIR studies of HDO spectra. *Journal of Physical Chemistry B* 103(18), 3778–3783.

Stangret, J. & Gampe, T. (2002). Ionic hydration behavior derived from infrared spectra in HDO. *Journal of Physical Chemistry A* 106(21), 5393–5402.

Stangret, J. & Kamieńska-Piotrowicz, E. (1997). Effect of tetraphenylphosphonium and tetraphenylborate ions on the water structure in aqueous solutions; FTIR studies of HDO spectra. *Journal of the Chemical Society-Faraday Transactions* 93(19), 3463–3466.

Stangret, J. & Kostrowicki, J. (1988). IR-study of aqueous metal perchlorate solutions. *Journal of Solution Chemistry* 17(2), 165–173.

Steinmaus, C., Yuan, Y., Bates, M. N. & Smith, A. H. (2003). Case-control study of bladder cancer and drinking water arsenic in the Western United States. *American Journal of Epidemiology* 158(12), 1193–1201.

Stumm, W. (1992). The Coordination Chemistry of the Hydrous Oxide-Water Interface. *Chemistry of the Solid-Water Interface*. pp 13–27. Wiley.

Stålhandske, C. M. V., Stålhandske, C. I., Persson, I., Sandström, M. & Jalilehvand, F. (2001). Crystal and solution structures of N,N-dimethylthioformamide-solvated copper(I), Silver(I), and gold(I) ions studied by X-ray diffraction, X-ray absorption, and vibrational spectroscopy. *Inorganic Chemistry* 40(26), 6684–6693.

Stålhandske, C., Persson, I., Sandström, M. & Kamienska-Piotrowicz, E. (1997). Structure of the solvated zinc(II), cadmium(II), and mercury(II) ions in N,N-dimethylthioformamide solution. *Inorganic Chemistry* 36(14), 3174–3182.

Su, C. & Puls, R. (2001). Arsenate and arsenite removal by zerovalent iron: Kinetics, redox transformation, and implications for in situ groundwater remediation. *Environmental Science & Technology* 35(7), 1487–1492.

Su, C. & Puls, R. W. (2008). Arsenate and arsenite sorption on magnetite: Relations to groundwater arsenic treatment using zerovalent iron and natural attenuation. *Water Air and Soil Pollution* 193(1-4), 65–78.

Sun, X. & Doner, H. (1996). An investigation of arsenate and arsenite bonding structures on goethite by FTIR. *Soil Science* 161(12), 865–872.

Sun, X. & Doner, H. (1998). Adsorption and oxidation of arsenite on goethite. *Soil Science* 163(4), 278–287.
Swedelius, F. (1800). Förgiftning af arsenik, lyckligen botad. *Kongl. Vetenskaps Academiens Handlingar* XXI, 68–70.
Tamura, Y., Yamaguchi, T., Okada, I. & Ohtaki, H. (1987). An X-Ray-Diffraction Study on the Structure of Concentrated Aqueous Cesium Iodide and Lithium Iodide Solutions. *Zeitschrift Fur Naturforschung Section a-a Journal of Physical Sciences* 42(4), 367–376.
Tarascon, J. M. & Armand, M. (2001). Issues and challenges facing rechargeable lithium batteries. *Nature* 414(6861), 359–367.
Teixeira, M. & Ciminelli, V. (2005). Development of a biosorbent for arsenite: Structural modeling based on X-ray spectroscopy. *Environmental Science & Technology* 39(3), 895–900.
Thirunavukkarasu, O., Viraraghavan, T. & Subramanian, K. (2003a). Arsenic removal from drinking water using granular ferric hydroxide. *Water Sa* 29(2), 161–170.
Thirunavukkarasu, O., Viraraghavan, T. & Subramanian, K. (2003b). Arsenic removal from drinking water using iron oxide-coated sand. *Water Air and Soil Pollution* 142(1-4), 95–111.
Tongraar, A., Liedl, K. R. & Rode, B. M. (1998). Born-Oppenheimer ab initio QM/MM dynamics simulations of Na^+ and K^+ in water: From structure making to structure breaking effects. *Journal of Physical Chemistry A* 102(50), 10340–10347.
Topel, Ö., Persson, I., Lundberg, D. & Ullström, A.-S. (2010). On the structure of the N,N ’-dimethylpropyleneurea and dimethylsulfoxide solvated gallium(III) and indium(III) ions and bromide complexes in solution and solid state, and the complex formation of the gallium(III) and indium(III) bromide systems in N,N ’-dimethylpropyleneurea. *Inorganica Chimica Acta* 363(5), 988–994.
Torapava, N., Persson, I., Eriksson, L. & Lundberg, D. (2009). Hydration and Hydrolysis of Thorium(IV) in Aqueous Solution and the Structures of Two Crystalline Thorium(IV) Hydrates. *Inorganic Chemistry* 48(24), 11712–11723.
Tossell, J. (1997). Theoretical studies on arsenic oxide and hydroxide species in minerals and in aqueous solution. *Geochimica et Cosmochimica Acta* 61(8), 1613–1623.
Tsai, S. Y., Chou, H. Y., The, H. W., Chen, C. M. & Chen, C. J. (2003). The effects of chronic arsenic exposure from drinking water on the neurobehavioral development in adolescence. *Neurotoxicology* 24(4-5), 747–753.
Tseng, C. H., Chong, C. K., Tseng, C. P., Hsueh, Y. M., Chiou, H. Y., Tseng, C. C. & Chen, C. J. (2003). Long-term arsenic exposure and ischemic heart disease in arseniasis-hyperendemic villages in Taiwan. *Toxicology Letters* 137(1-2), 15–21.
Tseng, C.-H. (2009). A review on environmental factors regulating arsenic methylation in humans. *Toxicology and Applied Pharmacology* 235(3), 338–350.
Tufano, K. J. & Fendorf, S. (2008). Confounding impacts of iron reduction on arsenic retention. *Environmental Science & Technology* 42(13), 4777–4783.
Wachter, W., Kunz, W., Buchner, R. & Hefter, G. (2005). Is There an Anionic Hofmeister Effect on Water Dynamics? Dielectric Spectroscopy of Aqueous Solutions of NaBr, NaI, $NaNO_3$, $NaClO_4$, and NaSCN. *The Journal of Physical Chemistry A* 109(39), 8675–8683.
Waddell, W. J. (2010). History of dose response. *Journal of Toxicological Sciences* 35(1), 1–8.
Vaishya, R. C. & Gupta, S. K. (2003). Arsenic removal from groundwater by iron impregnated sand. *Journal of Environmental Engineering-Asce* 129(1), 89–92.
Wasserman, G. A., Liu, X. H., Parvez, F., Ahsan, H., Factor-Litvak, P., van Geen, A., Slavkovich, V., Lolacono, N. J., Cheng, Z. Q., Hussain, L., Momotaj, H. & Graziano, J. H. (2004). Water arsenic exposure and children’s intellectual function in Araihazar, Bangladesh. *Environmental Health Perspectives* 112(13), 1329–1333.
Waychunas, G., Fuller, C., Rea, B. & Davis, J. (1996). Wide angle X-ray scattering (WAXS) study of "two-line" ferrihydrite structure: Effect of arsenate sorption and counterion variation and comparison with EXAFS results. *Geochimica et Cosmochimica Acta* 60(10), 1765–1781.

Waychunas, G., Rea, B., Fuller, C. & Davis, J. (1993). Surface-chemistry of ferrihydrite .1. EXAFS studies of the geometry of coprecipitated and adsorbed arsenate. *Geochimica et Cosmochimica Acta* 57(10), 2251–2269.

Vchirawongkwin, V., Rode, B. M. & Persson, I. (2007). Structure and dynamics of sulfate ion in aqueous solution - An ab initio QMCF MD simulation and large angle X-ray scattering study. *Journal of Physical Chemistry B* 111(16), 4150–4155.

Weast, R. C. (1975). *Handbook of Chemistry and Physics*. 56th. ed. CRC Press.

Weeks, M. E. (1932). The discovery of the elements. II. Elements known to the alchemists. *Journal of Chemical Education* 9(1), 11.

Vergnet Hydro. *Vergnet Hydro - Products*. [online] (2013-03-15). Available from: http://www.vergnet-hydro.com. [Accessed 2013-03-15].

Westerhoff, P., Highfield, D., Badruzzaman, M. & Yoon, Y. (2005). Rapid small-scale column tests for arsenate removal in iron oxide packed bed columns. *Journal of Environmental Engineering-Asce* 131(2), 262–271.

WHO (2003). *pH in Drinking-water. Background document for development of WHO Guidelines for Drinking-water Quality*. WHO.

Vinogradov, E. V., Smirnov, P. R. & Trostin, V. N. (2003). Structure of hydrated complexes formed by metal ions of Groups I-III of the Periodic Table in aqueous electrolyte solutions under ambient conditions. *Russian Chemical Bulletin* 52(6), 1253–1271.

Wolfe-Simon, F., Blum, J. S., Kulp, T. R., Gordon, G. W., Hoeft, S. E., Pett-Ridge, J., Stolz, J. F., Webb, S. M., Weber, P. K., Davies, P. C. W., Anbar, A. D. & Oremland, R. S. (2011). A Bacterium That Can Grow by Using Arsenic Instead of Phosphorus. *Science* 332(6034), 1163–1166.

Zabinsky, S., Rehr, J., Ankudinov, A., Albers, R. & Eller, M. (1995). Multiple-scattering calculations of X-ray absorption spectra. *Physical Review B* 52(4), 2995–3009.

Zakaznova-Herzog, V., Seward, T. & Suleimenov, O. (2006). Arsenous acid ionisation in aqueous solutions from 25 to 300 degrees °C. *Geochimica et Cosmochimica Acta* 70(8), 1928–1938.

Zeng, L. (2004). Arsenic adsorption from aqueous solutions on an Fe(III)-Si binary oxide adsorbent. *Water Quality Research Journal of Canada* 39(3), 267–275.

Zhang, J. S., Stanforth, R. S. & Pehkonen, S. O. (2007). Effect of replacing a hydroxyl group with a methyl group on arsenic (V) species adsorption on goethite (alpha-FeOOH). *Journal of Colloid and Interface Science* 306(1), 16–21.

Zong, C. (1999). Sphere packings. Springer.

8 Acknowledgements

Arriving to this late page, it is time to express a few words of gratitude towards those who have been crucially important, those who have been supportive in general and most importantly, to those I love.

This thesis would never have been written, was it not for my supervisor Professor **Ingmar Persson** who (twice) decided to give me the opportunity. You are quite possibly the smartest person in the room, but even more important is your optimistic view on life and science. Where others see problems, you see solutions! The piles of Papers with tasks and duties on your desk attempts to smother your joy of working, but when the dust has settled the professor will still be standing. Find as much time as possible to work for your own amusement, and the results are quite likely to turn out great. Also acknowledged is my assistant supervisor Dr. **Daniel Lundberg**, who worked hard teaching me everything from presentation technique and crystallography databases to a foolproof plan for securing seats in the parliament. I am certainly grateful for the amounts of free support given by DL-stöd, connection 1549. I hope you continue to think outside the box, and don't grow old even when you become a professor! I would also like to thank Dr. **Samuel Pare** at the University of Ouagadougou for taking good care of me at my visit in Burkina Faso, and for being committed to the arsenic problem.

Plenty of wonderful people inhabit the Department of Chemistry: Professor **Vadim Kessler**, it is almost impossible to be in the same room as you without learning something new. Also, your smooth and efficient department management is appreciated. Dr. **Gulaim Seisenbaeva**, always with a friendly smile, runs the most well-organized and efficient lab in the department. Involuntary chemist Dr. **Anke Herrmann** and her 48-channel crew is certainly starting to take off. In a few years you will be a professor and *Nature* begs you for articles. Dr. **Gunnar Almkvist**, my office mate for the first two years, you are skilled in your field and I hope you see the forest despite all the chopped-down

water-logged trees. Our secretary **Sonja Jansson** is always helpful in any matter. This is also the case with the student laboratory engineer Dr. **Bernt Andersson**. Keep your young mind, even when the last bottle of stock solution is prepared and the last troublesome instrument fixed.

Shahin Norbakhsh, my brother-in-arms, you are the captain of your ship and you don't need anyone's approval to bravely go where no man has gone before. Sail, fail and finally prevail!

With fellow solution chemist **Lars Eklund**, I have had many interesting discussions. I hope you get your potentials, angles and hydrogen bonds right, but I particularly wish you the greatest luck with your growing family! My physicist roommate **Josephina Werner** can easily explain hydrostatic paradoxes as well as Auger electrons for a chemist. **Tobias Bölscher** is a nice guy and I wish you the best luck with your micro-calorimeter work. Brand new PhD student **Martin Palmqvist**, enjoy the next few years - before you know it you are the one typing these sentences. During my time here, some colleagues accomplished their goals and left the Department of Chemistry with PhD:s; Dr. **Olesya Nikonova**, Dr. **Natallia Torapava** and Dr. **Kai Wilkinson**. You are all great people and I wish you the best out there.

Professor **Lennart Kenne** left us in a much more tragic way, much too soon. I will certainly remember all the nice organic people; **Lena Lundqvist**, **Eric Morssing Vilén**, **Gustav Nestor**, **Christina Nord**, **David Hansson**, **Frida Wende**, Dr. **Anders Sandström**, Dr. **Peter Agback**, Dr. **Pierre Andersson**, Dr. **Anders Broberg**, Dr. **Elsa Coucheney**, Dr. **Jan Eriksson**, Dr. **Mattias Fredriksson**, Dr. **Suresh Gohil**, Dr. **Ali Moazzami** and Professor **Corine Sandström**. When one thinks of it, carbon isn't such a bad element after all. Present and former **visiting colleagues** are acknowledged, although I am running out of my three pages of space and cannot fit in all your names!

I would also like to thank my former employer **METLAB miljö AB**, and in particular managing director **Lars Månsson**, for an excellent introduction to working life and - I think - to a scientific way of thinking. I believe that everyone at SLU chemistry is now aware of the greatness of METLAB, and I will continue to preach for anyone prepared to listen.

My mother, **Sonja Mähler**, may not be a great chemist but certainly a great mom. You raised me to a decent guy, and you taught me to say what I think and to be myself. Perhaps everyone does not agree this is a good thing, but I am very grateful for what you have done. My father, **Charlie Lundmark**, have many virtues such as an open mind and a fearless attitude to challenges. *"I have never done it before, but I am pretty sure I can"* is a quote that can be applied to almost any situation, and it got stuck to my brain. **Eva Lundmark**, you are always nice to me and wise about philosophical matters. My brother

Linus Mähler, I am very happy for your successful career and only marginally envious of your car and your business trips. My brother **Viktor Mähler**; I am equally happy for your successful studies and appointments. I would however also like to give a small advice to my brothers Linus and Viktor. I feel a slight tension in your behavior and state of mind, and I have come to the conclusion that it might originate in your production of inferior woodwork butter knives, your repeated losses in different righteously performed family games or perhaps in your inability to correctly recite holy texts out of mind. Don't worry about it - there can be only one truly big brother.

While I rarely meet my other siblings **Julia Lundmark**, **Oskar Lundmark** and **Alva Lundmark**, the three of you are also important to me. In my mind I still think of you as one-meter-high kids, but I am happy that all of you are starting up exciting lives as young adults.

My stepdaughter **Roxana Korkchi**: I guess that I more often, should emphasize that you mean a lot to me. In my present sentimental mood, I cannot resist the urge to give you a piece of advice. While it is always good to try to improve your weak sides, my main advice for now is to focus on all the things you are good at. You are good at handling people, you do not fear to contact either unknowns or those of authority, and you have no problem to express your opinions - not even at TV. In a land of shy and easily embarrassed people, don't be surprised if people skills turn out to be even more useful than chemistry. Also remember that making the wrong decision is usually not a big problem, while making no decision at all can be a terrible mistake.

My wonderful daughter **Hilda Mähler** is two years old as this thesis is printed, and it will probably take a few years until you read these lines. I imagine how you find a dusty old thesis tucked into a bookshelf somewhere, and starts to read the acknowledgements for the fun of it (such things happens in the future, right?). This is a message from 2013, which travelled through time and space to reach your eyes: Your dad loves you as limitless as a teenager, young adult or grown-up, as he loved the little princess who wanted to dance, climb the stairs or ride the slide at the playground. No conditions whatsoever. This said, I would still appreciate if you by now have stopped the habit of intentionally throwing food on the floor.

I wish to thank my wife **Roya Rahbar**, for being supportive with my work, but especially for being you. You put up with my sometimes irritating flaws and I love you so much. Since I met you, my life has become meaningful. You may not always believe me on that point, but remember that I knew me a long time before you knew me. We are a great team and there is no one else I would rather have by my side when setting out at new paths to explore the wonderful possibilities of life.

8.1 Funding and support

Research in this project has been funded by The Swedish International Development cooperation Agency (SIDA) as well as the Swedish Research Council (VR). Both are greatly acknowledged for their support. Beam time at beam-line I811 was kindly granted by MAX-lab synchrotron radiation source, Lund University, Sweden. The beam-line itself was funded by the Swedish Research Council and the "Knut and Alice Wallenbergs Stiftelse". Also acknowledged is GEH Wasserchemie GmbH & Co. KG, for supplying granular ferric hydroxide free of charge.

Appendix I - Hydrogen atoms in water molecules

Using data for the water oxygen radius (Beattie *et al.*, 1981), oxygen-oxygen distances in ice (Fortes *et al.*, 2004) and the intramolecular O-H distance of a water molecule (Soper, 2000), the size of the water hydrogen can be roughly estimated.

Using the assumption of hydrogen atoms as hard spheres embedded in a spherical electron cloud of an oxygen atom without significantly disturbing it, a radius of 0.43 Å for such a hydrogen atom can be estimated, as shown below. The hydrogen atom would extend the oxygen sphere surface with only 0.07 Å.

While the assumption above may be a simplification and the referenced d_{OH} distance somewhat uncertain, the figure below serves to underline the small demand for space by the hydrogen atoms in a water molecule.

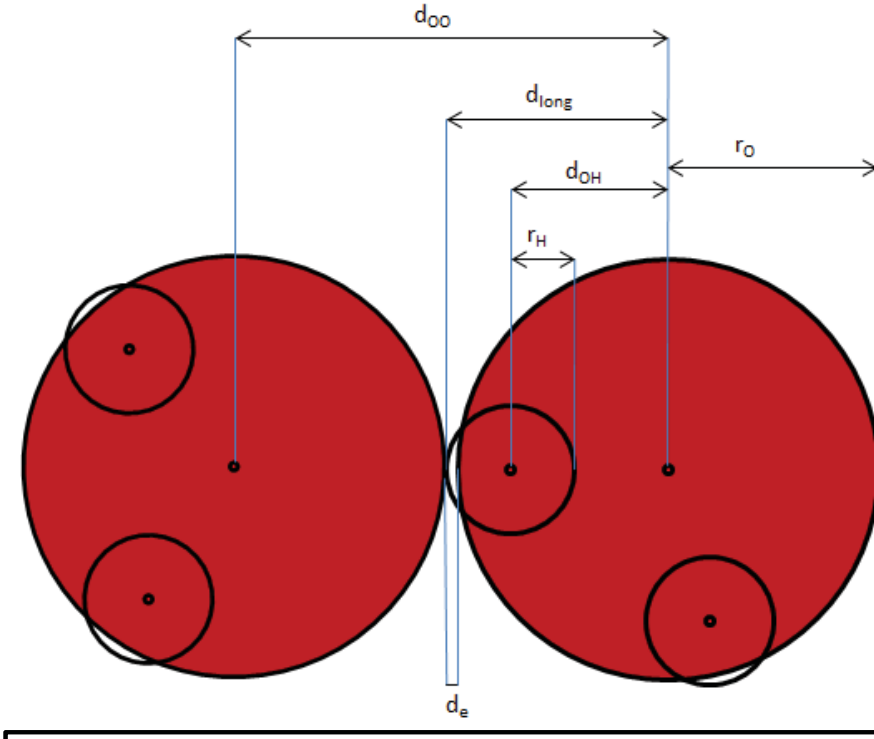

r_O = 1.34 Å (Beattie *et al.*, 1981)	$d_{long} = d_{OO} - r_O$ = 2.75 Å-1.34 Å = 1.41 Å
d_{OO} = 2.75 Å (Fortes *et al.*, 2004)	$d_e = d_{long} - r_O$ = 1.41 Å - 1.34 Å = 0.07 Å
d_{OH} = 0.98 Å (Soper, 2000)	$r_H = d_{long} - d_{OH}$ = 1.41 Å - 0.98 Å = 0.43 Å

Beattie, J., Best, S., Skelton, B. & White, A. (1981). Structural Studies on the Cesium Alums, $CsM^{iii}[SO_4]_2*12H_2O$. *Journal of the Chemical Society-Dalton Transactions* (10), 2105–2111.

Fortes, A. D., Wood, I. G., Grigoriev, D., Alfredsson, M., Kipfstuhl, S., Knight, K. S. & Smith, R. I. (2004). No evidence for large-scale proton ordering in Antarctic ice from powder neutron diffraction. *Journal of Chemical Physics* 120(24), 11376–11379.

Soper, A. K. (2000). The radial distribution functions of water and ice from 220 to 673 K and at pressures up to 400 MPa. *Chemical Physics* 258(2–3), 121–137.

Appendix II - Estimation of the francium ion radius

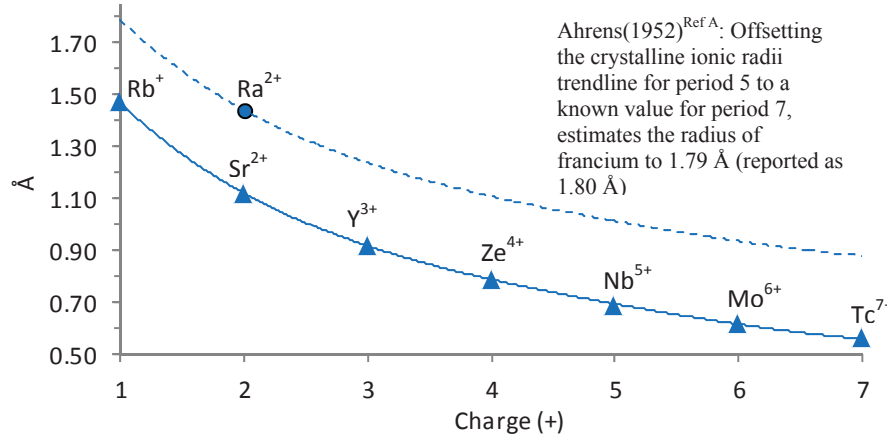

Ahrens(1952)[Ref A]: Offsetting the crystalline ionic radii trendline for period 5 to a known value for period 7, estimates the radius of francium to 1.79 Å (reported as 1.80 Å)

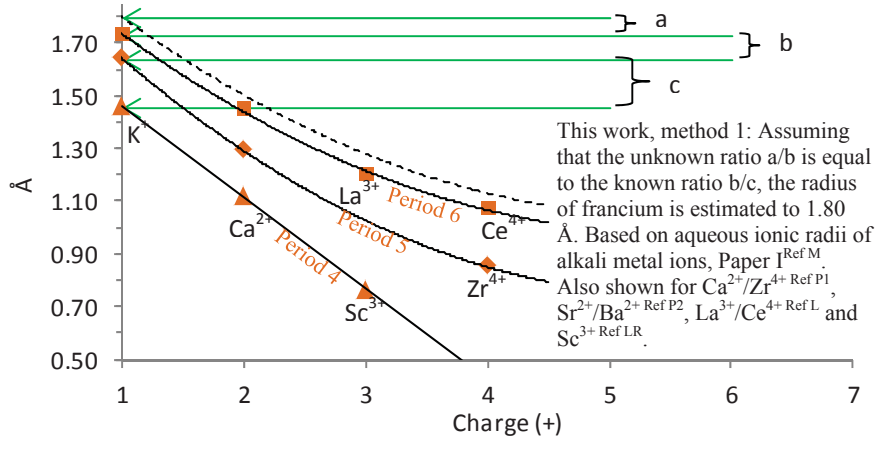

This work, method 1: Assuming that the unknown ratio a/b is equal to the known ratio b/c, the radius of francium is estimated to 1.80 Å. Based on aqueous ionic radii of alkali metal ions, Paper I[Ref M]. Also shown for Ca^{2+}/Zr^{4+}[Ref P1], Sr^{2+}/Ba^{2+}[Ref P2], La^{3+}/Ce^{4+}[Ref L] and Sc^{3+}[Ref LR].

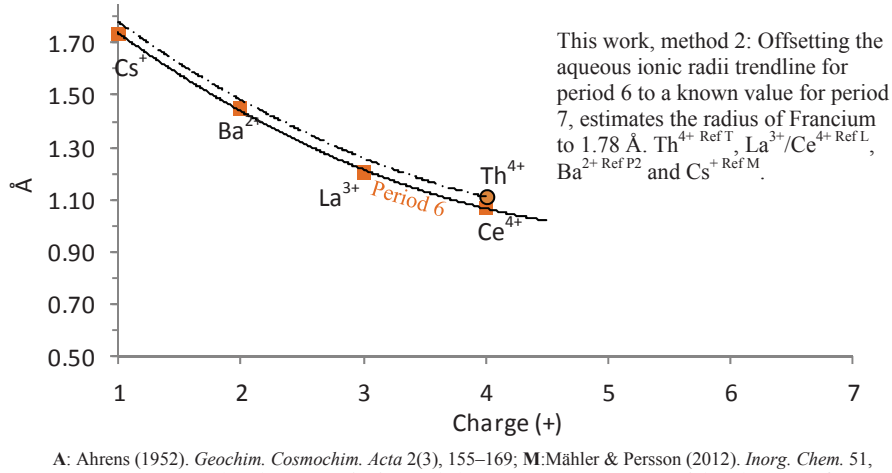

This work, method 2: Offsetting the aqueous ionic radii trendline for period 6 to a known value for period 7, estimates the radius of Francium to 1.78 Å. Th^{4+}[Ref T], La^{3+}/Ce^{4+}[Ref L], Ba^{2+}[Ref P2] and Cs^{+}[Ref M].

A: Ahrens (1952). *Geochim. Cosmochim. Acta* 2(3), 155–169; **M**:Mähler & Persson (2012). *Inorg. Chem.* 51, 425-438.; **P1**:Persson (2010). *Pure Appl. Chem.* 82(10), 1901–1917; **P2**:Persson *et al.* (1995). *Z. Naturfors. Sect. A*- 50(1), 21–37; **L**: Lundberg *et al.* (2010). *Inorg. Chem.* 49(10), 4420–4432; **LR**: Lindqvist-Reis *et al.* (2006). *Dalton Trans.* (32), 3868–3878. **T**: Torapava *et al*. (2009). *Inorg. Chem.* 48(24), 11712–11723.